TECHNISCHE UNIVERSITÄT WIEN
Vienna University of Technology

DIPLOMARBEIT

Cluster of human spiral ganglion neurons: A computational model study of ephaptic coupling effects

Ausgeführt am Institut für
Analysis und Scientific Computing
der Technischen Universität Wien
unter der Anleitung von
Ao.Univ.Prof.i.R. Dipl.-Ing. Dr.rer.nat. Dr.sc.med. Dr.techn. **Frank Rattay**
Projektass. Dipl.-Ing. Mag. Dr.techn.Danner, **Simon Michael**

durch
Igor Saburov
Molkereistrasse 1/2053/1
1020 Vienna

September 15, 2014

Abstract

Motivations of the thesis: Cochlear Implants are the medical option for people, who severe to profound hearing loss. Since my thesis related with human auditory system, considering the human auditory nerves is very important topic. Human auditory neurons show micro-anatomical peculiarities which differ considerably from other species, for instance human spiral ganglion neuron bodies are unmyelinated and often arranged in functional units covered by common satellite glial cells. Since human spiral ganglion cells are not experimentally accessible, theoretical analysis concerning single neuron response has to be performed. Nonetheless the physiology of hearing is not totally understood, e.g. speech recognition and perception in noisy environment, attenuation effects and the temporal fine structure of the neural pattern.

Methods of the investigations: The anatomical data presented in the thesis are based on several human cochlea and compose the fundament of the subsequent computer simulations which provide an appropriate method for single cell analysis. The electrical activity of cochlear neurons can be deducted from solving systems of differential equations which will enhance our understanding of action potential initiation and propagation of nerve impulses. A new model for simulating the natural spiking behavior of human cochlear neurons as well as their excitability to microstimulation by electrodes were presented in my thesis.

Final results: Hierarchial cluster analysis of acquired volumetric data of unmyelinated human auditory cell somata indicates the existence of four distinct populations of auditory nerves within the human cochlea. The unmyelinated soma region reduces the safety factor of AP transmission whereas certain sensitive parameter can be identified leading to divergent excitation profiles. For successful ephaptic stimulation the spikes of adjacent neurons get synchronized. Some inhibiting effects can also be observed due to large current loss on the sensitive human soma region. Mathematical modeling and computer simulation have become important tool for many clinical and medical applications. Especially further development for electrical prosthesis leading to better implant user performance is achieved by adapting stimulation strategies according to results obtained by computer simulation. The results of the thesis predict the contemporary models shall be adapted according to the unique human in order to improve pending studies.

Zusammenfassung

Motivation der Diplomarbeit: Cochlea-Implantate sind eine medizinische Option für Menschen mit schwerwiegendem Hörverlust. Da meine Diplomarbeit mit menschlichem Gehör in Zusammenhang steht, ist die Berücksichtigung der menschlichen Gehörnerven ein wichtiges Thema. Die menschlichen Cochlea - Neuronen zeigen mikro-anatomische Besonderheiten, die sich beträchtlich von denen anderer Spezien unterscheiden. Beispielsweise sind menschliche Spiralganglien - Zellkörper myelinfrei und oftmals in funktionellen Einheiten arrangiert, welche von Mantelzellen umgeben sind. Da menschliche Spiralganglienzellen nicht experimentell zugänglich sind, muss eine theoretische Analyse der einzelnen Neuronen - antworten durchgeführt werden. In vielen Teilen ist die Physiologie des Hörens nicht vollkommen erforscht. Zu diesen Gebieten zählen bsw. die Stimmerkennung und - Aufnahme in lauten Umgebungen, Dämpfungseffekte und die feine Temporalstruktur neuronaler Muster.

Untersuchungsmethoden: Die humanen anatomischen Daten, die in dieser Arbeit präsentiert werden, basieren auf verschiedenen Cochlea messungen und bilden die Basis der Computersimulationen, welche eine geeignete Methode für die Analyse einzelner Zellen darstellen. Die elektrische Aktivität der Cochlea neuronen kann durch Lösungen von Systemen von Differentialgleichungen simuliert werden,um die Initiierung von Aktionspotentialen und Vorhersage von Nervenimpulsen besser zu verstehen. Ein neues Modell zur Simulation des Feuerungsverhaltens menschlicher Cochlea neuronen, sowie deren Erregbarkeit durch Mikrostimulationen durch Elektronen, werden in dieser Arbeit präsentiert.

Endresultate: Hierarchische Cluster-Analysen akquirierter volumetrischer Daten der myelinfreien menschlichen Cochleazellen-Somata deuten auf die Existenz von vier ausgeprägten Populationen von akkustischen Nerven innerhalb der menschlichen Cochlea hin. Die myelinfreie Soma-Region reduziert den Sicherheitsfaktor der Aktionspotentialbertragung, wobei bestimmte sensitive Parameter, welche zu abweichenden Erregungsprofilen führen, entdeckt werden können. Für eine erfolgreiche ephaptische Stimulationen werden die Spitzen angrenzender Neuronen synchronisiert. Einige hemmende Effekte können auch beobachtet werden, welche durch den grossen Stromverlust im sensitiven Teil der menschlichen Soma-Region ausgelöst werden. Mathematische Modellierung und Computersimulation haben sich zu einer wichtigen Methode in vielen klinischen und medizinischen Anwendngen etabliert. Insbesondere die Weiterentwicklung elektrischer Prothesen, die zu einer Verbesserung der Hörfhigkeit führen, werden durch

Strategien, welche aus Ergebnissen von Computersimulationen gewonnen werden, entwickelt. Die Ergebnisse dieser Diplomarbeit zeigen, dass die Modelle der einzigartigen Situation des Menschen angepasst werden sollen, um anstehende Studien zu verbessern.

Acknowledgements

I would like to express gratitude and thank to:

- My supervisor - DDDr. Frank Rattay, who has been a great advisor and answered me all the uncleared questions, that has appeared during the whole working process of my thesis.I really thank him for every meeting, that he spend with me during our meeting hours on Monday‘s.

- My second supervisor - Dr. Thomas Potrusil, who has given me a material for my thesis research. And, of course, thank you Thomas for answering on all my questions via e-mails. It was great explanation of problems, that I had during my thesis.

- Erasmus Mundus Action 2 Consortium, who sponsored me the whole my Master studies in Vienna and therefore make a significant contribution in my teaching process in Austria.

- My family and friends and all the people, who were always with me and gave me a good advice and support in a hard situations and helped me to cope easily with all the problems during my studies in Vienna.

Igor Saburov

List of Abbreviations and Symbols

- α_m,α_n,α_h - transfer rates from closed to open state [1/ms]
- β_m,β_n,β_h - transfer rates from closed to open state [1/ms]
- ρ_e - extracellular resistivity[$k\Omega cm$]
- ρ_i - intracellular resistivity[$k\Omega cm$]
- $[Cl]_e$ - extracellular concentration of chloride ions [mol/l]
- $[Cl]_i$ - intracellular concentration of chloride ions [mol/l]
- $[K]_e$ - extracellular concentration of potassium ions [mol/l]
- $[K]_i$ - intracellular concentration of potassium ions [mol/l]
- $[Na]_e$ - extracellular concentration of sodium ions [mol/l]
- $[Na]_i$ - intracellular concentration of sodium ions [mol/l]
- AP - Action Potential
- BM - Basilar Membrane
- C_m - Membrane capacitance [$\mu m/cm^2$]
- Ca^{2+} - calcium ion
- Cl^- - chloride ion
- CNS - Central Nervous System
- CRRSS - Chiu, Ritchie, Rogert, Stagg and Sweeney
- ECS - extracellular space
- F - Faraday Constant, F=9.64845 [C/mol]

- FH - Frankenhaeser and Huxley
- $G_{K,max}$ - maximum value of potassium conductance $[mS/cm^2]$
- G_K - potassium conductance $[mS/cm^2]$
- $G_{Na,max}$ - maximum value of sodium conductance $[mS/cm^2]$
- G_{Na} - sodium conductance $[mS/cm^2]$
- GAUSS - Gaussian noise current term
- $I_{capacitive}$ - capacitive current $[\mu A/cm^2]$
- I_{ion} - ionic current $[\mu A/cm^2]$
- I_k - potassium current $[\mu A/cm^2]$
- I_{Na} - sodium current $[\mu A/cm^2]$
- I_m - membrane current $[\mu A/cm^2]$
- I_{noise} - noise current $[\mu A/cm^2]$
- I_{ohm} - ohmic current $[\mu A/cm^2]$
- I_{inj} - stimulation current $[\mu A/cm^2]$
- ICS - intracellular space
- IHC - inner hair cell
- OHC - outer hair cell
- k- temperature coefficient, acceleration factor
- K^+ - potassium ion
- K_{noise} - noise factor $[\mu A m s^{-1/2}]$
- l-length

- m,n,h - gating variables, probability for a membrane gating process
- Na^+ - sodium ion
- nm - number of myelin layers
- OC - Organ of Corti
- P_{Cl} - permeability of chloride ions [cm/s]
- P_k - permeability of potassium ions [cm/s]
- P_{Na} - permeability of sodium ions [cm/s]
- PNS - peripheral nervous system
- Q - charge
- R - Gas Constant, R=8.31 [J/mol.K]
- R_K - resistance of membrane for potassium
- R_L - resistance of membrane for other ions
- R_{Na} - resistance of membrane for sodium
- SM - scala media
- ST - scala tympani
- SV - scala vestibuli
- T - absolute Temperature
- TC - Tunnel of Corti
- TM - Tectoral Membrane
- TMa - Tympanic Membrane
- V_e - extracellular potential [mV]

- V_i - intracellular potential [mV]
- V_k - Nernst potential of potassium [mV]
- V_l - Nernst potential of other ions, leakage voltage [mV]
- V_m - transmembrane potential [mV]
- V_{Na} - Nernst potential of sodium [mV]
- V_{rest} - resting membrane potential [mV]
- PNS - Peripheral Nervous System
- SGC - Spiral Ganglion Cells
- gE - cluster conductance of one layer of myelin [mS/cm^2]
- AP_{height} - local parameter: maximal overshot of membrane potential [mV]

Contents

Abstract i

Zusammenfassung ii

Acknowledgements iv

List of Abbreviations and Symbols iv

1 Introduction 1

1.0.1 Thesis Organization 3

2 Nervous system 4

2.1 Anatomy of Human Neurons 6

2.1.1 Cell Membrane 6

2.1.2 Soma 7

2.1.3 Dendrites 8

2.1.4 Axon 8

2.1.5 Synapse 9

2.2 Types of Neurons 11

2.2.1 Functional classification of Neurons 12

2.2.2 Nervous System 13

2.3 Passive Electrical Behavior 14

2.3.1 Structure of the Biological Membrane 14

2.3.2 Passive State - Equilibrium 16

2.3.3 Nernst and Goldman equations 17

2.4 Active Electrical Behavior 19

2.4.1 Action Potential(AP) 20

2.4.2 HH,FH,CRRSS,SE,SRB - Models 23

2.4.3 Sodium conductance 25

2.4.4 Potassium conductance 25

2.4.5 Inactivating h-particle 26

3 The Human Ear **30**

3.1 The Inner Ear 31

3.2 Cochlea, Organ of Corti 32

3.3 The organ of Corti and auditory hair cells 35

3.4 Hair Cells 36

3.4.1 Inner Hair Cell(IHC) 37

3.4.2 Outer Hair Cell(OHC) 38

3.4.3 Type I and type II neurons 38

3.5 Human Specialities 40

4 Models of human cochler Neurons 44

4.1 Compartment model 44

4.2 Cluster modeling 49

4.2.1 Cluster1 51

4.2.2 Cluster2 56

4.2.3 Cluster3 60

4.2.4 Intracellular Spike Trains 64

4.2.5 Cluster4 67

5 Cell Synchronization 77

5.1 Noise Effects 78

5.2 Unidirectional Coupling 78

5.2.1 Cluster1 79

5.2.2 Cluster2 81

5.2.3 Cluster3 83

5.2.4 Cluster4 85

5.3 Bidirectional Coupling 89

5.3.1 Cluster1 90

5.3.2 Cluster2 92

5.3.3 Cluster3 94

5.3.4 Cluster4 96

6 Conclusion **100**

Bibliography **101**

Chapter 1

Introduction

First our knowledge about neural coding in mammalian cochlear neurons is based on animal experiments. (Kiang 1966, Brugge et al. 1969, Sachs and Abbas 1974, Shamma 1985, Javel 1994, Rattay and Lutter 1997). The somatic region of the afferent human cochlear are quite unique. Firstly most cell bodies of type I neurons are unmyelinated and secondly many of them are gathered to clusters 2-4 (Tylstedt et al. 1997) neurons having a common insulation by myelin. The cell bodies differ not only in size, i.e., 25-30m in man (Spoendlin and Schrott 1989) and about 20 m in cat (Liberman and Oliver 1984), but also in number of myelin layers surrounding them. According to (Ota and Kimura 1980) 94% of human spiral ganglion neurons are unmyelinted and mostly surrounded by one to several layers of satelite cells. The pre- and postsomatic areas, the lengths of which vary a lot, are not shielded by myielin, either. On the other hand, in all mammalians studied so far 90-95% of the spiral ganglion cells are large in size and myelinated (Spoendlin 1971). It is almost a reverse proportion between man and cat. The morphological difference is of major relevance for the propagation of an action potential. Both human particularities are expected to affect essentially the neural pattern resulting in a special human physiologic hearing performance. Analyzing the electrical features of a non-or poorly myelinated somatic region one can conclude that the human afferent cochlear neuron is essentially less robust in spike conduction as in the preferred experimental animals cat and guinea pig (Rattay et al. 2001a). This is mainly a consequence of the large capacitance of the

soma which consumes most of the current provided by the active peripheral axon and so it is questionable if enough intracellular current is available to prepare excitation in the central axon in order to conduct a spike. The danger of loosing most of the spikes could be reduced by the myelin sheets of the cluster or by a proper combination of geometric and electrical parameters in the presomatic region. Loading the somatic capacitance causes a larger delay: Comparing the reactions of a human and cat cochlear neuron, it has been found 400 μs in man and 200 μs in cat (Rattay et al. 2001a), a result that was supported by neural response telemetry recording with cochlear implants (Dillier et al. 2002, Cohen et al. 2004).

Kimura et al. 1987 found in macaque monkeys four types of cochlear neurons, one with unmyelinated perikaryon and myelinated axons. (Tylstedt and Rask-Andersen 2001) speculate whether unique formations between human spiral ganglion cells, which have not been observed in other species, may constitute interactive electrotonic or phaptic transmission pathways. These may be in the low-frequency region and may increase plasticity and signal acuity related to the coding speech. Clusters could also work as filters in order to suppress spontaneous spikes without signal information. For example, (Rattay et al. 1998) and (Svrcek-Seilek 1998) have shown that e.g., Brownian motion of inner hair cell stereocilia enhances weak auditory signals resulting in spontaneous with and without signal information. In a recent study (Machery et al. 2008), it was shown electrophysiologically and psychophysically that the human auditory system exhibits the opposite pattern, being more sensitive to anodic simulation. These findings are explained by the computational model of the human auditory nerve (Rattay 1999, Rattay et al. 2001a, Rattay et al. 2001b). As nerve fiber model analysis and computer simulations can be valuable tools to show the functional relevance of morphological data. The goal of the thesis is a better understanding of the functions of the cochlear. This is also of importance for developing next generation hearing aids. This thesis provides simulations concerning the nonmyelinated soma and gives a first approach to derive a mathematical model of the neuron clusters to study their influence on the spiking behaviour of the surrounded neurons.

1.0.1 Thesis Organization

Chapter 2 gives us an overview of the main functional and structural units of the nervous system. This part contains types of neurons, the main components of nervous system (CNS, PNS), as well as the main equations, which were used for describing main biophysical models.

Chapter 3 provides an anatomical overview of the human cochlea and outlines the physiological process of hearing. This part offers a summary of a complex organization of the hearing organ, the neural parts and different types of cells in the hearing process.

Chapter 4 provides a general biophysical model of an auditory neuron, which is shown by the underlying physical laws of electrical circuits and the derived differential equations. These equations enable to calculate time course of the transmembrane potential for every functional subunit to study the resulting excitation pattern in respect of time. The four detected neuron clusters which have been just recently investigated by cooperation partner of the MedUni IBK. The effect of ephaptic coupling between the SGC sharing a common myelin layer over their somata was analyzed.

Chapter 5 shows the synchronization effects for four different human clusters for uni- and bidirectional coupling. In this experiments we include noise factor k_{noise}= 0.05 $\mu AmS^{-1/2}$, which is common to all compartments of the neuron.

The summary and conclusion of the computer simulations including the limitations of the mathematical models and ideas for further experiments are provided in Chapter 6. The computer simulations were performed with the MatLab 2012b programm.

Chapter 2

Nervous system

The neuron is a functional and structural unit of the nervous system. A typical neuron consists of the soma or cell body, the axon and dendrites. The neuron receives the afferent signals (excitatory or inhibitatory) from a few to sometimes several thousands of other neurons via its dendrites and sums the signals along the cell membrane of the soma. The axon arises from the axon hillock of the soma and is responsible for the transmission of efferent neural signals to nearby or distant effectors and adjacent neurons. Along the axon, the plasma membrane of the soma continues as the axolemma. The axolemma is surrounded by oligodendrocytes in the central nervous system (CNS), and by Schwann cells in the peripheral nervous system. A nerve fiber consists of an axon plus its sheath. In some neurons, Schwann cells form multiple concentric double phospholipid layers around an axon, comprising the myelin sheath that insulates the axon from ion current. The sheath is interrupted every 1.5mm or so at the nodes of Ranvier.

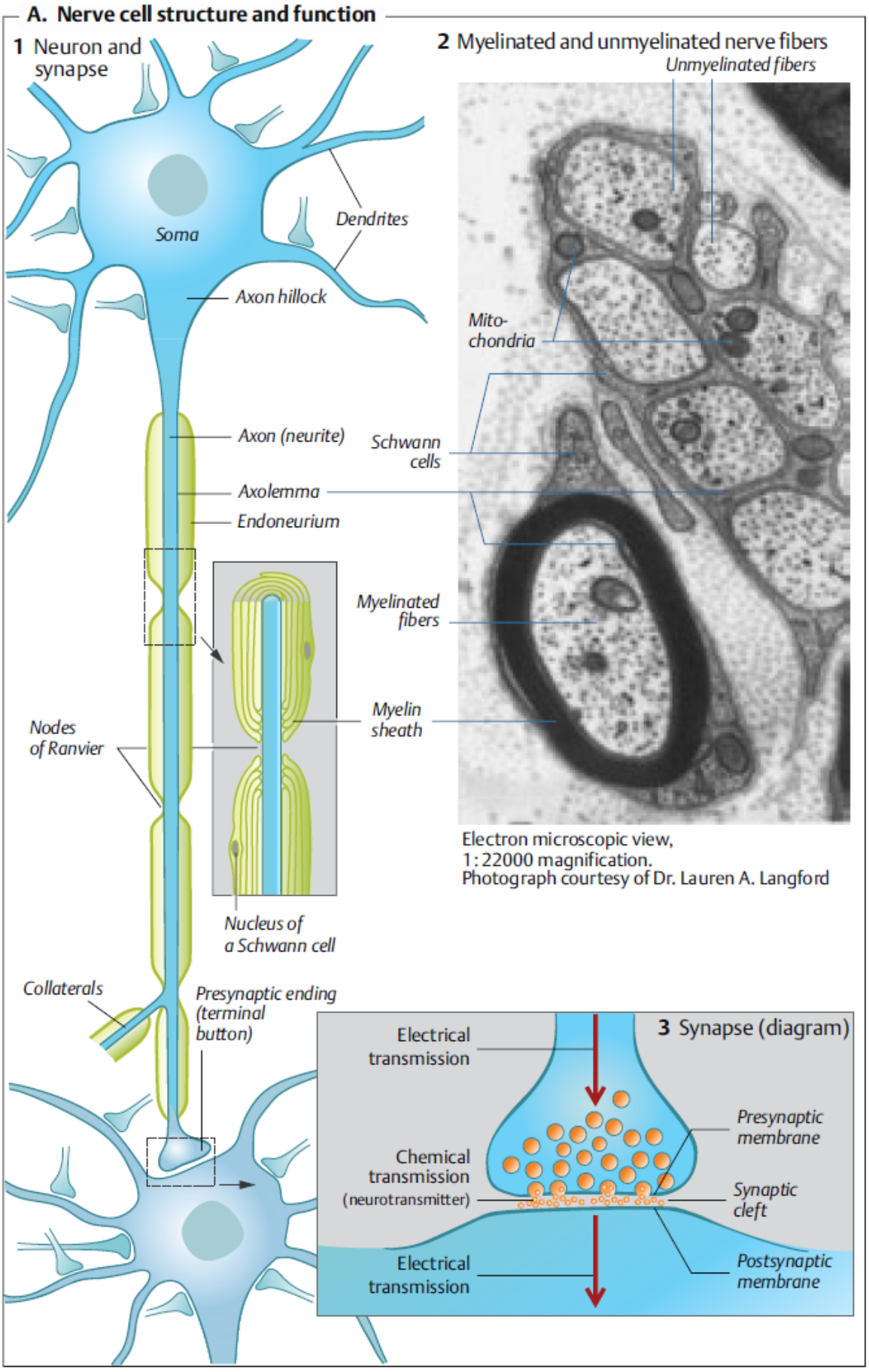

Figure 2.1: Nerve cell structure and function (Silbernagl 2009)

2.1 Anatomy of Human Neurons

2.1.1 Cell Membrane

The main job of cell membrane is to separate the cell interior from the extracellular space. The cell membrane is phospholipid bilayer that may be either smooth or deeply infolded. Depending on the cell type, the cell membrane contains variable amounts of phospholipids, cholesterol and glycolipids. The electrical properties of the membrane enable the generation and transmission of information coded in a nerve impulse, which is also called action potential.

The fatty acids that constitute most of the cell membrane are called phosphoglycerides. A phosphoglyceride consists of phosphoric acid and fatty acids called glycerides. The head of the molecule is hydrophilic (‘like‘ water). The fatty acids have tails consisting of hydrocarbon chains which are hydrophobic (‘don‘t like‘ water). The bilayer is the main structure of the cell membrane. From the bioelectric view, the ionic channels constitute an important part of the cell membrane. These are macromolecular pores through which sodium, potassium and chloride ions flow through the membrane. The flow of these ions forms the basis of bioelectric phenomena. Figure. 2.2 shows the construction of a cell membrane.

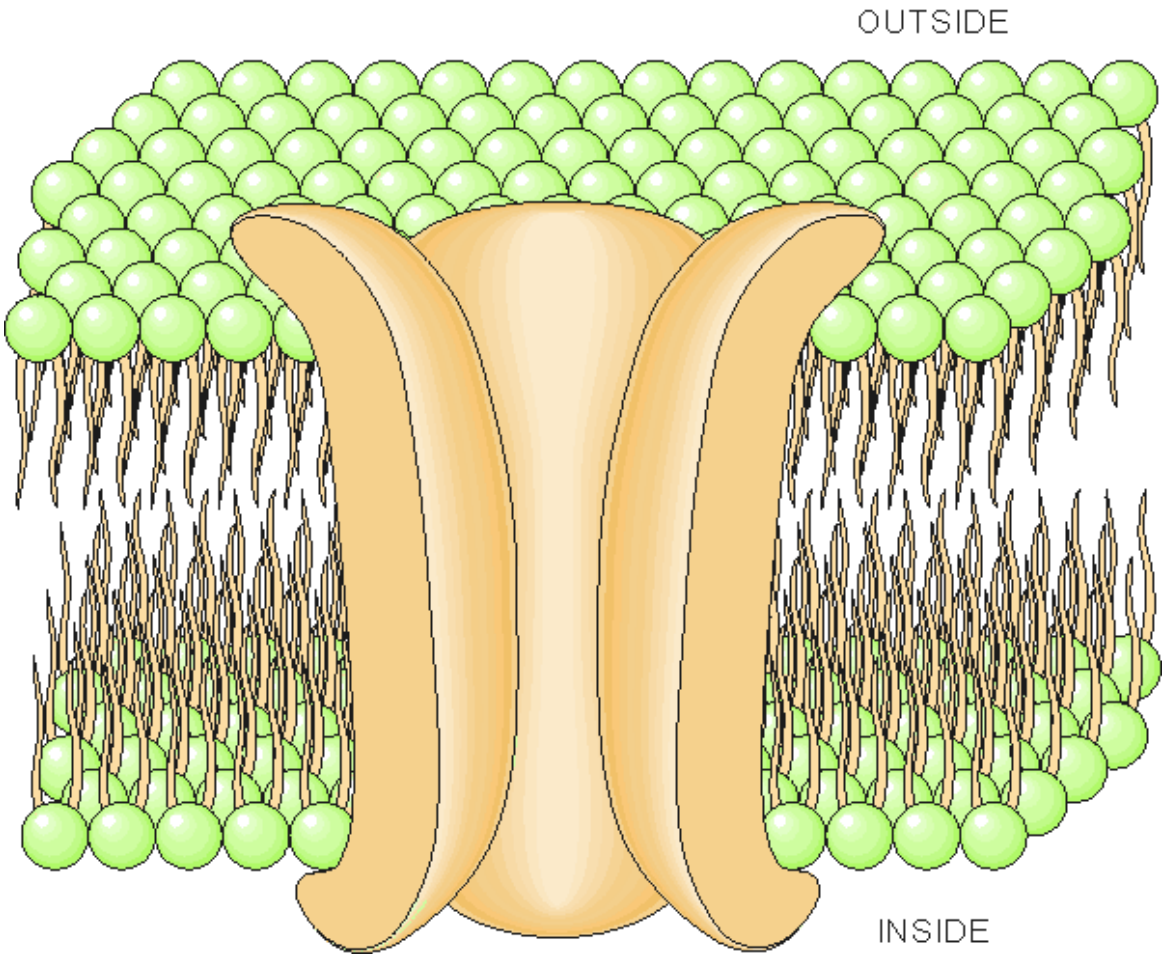

Figure 2.2: The construction of a cell membrane. The main constituents are two lipid layers, with the hydrophobic tails pointing inside the membrane (away from the aqueous intracellular and interstitial mediums). The macromolecular pores in the cell membrane form the ionic channels through which sodium, potassium, and chloride molecules flow through the membrane and generate the bioelectric phenomena.(Malmivuo, Plonsey 1995)

2.1.2 Soma

Soma is the cell‘s body and has typically cell components used for cell maintenance: the membrane (a lipid bilayer), which separates and protects the cell from its environment; the nucleus (with a large nucleolus), which contains the genetic information of the cell; endoplasmic reticulum and ribosomes, where proteins are produced; mitochondria, the energy power houses of the cell; golgi apparatus, where proteins are packaged in vesicles for secretion outside the cell; and the other miscellaneous organelles; the soma is usually large (Figure 2.1).

2.1.3 Dendrites

Dendrites are the 'input' of the neuron. They receive information from other neurons or the external environment and transfer to the cell body (soma) or axons. Dendrites are numerous, relatively short, and branch extensively in a tree-like fashion. Dendrites have numerous spines on them and provide a greater surface area for other neurons to synapse on. Dendrites receive information from other cells at these synapses. This makes dendrites *postsynaptic*. The connection between axons that synapse on dendrites is called *axodendritic*. Meanwhile the connection between dendrites that synapse on other dendrites is called *dendrodendritic*.

2.1.4 Axon

Axon is the 'output' of the neuron. It transfer the information to other neurons. Axon begins at *axon hillock*, which is swelling at the junction of axon and soma where there are many Na^+ channels and the action potential starts. They are usually long (some reaching several feet). Axon have *terminal boutons* at the end of the axon where the synapse is located. This makes axons *presynaptic*, also it swelling at the terminal bouton (where the neuron synapses with another neuron). Contains numerous vesicles which hold neurotransmitter. Axon has many Ca^{2+} channels in the membrane, forms presynaptic membrane in any kind of axonal synapse. The space between the terminal boutons and and the next cell is known as *synaptic cleft*, and approximately 20nm thick. Most of the axons are myelinated: have *myelin sheath* that are made by Schwann cells or oligodendrocytes. Myelin acts as insulator to help conduction of Ation potential. Also there are openings between Schwann cells called *Nodes of Ranvier*. These help with the conduction of Action potentials. Some of the axons are not myelinated (typically shorter axons). Axon synapse on other cells in various forms:

•Axoaxonal: Axon is connected to another neurons axon

•Axodendritic: Axon is connected to another neurons dendrites

•Axosomatic: Axon is connected directly to another neurons soma

•In neuromuscular junctions, axons synapse directly on muscles

2.1.5 Synapse

A synapse is the site where the axon of neuron communicates with effectors or other neurons (Figure 2.3). Depending on the type of neurotransmitter and postsynaptic receptor involved, the transmitter will either have an excitatory effect or inhibitory effect on the postsynaptic membrane. Since the postsynaptic membrane normally does not release neurotransmitters, nerve impulses can pass the synapse in one direction only. The synapse therefore acts like a valve that ensures the orderly transmission of signals. Synapses are also the sites at which neuronal signal transmissions can be modified by other (excitatory or inhibitory) neurons.

Action potential arriving at the presynaptic terminal cause voltage-gated calcium ion channel to open. Calcium ions Ca^{2+} diffuse into the cell and cause synaptic vesicles to release acetylcholine, a neurotransmitter molecule. Acetylcholine molecules diffuse from the presynaptic terminal across the synaptic cleft and bind to their receptor sites on the ligand-gated sodium ions Na^{+} channels. This causes the ligand-gated sodium ion channels to open and sodium ions diffuse into the cell, making the membrane potential more positive. If the membrane potential reaches threshold level, an action potential will be produced. (Figure 2.3)

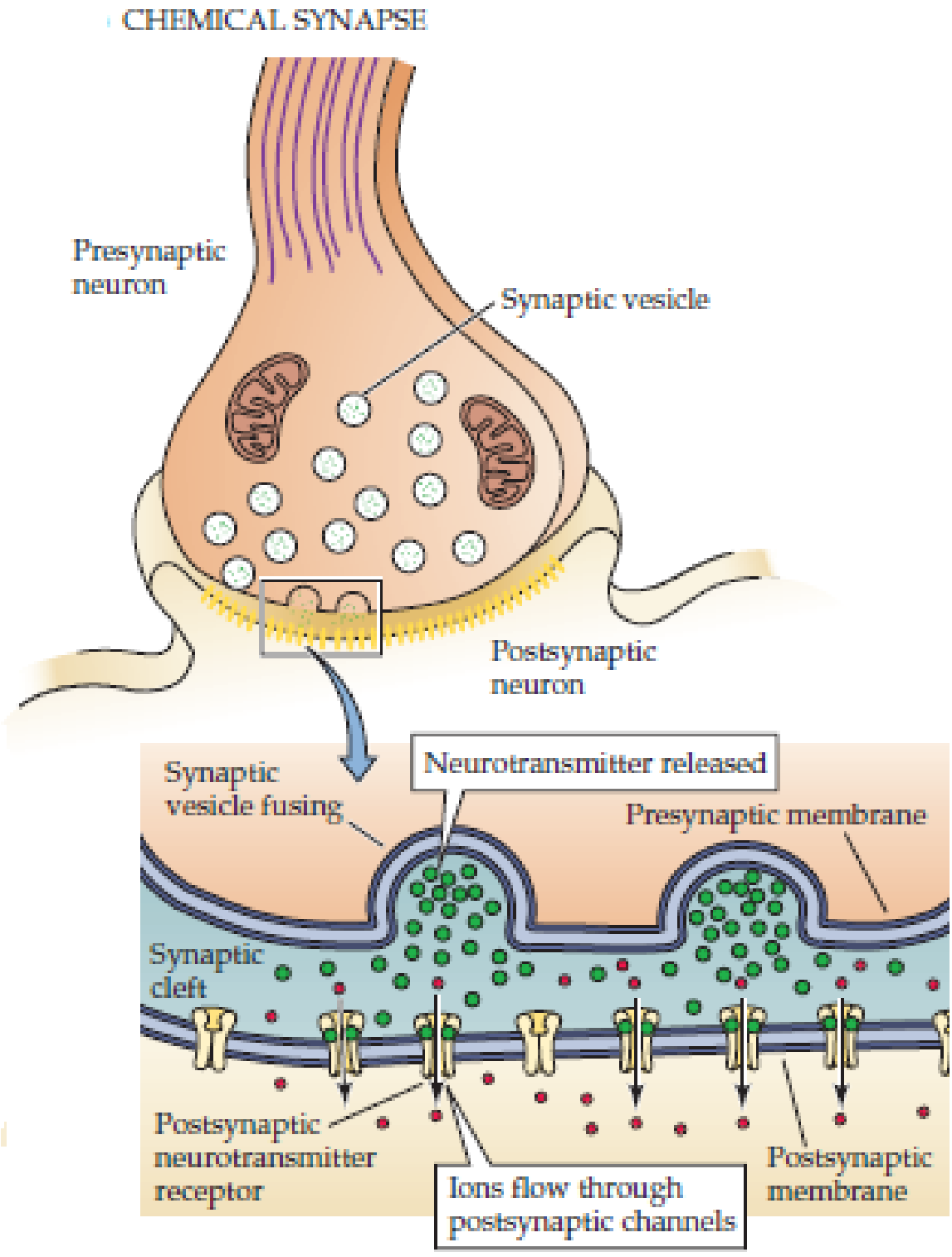

Figure 2.3: Chemical Synapse (Purves 2004)

2.2 Types of Neurons

There are many types of neurons considering their morphometric features. Neurons can be distinguished concerning their structural and functional differences which are includes in following sections. Neurons have different shapes:

(a) Unipolar: Has only one process extending from the soma, branching into dendrites or axon terminals (typical of invertebrate animals)

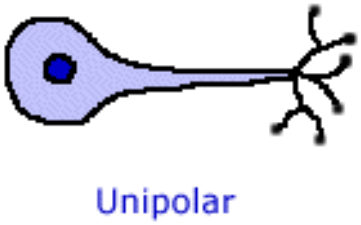

Figure 2.4: Unipolar Neuron Shape `http://www.columbia.edu/cu/psychology/courses/1010/mangels/neuro/neurocells/neurocells.html`

(b) Bipolar: The neuron, it has one input process from dendrites and one output process to dendrites (typical of sensory neurons: visual, auditory, olfactory)

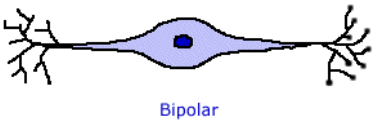

Figure 2.5: Bipolar Neuron Shape `http://www.columbia.edu/cu/psychology/courses/1010/mangels/neuro/neurocells/neurocells.html`

(c) Multipolar: One axon but many dendrites extending directly from the soma (used for motor and sensory processing). This is the prototypical neuron

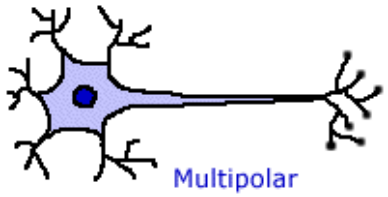

Figure 2.6: Multipolar Neuron Shape `http://www.columbia.edu/cu/psychology/courses/1010/mangels/neuro/neurocells/neurocells.html`

(d) Pseudounipolar: Were originally bipolar, but the dendrites and axon extensions have fused (typical of the dorsal root ganglia in the spinal cord)

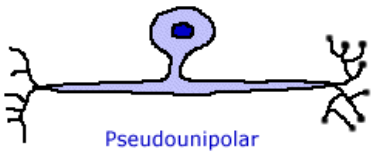

Figure 2.7: Pseudounipolar Neuron Shape `http://www.columbia.edu/cu/psychology/courses/1010/mangels/neuro/neurocells/neurocells.html`

2.2.1 Functional classification of Neurons

There are three major classes of neurons:

Sensory neurons- these run from the various types of stimulus receptors(touch, odor, taste, sound, vision) to the central nervous system (CNS), the brain and spinal cord.

Motor neurons - these transmit impulses from the central nervous system to the muscles and glands that carry out response. Most motor neurons are stimulated by interneurons, although some are stimulated directly by sensory neurons.

Interneurons- these are found exclusively within the spinal cord and brain. They are stimulated by signals reaching them from sensory neurons, other interneurons or both. Interneurons

are also called association neurons.

Concerning the action two types of neurons can be distinguished:

Excitatory neurons - they excite their target neurons through excitatory neurotransmitters.

Inhibitory neurons- they are often interneurons which inhibit their target neurons.

2.2.2 Nervous System

The **central nervous system (CNS)** consists of the spinal cord and brain. These complex organs include not only neural tissue, but also blood vessels and the various connective tissues that provide physical protection and support. The CNS is responsible for integrating, processing, and coordinating sensory data and motor commands. Sensory data convey information about conditions inside or outside the body.

The **peripheral nervous system (PNS)** includes all the neural tissue outside the CNS. The PNS delivers sensory information to the CNS and carries motor commands to peripheral systems and tissue. Bundles of axons or nerve fibers carry sensory information and motor commands in the PNS. We can divide the PNS into afferent and efferent divisions, each with different functions. The **afferent division** (afferens, to bring to) of the PNS brings sensory information to the CNS from receptors in peripheral tissues and organs. The **efferent division** (effero, to bring out) of the PNS carries motor commands from the CNS to glands, muscles, and adipose tissue. These target organs, which respond by doing something, are called effectors. The efferent division has both somatic and autonomic components.

Neuroglia consists of roughly half of the volume of the nervous system. The organization of neural tissue in the CNS differs from the PNS, because the CNS contains a greater amount of neuroglial cell types. Figure 2.8 shows the major neuroglial populations in the CNS and PNS.

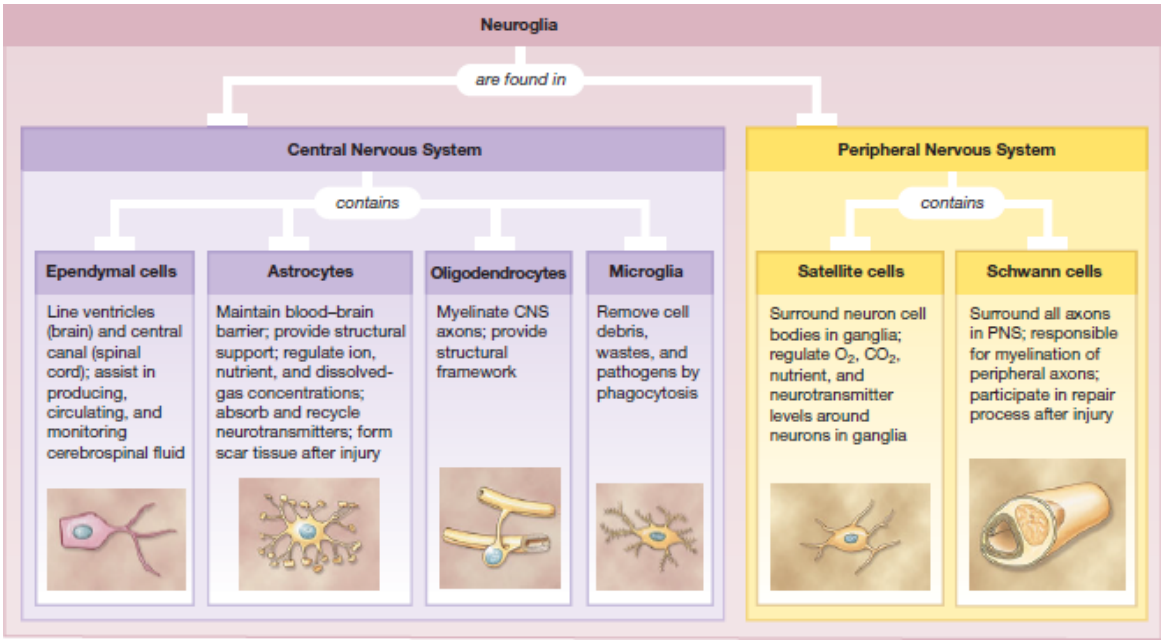

Figure 2.8: The major neuroglial populations (Martini, Nath 2012).

2.3 Passive Electrical Behavior

As it mentioned before, the biological membrane responsible for the signal processing in human nerve cells, i.e., the electrical excitability. Due to the certain structure the membrane has passive and active electrical properties.

2.3.1 Structure of the Biological Membrane

The membrane contains different proteins which differ in their location (Figure 2.9). There are proteins attached to the membrane inside and outside the cell, proteins which are embedded in one lipid layer and the channel proteins which pass the whole membrane and connecting the intracellular space and extracellular space. Some types of ions are able to pass these channels if they are open.

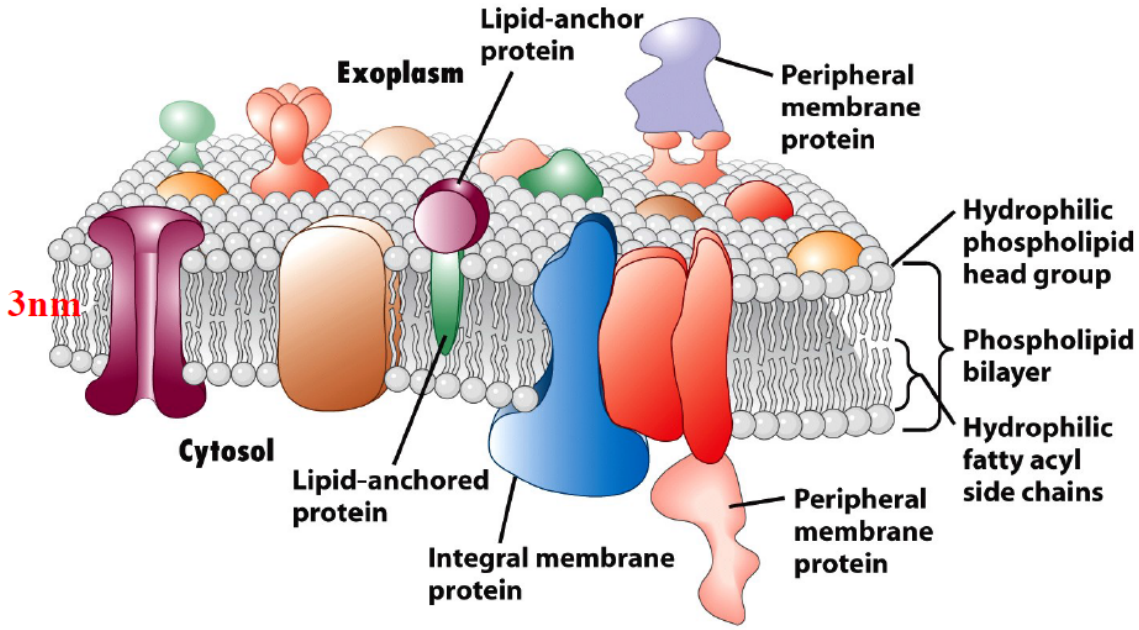

Figure 2.9: Structure of biological membrane (Lodish 2008)

To achieve ion transport, membranes have a variable number of channels (pores) specific for different ion species Na^+,Ca^{2+},K^+,Cl^-, etc.. The conductance of the cell membrane is therefore determined by the type and number of ion channels that are momentarily open. Patch-clamp techniques permit the direct measurement of ionic currents through single ion channels. (Figure. 2.10)

Patch-clamp technique enables to record ionic currents through single channels (Figure 2.10). The first step is lowering the fire-polished tip of a glass recording electrode, 1-5μm in diameter, onto the membrane of the neuron(part a). The applying suction through the electrode tip (part b). A tight seal forms between the walls of the electrode and the patch of membrane. If the electrode is then withdrawn from the cell, the membrane patch can be torn away (part c), and ionic currents can be measured as steady voltages as applied across the membrane (part d). If the patch has a voltage-gated Na^+-channel, then the membrane potential from 65 to 40 mV will cause the channel to open, and current I will flow through it(part e).The amplitude of the measured current at a constant membrane voltage reflects the channel conductance, and the duration of the current reflects the time the channel is open.

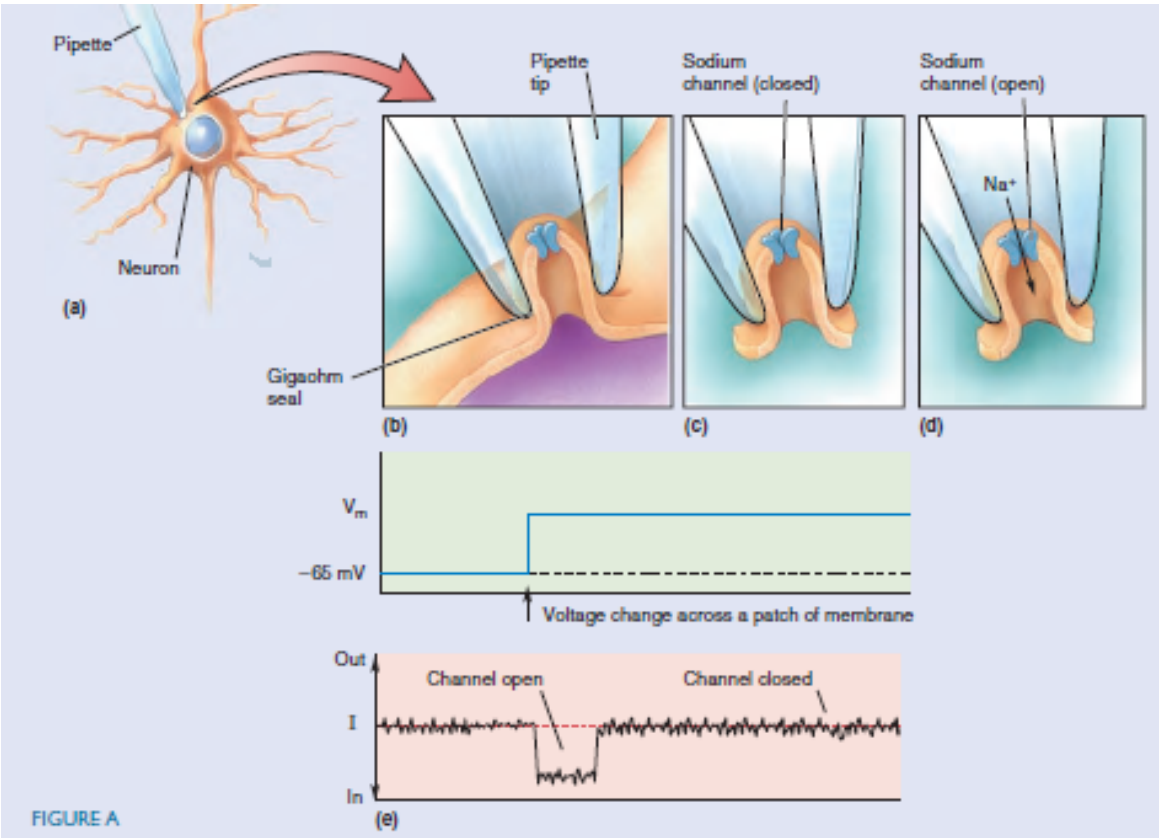

Figure 2.10: Patch-clamp technique (Bear et al. 2007)

2.3.2 Passive State - Equilibrium

The neuronal membrane potential depends on the ionic concentrations on either side of the membrane. The important point is K^+ is more concentrated on the inside, and Na^+ and Ca^{2+} are more concentrated on the outside. Ionic concentration gradients are established by the actions of ion pumps in the neuronal membrane. There two main ion pumps: the *sodium-potassium pump* and *calcium pump*. The sodium-potassium pump is an enzyme that breaks down ATP in the presence of internal Na^+. The chemical energy released by this reaction drives the pump, which exchanges internal Na^+ for external K^+. The actions of this pump ensure that K^+ is concentrated inside the neuron and that Na^+ is concentrated outside the neuron. The pump pushes these ions across the membrane against their concentration gradients. (Figure.2.11).

The calcium pump is also an enzyme that actively transports Ca^{2+} out of cytosol across the cell membrane. Ion pumps are the unsung heroes of cellular neurophysiology. They work in the

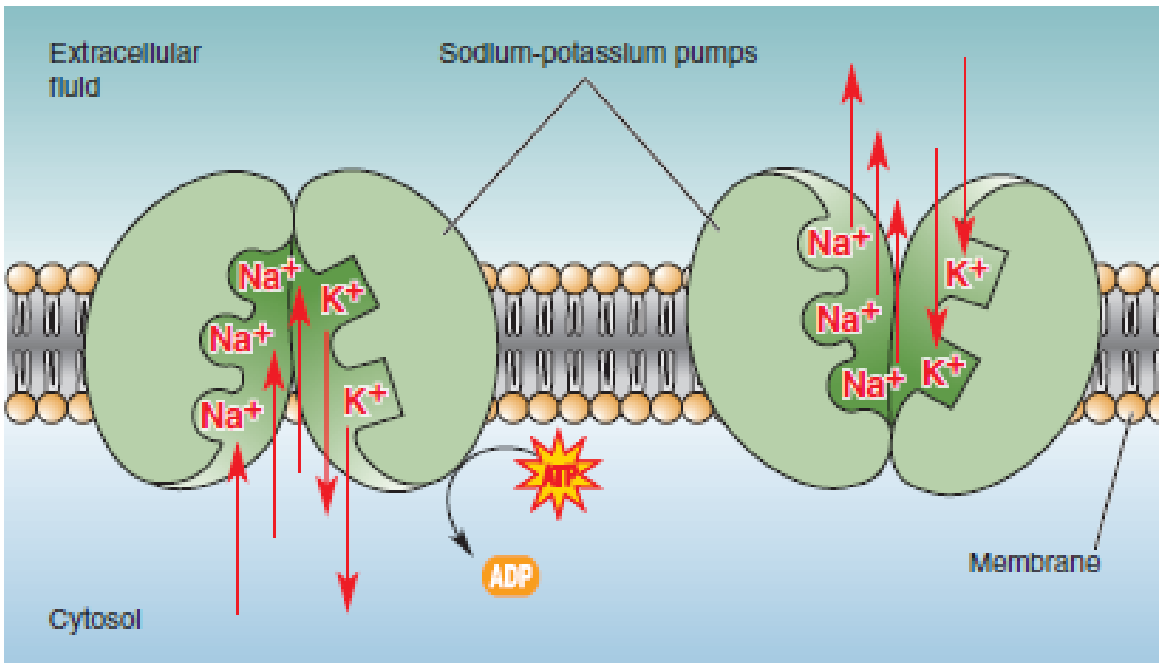

Figure 2.11: Sodium-potassium pump (Bear et al. 2007)

background to ensure that the ionic concentration gradients are established and maintained. These proteins may lack the glamour of a gated ion channel, but without ion pumps, the resting membrane potential would not exist, and the brain would not function.

Ion	Concentration outside (in mM)	Concentration inside (in mM)	Ratio,Out:In	E_{ion},(at 37C)
K^+	5	100	1:20	-80mV
Na^+	150	15	10:1	62mV
Ca^{2+}	2	0.0002	10.000:1	123mV
Cl^-	150	13	11.5:1	-65mV

Table 2.1: The concentration of ions in the cell(Bear et al. 2007)

2.3.3 Nernst and Goldman equations

Each ion has its own equilibrium potential - the steady electrical potential that would be achieved if the membrane were permeable only to that ion. So we can say about potassium equilibrium potential - E_k; sodium equilibrium potential - E_{Na}; the calcium equilibrium potential - E_{Ca} and so on. And knowing the electrical charge of the ion and the concentration difference across the membrane, we can easily deduce whether the inside of the cell would be positive or negative equilibrium. The exact value of an equilibrium potential in V can be calcu-

lated using an equation derived from the principles of physical chemistry - the Nernst equation, which is taken from consideration of the ion charge, the temperature and the ratio of the external and internal ion concentrations. Using the Nernst equation we can calculate the value of the equilibrium potential for any ion. A different internal concentration,c_i, and external ion concentration,c_e, cause the membrane voltage,E_m, when one type of ions is involved:

$$E_m = \frac{RT}{zF} \ln \frac{c_e}{c_i} \tag{2.1}$$

where the gas constant R=8.31441 J/(mol.K); temperature, T, is in Kelvin; z is valence and the Faraday constant represents the charge of one mol of single-valenced ions F=96485 c/mol. At room temperature, the factor $\frac{RT}{F}$ is about 25mV. At body temperature (37C), the Nernst equation for the important ions - K^+, Na^+,Cl^-, and Ca^{2+} - simplifies to :

$$E_k = 61.54mV \log \frac{K_o^+}{K_i^+} \tag{2.2}$$

$$E_{Na} = 61.54mV \log \frac{Na_o^+}{Na_i^+} \tag{2.3}$$

$$E_{Cl} = -61.54mV \log \frac{Cl_o^-}{Cl_i^-} \tag{2.4}$$

$$E_{Ca} = 30.77mV \log \frac{Ca_o^{2+}}{Ca_i^{2+}} \tag{2.5}$$

The Goldman equation defines the steady state membrane voltage $E_m = E_{rest}$ when several ion types are involved. When K^+,Na^+, and Cl^- ions are considered it reads as:

$$E_m = \frac{RT}{F} \ln \frac{P_k[K]_e + P_{Na}[Na]_e + P_{Cl}[Cl]_i}{P_k[K]_i + P_{Na}[Na]_i + P_{Cl}[Cl]_e} \tag{2.6}$$

where $[K]$ is potassium concentration , P_k, P_{Na} and P_{Cl}, are permeabilities measured in centimeters per second (cm/sec). Sodium and potassium are anions, but chloride is cathodic, so,$[Cl]_i$ appears in the numenator in contrast to the anionic concentrations. In the resting state, the membrane is most permeable to potassium ions, and the resting membrane voltage of about -70mV is close to the potassium Nernst potential. The nonlinear conductance of the neural cell membrane depends on different classes of ion channels (Destexhe et al. 1994) and on the activity of ion pumps:

(a) Voltage-dependent gating dominates excitation and neural signal propagation in the axon; open/close kinetics depend on the voltage across the cell membrane.

(b) Calcium-dependent gating occurs mainly at the soma and dendrites; the calcium concentration regulates the opening of the channels as opening depends on intracellular calcium ion binding.

(c) Transmitter gating and second messenger gating occurs at the pre-and postsynaptic membrane.

(d) Ion pumps are membrane molecules that consume energy pump ions across the cell membrane in order to restore the high individual ion concentration on one side of the cell (e.g., high external sodium and high internal potassium concentration).(Rattay et al.2003)

2.4 Active Electrical Behavior

Neurons are electrically excitable cells and therefore able to transmit information through the body. All information is coded in an electrical signal resulting in a change of the membrane potential V_m. The ability of nerve cells to generate and transport these signals so called, Action Potentials (APs), results from the active mechanisms of a membrane.

2.4.1 Action Potential(AP)

The AP is shown on figure 2.12. This graph shows the display of oscilloscope as membrane potential versus time. The AP has its own specific parts. The first part, called *rising phase*,is characterized by a rapid depolarization of the membrane. This change of membrane potential continues until V_m reaches the a peak value of about 40mV. The part of the AP where the inside of the neuron is positively charged with respect to the outside is called the *overshoot*. The next part is *falling phase* is a rapid repolarization until the membrane is actually more negative than the resting potential. The last part is called *undershoot* or *after-hypolarization*. Finally, there is a gradual restoration of the resting potential. From beginning to the end, AP lasts about 2 msec.

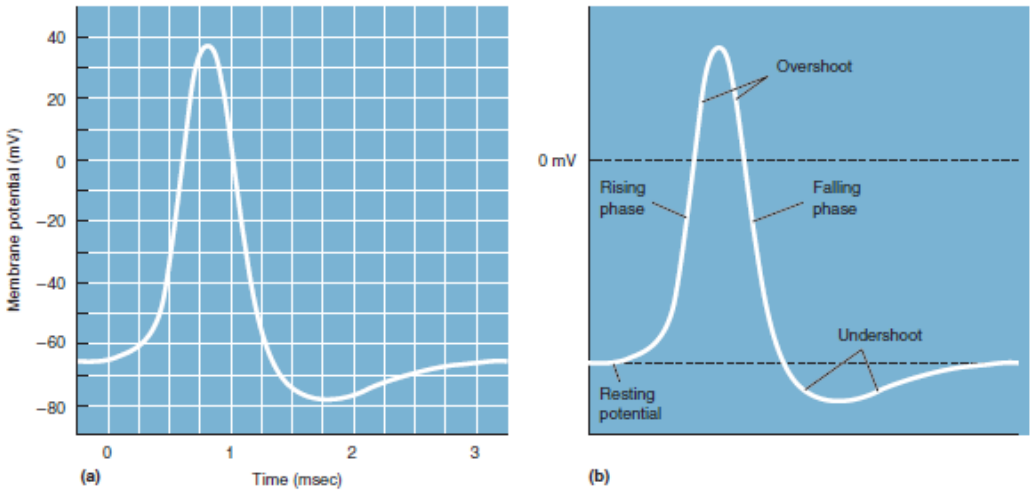

Figure 2.12: a) AP displayed by oscilloscope b) The parts of an AP (Bear et al.2007)

If for example, we pass continuous depolarizing current in a neuron via microelectrode, we will generate not one, but a lot of APs. (Figure 2.13).

Firing frequency increases with the amount of depolarizing current, there is a limit to the rate at which a neuron can generate APs. The maximum firing frequency is about 1000 Hz; once an AP is initiated, it is impossible to initiate another one for about 1ms. This period of time calls the *absolute refractory period* . Deploarization of the cell during the AP is caused by the inflow of Na^+ ions across the membrane, and repolarization is caused by the outflow of K^+ ions. Assume that the both potassium and sodium channels are closed, and the membrane

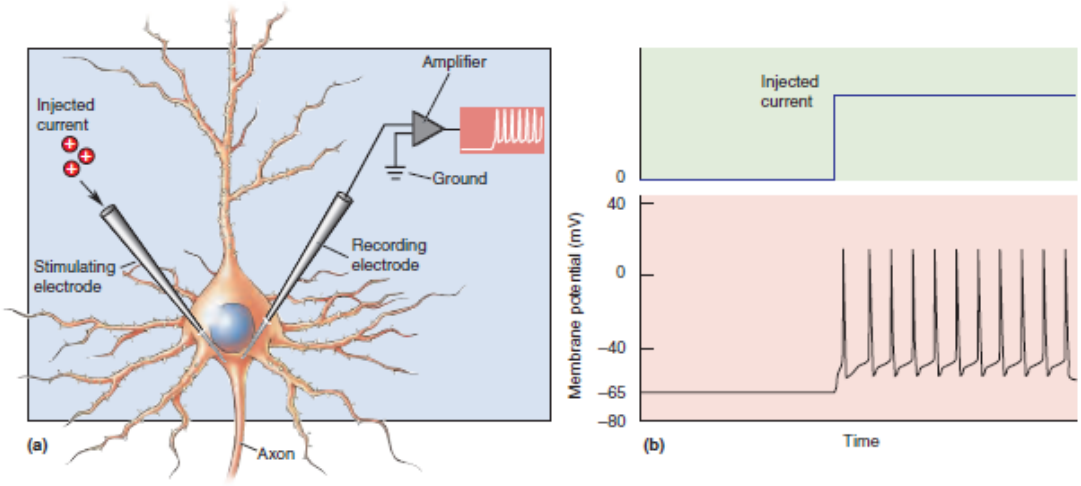

Figure 2.13: The effect of injecting positive charge into a neuron a) Two electrodes are used, one for the recording the membrane potential relative to the ground and the second for the stimulating the neuron with electrical current. b) the depolarization of the membrane to start APs. (Bear et al.2007).

potential V_m is equal to 0mV.Then open the potassium channel , so the K^+ ions will flow out of the cell, until the inside becomes negatively charged, and $V_m = E_k$. Focus our attention on the movement of K^+ that took the membrane potential from 0mV to -80mV. Consider these three points:

(1) The movement of K^+ ions across the membrane is an electrical current. It is possible to represent it as I_k.

(2) The number of open potassium channels are proportional to an electrical conductance. It is possible to represent it as g_k.

(3) Membrane potassium current, I_k, will flow only if $V_m \neq E_k$. The driving force on K^+ is defined as the difference between the real membrane potential - V_m and the equilibrium potential - E_k and can be represented as $V_m - E_k$.

So the relationship between ionic driving force, ionic conductance and amount of ionic current in general way can be written as:

$$I_{ion} = g_{ion}(V_m - E_{ion}) \tag{2.7}$$

When repetitive stimuli are applied the neuron shows refractory behavior, characterized by a rise in the excitation threshold. (Figure 2.14). When the sodium channels are return to activate, open state in the inwardly repolarization phase the neuron is able to be activated by a much stronger current with a resulting smaller depolarization and is said to be relatively refractory. The duration of the whole AP in neuron is about 1ms.

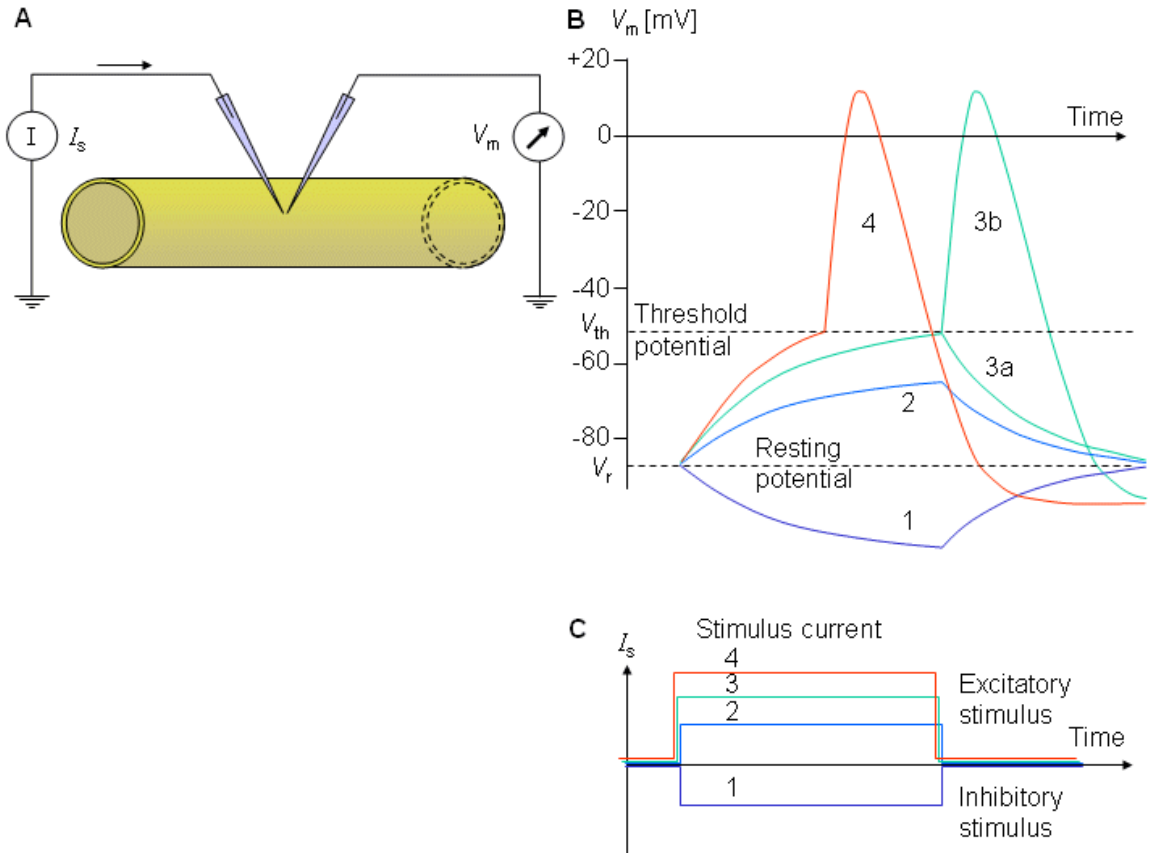

Figure 2.14: (A) All-or-nothing principle with the corresponding states of the ion channels (Hummel and Taylor 2007). Experimental arrangement for measuring the response of the membrane potential (B) to inhibitory (1) and excitatory (2, 3, 4) stimuli (C). The current stimulus (2), while excitatory is, however, subthreshold, and only a passive response is seen. For the excitatory level (3), threshold is marginally reached; the membrane is sometimes activated (3b), whereas at other times only a local response (3a) is seen. For a stimulus (4), which is clearly transthreshold, a nerve impulse is invariably initiated. (Malmivuo, Plonsey 1995)

2.4.2 HH,FH,CRRSS,SE,SRB - Models

'Our object here is to find equations which describe the conductances with reasonable accuracy and are sufficiently simple for theoretical calculation of the action potential and refractory period. For sake of illustration we shall try to provide a physical basis for the equations, but must emphasize that the interpretation given is unlikely to provide a correct picture of the membrane'.(Hodgkin and Huxley, 1952d). It was the first model to describe the ionic basis of excitation correctly. For this work they receive a Nobel Prize in 1963 (Hodgkin and Huxley, 1952a; Hodgkin and Huxley, 1952b; Hodgkin and Huxley, 1952c). They use the parallel conductance model (called also chord conductance model) (Junge 1992) to describe the electric current flowing across the membrane. It consists of 4 main components:

(1) Current carried by sodium ions.

(2) Current carried by potassium ions.

(3) Current carried by other ions(leakage current, constituting mainly chloride ions).

(4) Capacitive(displacement) current.

In this model (Figure.2.15) is the current from inside to outside is considered to be positive.

For this model, the ion permeability for sodium, potassium and leakage currents are written in a form as:

$$G_{Na} = \frac{I_{Na}}{V_m - V_{Na}} \tag{2.8}$$

$$G_K = \frac{I_K}{V_m - V_K} \tag{2.9}$$

$$G_L = \frac{I_L}{V_m - V_L} \tag{2.10}$$

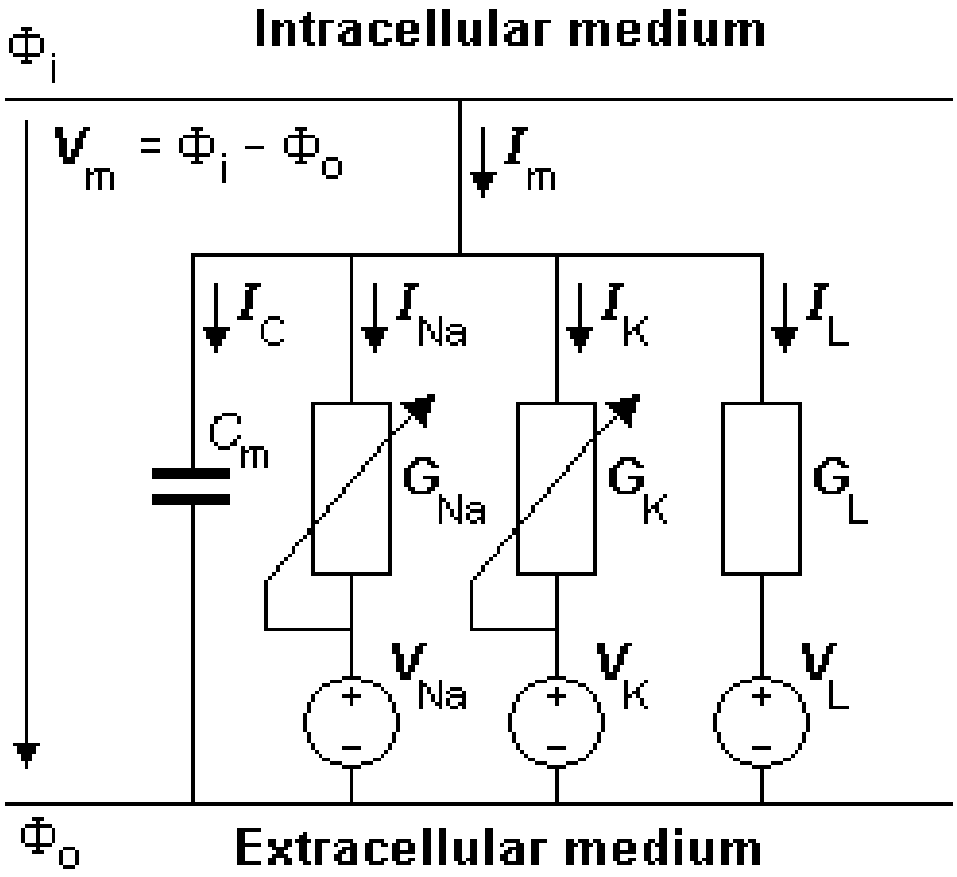

Figure 2.15: The equivalent circuit of the Hodgkin-Huxley model. The voltage sources show the polarity of the positive value. The calculated Nernst voltages of sodium, potassium, and chloride designate the value of corresponding voltage sources. (Malmivuo, Plonsey 1995).

G_{Na}, G_K, G_L - membrane conductance per unit area for sodium, potassium and leakage ions[S/cm^2]

I_{Na}, I_K, I_L - electric current per unit area for sodium, potassium and leakage ions[mA/cm^2]

V_{Na}, V_K, V_L - Nernst voltage for sodium, potassium and leakage ions[mV]

V_m - membrane voltage [mV]

For the HH-model, the expression for the total transmembrane current density is the sum of the capacitive and ionic components. The equation has the form:

$$I_m = C_m \frac{dV_m}{dt} + (V_m - V_{Na})G_{Na} + (V_m - V_K)G_K + (V_m - V_L)G_L \tag{2.11}$$

where,

I_m - membrane current per unit area[mA/cm^2]

C_m - membrane capacitance per unit area[F/cm^2]

V_m - membrane voltage[mV]

V_{Na}, V_K, V_L - Nernst voltage for sodium, potassium and leakage ions [mV]

G_{Na}, G_K, G_L - sodium, potassium, and leakage conductance per unit area [S/cm^2]

2.4.3 Sodium conductance

$$m \underset{\alpha_m}{\overset{\beta_m}{\longleftrightarrow}} (1-m) \tag{2.12}$$

An equation for the behavior of sodium activation may be written, namely that m satisfies a first-order process:

$$\frac{dm}{dt} = \alpha_m(1-m) - \beta_m m \tag{2.13}$$

The potassium conductance per unit area is then the conductance of a single channel times the number of open channels. Alternatively, if G_{Na} max is the conductance per unit area when they are occupied simultaneously by three activating m-particles and not blocked by an inactivating h-particle:

$$G_{Na} = G_{Na\,\max} m^3 h \tag{2.14}$$

2.4.4 Potassium conductance

$$n \underset{\alpha_n}{\overset{\beta_n}{\longleftrightarrow}} (1-n) \tag{2.15}$$

An equation for the behavior of potassium activation may be written in the same manner as for the sodium, namely that m satisfies a first-order process:

$$\frac{dn}{dt} = \alpha_n(1-n) - \beta_n n \tag{2.16}$$

The potassium conductance per unit area is then the conductance of a single channel times the number of open channels. Alternatively, if G_{Kmax} is the conductance per unit area when all channels are open, then if only the fraction n^4 are open, we have:

$$G_K = G_{K\,\max} n^4 \tag{2.17}$$

2.4.5 Inactivating h-particle

The parameter h represents the probability that an h-particle is in the non-inactivating (i.e., open) state. Thus $(1-h)$ represents the number of the h-particles in the inactivating (i.e., closed). The movement of these particles is also governed by first-order kinetics: The parameter h represents the probability that an h-particle is in the non-inactivating (i.e., open) state. Thus $(1-h)$ represents the number of the h-particles in the inactivating (i.e., closed). The movement of these particles is also governed by first-order kinetics:

$$1 - h \underset{\beta_h}{\overset{\alpha_h}{\longleftrightarrow}} h \tag{2.18}$$

$$\frac{dh}{dt} = \alpha_h(1-h) - \beta_n h \tag{2.19}$$

The leakage conductance is assumed to stay constant:

$$G_L = \text{constant} \tag{2.20}$$

In 1964, Frankenhaeuser and Huxley developed a model for the myelinated frog axon node (FH model) assuming HH-like gating mechanisms, but they derived the ion current formulation from the Nernst-Planck equation and added a nonspecific current density i_p (Frankenhaeuser 1964):

$$\frac{dV}{dt} = [-i_{Na} - i_K - i_p - i_L + i_{stimulus}]/C \tag{2.21}$$

$$i_{Na} = P_{Na} m^2 h \frac{EF^2}{RT} \frac{[Na]_o - [Na]_i \exp(EF/RT)}{1 - \exp(EF/RT)} \tag{2.22}$$

$$i_k = P_k n^2 \frac{EF^2}{RT} \frac{[K]_o - [K]_i \exp(EF/RT)}{1 - \exp(EF/RT)} \tag{2.23}$$

$$i_p = P_p p^2 \frac{EF^2}{RT} \frac{[Na]_o - [Na]_i \exp(EF/RT)}{1 - \exp(EF/RT)} \tag{2.24}$$

$$i_L = g_L(V - V_L) \tag{2.25}$$

$$\frac{dm}{dt} = -(\alpha_m + \beta_m)m + \alpha_m \tag{2.26}$$

$$\frac{dn}{dt} = -(\alpha_n + \beta_n)n + \alpha_n \tag{2.27}$$

$$\frac{dh}{dt} = -(\alpha_h + \beta_h)h + \alpha_h \tag{2.28}$$

$$\frac{dp}{dt} = -(\alpha_p + \beta_p)p + \alpha_p \tag{2.29}$$

$$\tag{2.30}$$

Sodium current plays the dominant role in the action potential of the mammalian node of Ranvier, and in contrast to the axon model of squid and frog there are almost no potassium currents (Horackova et al. 1968; Chiu et al. 1979; Schwarz and Eikof 1987). The CRRSS model, named after Chiu, Ritchie, Rogert, Stagg, and Sweeney, describes a myelinated rabbit nerve node extrapolated from orginal 14 °C data to 37 °C (Chiu et al. 1979; Sweeney et al. 1987):

$$\frac{dV}{dt} = [-g_{Na}m^2h(V - V_{Na}) - g_L(V - V_L) + i_{stimulus}]/C \tag{2.31}$$
$$\frac{dm}{dt} = [-(\alpha_m + \beta_m)m + \alpha_m]^k \tag{2.32}$$
$$k = 3^{0.1T-3.7} \tag{2.33}$$
$$\frac{dh}{dt} = -(\alpha_h + \beta_h)h + \alpha_h \tag{2.34}$$
$$\tag{2.35}$$

Schwarz and Eikhof obtained a model of FH type from voltage clamp experiments on rat nodes (Schwarz and Eikhof 1987). From the original data, the Schwarz-Eikhof (SE) model results by assuming a nodal area of 50 μm^2 (Rattay 1990; Rattay 1993):

$$\frac{dV}{dt} = [-i_{Na} - i_K - i_L + i_{stimulus}]/C \tag{2.36}$$
$$i_{Na} = P_{Na}m^3h\frac{EF^2}{RT}\frac{[Na]_o - [Na]_i \exp(EF/RT)}{1 - \exp(EF/RT)} \tag{2.37}$$
$$i_L = g_L(V - V_L) \tag{2.38}$$
$$E = V + V_{rest} \tag{2.39}$$
$$\frac{dm}{dt} = -(\alpha_m + \beta_m)m + \alpha_m \tag{2.40}$$
$$\frac{dn}{dt} = -(\alpha_n + \beta_n)n + \alpha_n \tag{2.41}$$
$$\frac{dh}{dt} = -(\alpha_h + \beta_h)h + \alpha_h \tag{2.42}$$
$$\frac{dp}{dt} = -(\alpha_p + \beta_p)p + \alpha_p \tag{2.43}$$
$$\tag{2.44}$$

(Schwarz et al. 1995) derived the SRB model from human nerve fibers at room temperature. Single-action potentials are little effected by removing the fast or slow potassium currents, but a slow K conductance was required to limit the repetitive response of the model to prolonged

stimulating currents. SRB model follows and they were the first to develop a model of a human nerve fiber, including the nodes of Ranvier also for a temperature of T=37 °C:

$$\frac{dV}{dt} = [-i_{Na} - i_{K,fast} - i_{K,slow} - i_L + i_{stimulus}]/C \tag{2.45}$$

$$i_{Na} = P_{Na} m^2 h \frac{EF^2}{RT} \frac{[Na]_o - [Na]_i \exp(EF/RT)}{1 - \exp(EF/RT)} \tag{2.46}$$

$$i_{k,fast} = g_k n^4 (V - V_k) \tag{2.47}$$

$$i_{k,slow} = g_{k,slow} p (V - V_k) \tag{2.48}$$

$$i_L = g_L (V - V_L) \tag{2.49}$$

$$E = V + V_{rest} \tag{2.50}$$

$$\frac{dm}{dt} = -(\alpha_m + \beta_m) m + \alpha_m \tag{2.51}$$

$$\frac{dn}{dt} = -(\alpha_n + \beta_n) n + \alpha_n \tag{2.52}$$

$$\frac{dh}{dt} = -(\alpha_h + \beta_h) h + \alpha_h \tag{2.53}$$

$$\frac{dp}{dt} = -(\alpha_p + \beta_p) p + \alpha_p \tag{2.54}$$

$$\tag{2.55}$$

The dendrite and especially the soma region is more difficult to simulate because a variety of ion channel types are involved. Some membrane models are available (Beluzzi et al 1991; Winslow et al. 1991; McCormick et al. 1992; Traub et al. 1994; DeSchutter et al. 1999; Fohlmeister et al. 1997a; Fohlmeister et al. 1997b), but even in these models we cannot rely on a precise individual measurement of all the ion components that vary in channel density and open/close kinetics. (Rattay et al.2003).

Chapter 3

The Human Ear

The human ear is divided into three sections, the outer, middle and inner ear and plays an important role in hearing.

The outer ear consists of the pinna (auricle) that leads into the external auditory canal. It collects sound waves from a wide area and funnels the sound into the external ear passage. On the inside surface of the outer ear is the tympanic membrane (eardrum). It is stretched across the end of the auditory canal separating the outer ear from the middle ear.

The middle ear consists of small bones called ossicles. They are the malleus (hammer), the incus (anvil) and the stapes (stirrup). They transfer sound waves to the inner ear. Located covering an opening into the inner ear is called the oval window. Below is another membrane called the round window that stretches across the opening and adjoins the cochlea in the inner ear.

The inner ear comprises a coiled structure called the cochlea. The snail-like spiral coiled tube contains the receptors for sound and the vestibular apparatus that is associated with a sense of balance. The cochlear duct contains the organ of Corti, which contains auditory receptor cells. The auditory nerve transmits sound vibrations to the brain.

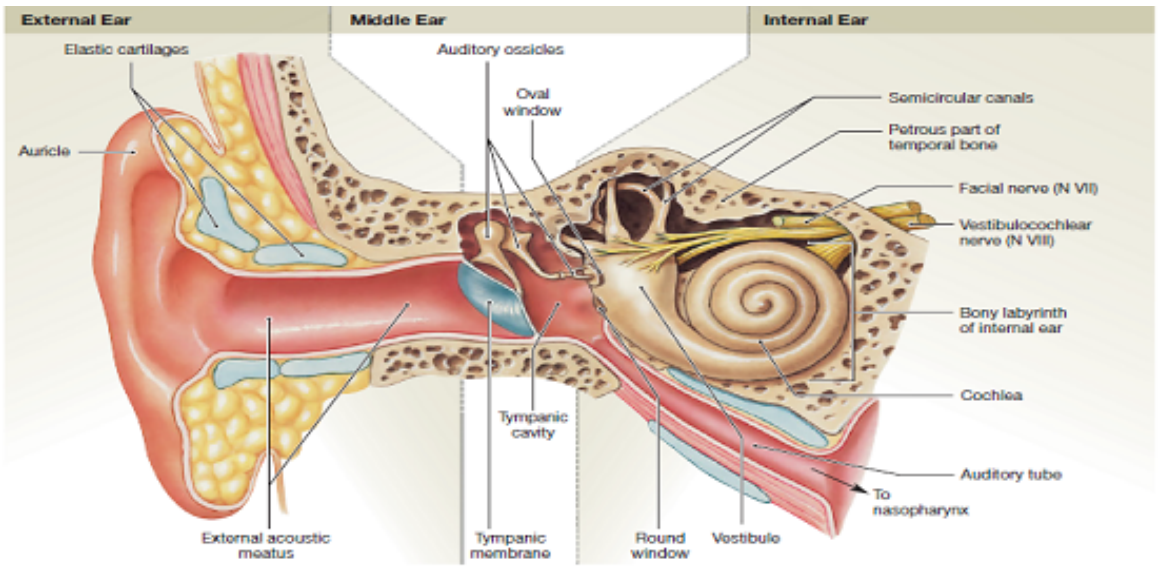

Figure 3.1: Anatomy of the Ear: The boundaries separating the three anatomical regions of the ear(external, middle and inner) are indicated by the dashed lines. (Martini, Nath 2011)

3.1 The Inner Ear

The senses of equilibrium and hearing are provided by receptors in the inner ear (Figure 2).

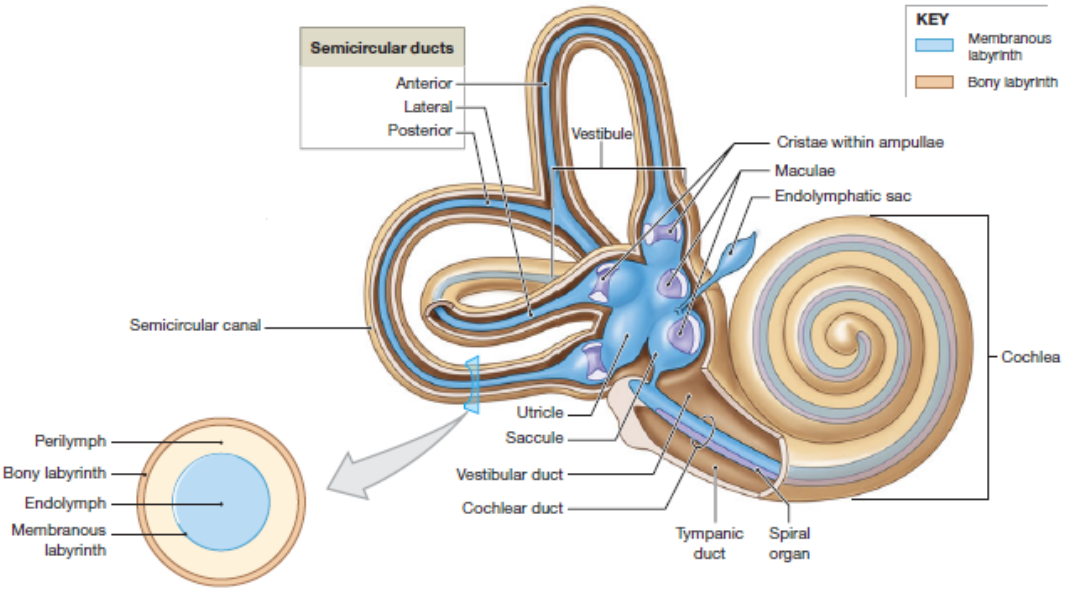

Figure 3.2: The Inner Ear. The bony and membranous labyrinths. (Martini, Nath 2011)

The superficial contours of the internal ear are formed by *bony labyrinth* - layer of dense bone. The inner contours of the bony labyrinth closely follow the contours of the *membranous labyrinth* - interconnected network of fluid-filled tubes. The receptors of the internal ear are found in these tubes. Between the bony and membranous labyrinths flows liquid that closely resembles cerebrospinal fluid - *perilymph*. The membranous labyrinth contains fluid with electrolyte concentrations different from those of typical body fluids - *endolymph*. The bony labyrinth can be divided into the *vestibule*, three semicircular canals, and the cochlea. The vestibule consists of a pair of membranous sacs: *the saccule* and *the utricle*. Receptors in the saccule and utricle provide sensations of gravity and linear acceleration. *The semicircular canals* enclose slender semicircular ducts. Receptors in the semicircular ducts are stimulated by rotation of the head. The combination of vestibule and semicircular canals is called the vestibular complex. The fluid-filled chambers within the vestibule are continuous with those of the semicircular canals.

3.2 Cochlea, Organ of Corti

The *cochlea* is a spiral shaped, bony chamber that contains the *cochlear duct* of the membranous labyrinth. Receptors within the cochlear duct provide the sense of hearing. The duct is sandwiched between a pair of perilymph-filled chambers. The entire complex makes turns around a central bony hub, much like a snail shell. The walls of the bony labyrinth consist of dense bone everywhere except at two small areas near the base of the cochlear spiral (Figure 3.3). *The round window* is a thin, membranous partition that separates the perilymph of the cochlear chambers from the air-filled middle ear. Collagen fibers connect the bony margins of the opening known as the oval window to the base of the stapes.

The Cochlea contains several fluid-filled compartments . Two of them (*scala tympani* and *scala vestibuli* are considered to be continuous) are filled with a high-sodium solution - perilymph, and another is filled with high potassium solution - endolymph. So the term ‘cochlear duct‘’ labels a compartment bounded by including Reissner‘s membrane, the spiral ligament, the stria vascularis, the basilar membrane (BM), and the spiral limbus. The scala vestibuli (SV) is separated from the scala media (SM) by Reissner‘s membrane, a thin epithelial sheet consisting of

two cell layers. Reissner's membrane is separate the fluids in the SV and ST . Typical fluids filling extracellular spaces in the body are perilymph, which is basically dilute NaCl solution, but with a low K^+ concentration. In contrast, the fluid in SM, called endolymph, has a high K^+ concentration with low Na^+ and Ca^{2+} concentrations. The endolymph is generated in the stria vascularis, a specilized epithelium in the lateral wall of the SM by a complex multicellular active transport system (Wangemann, Schacht 1996).

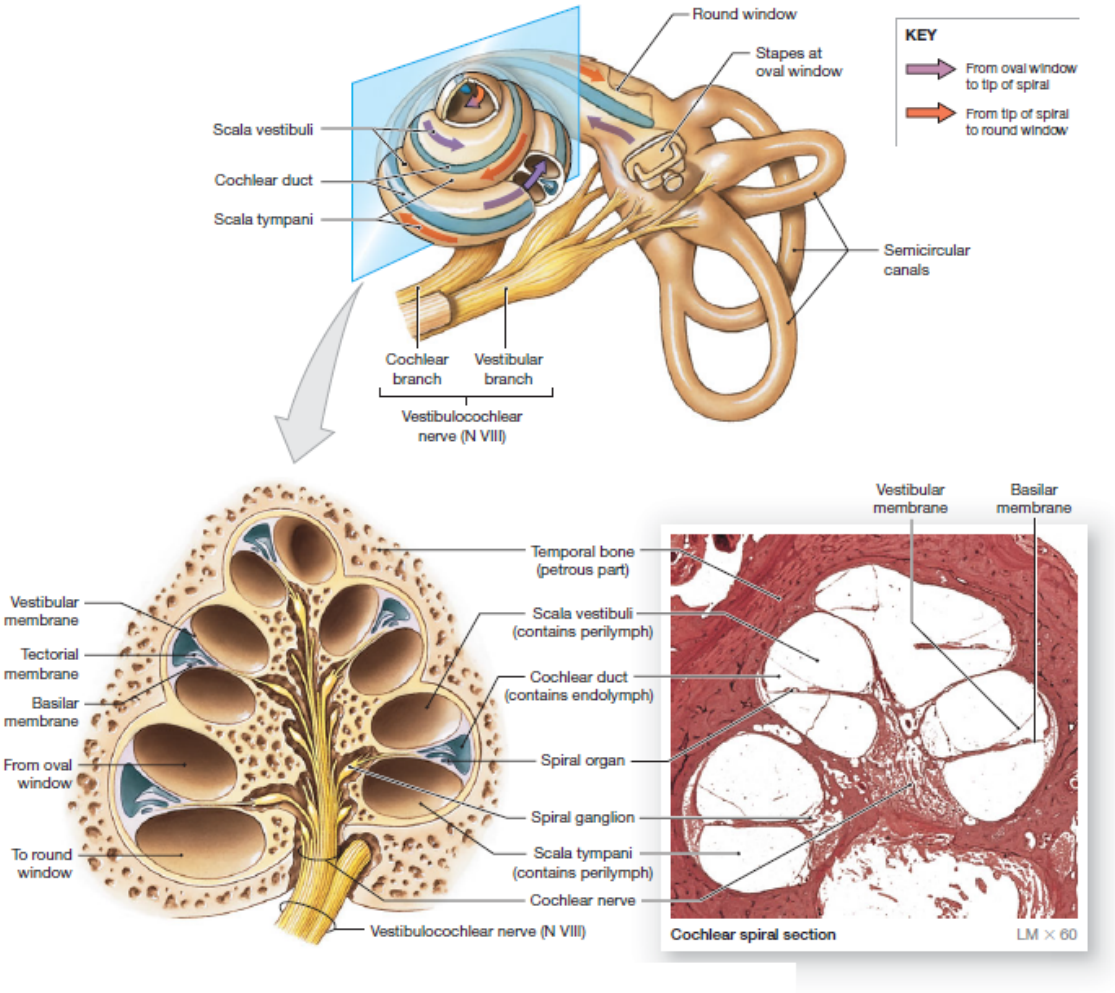

Figure 3.3: Cross section of Cochlea (Martini, Nath 2011)

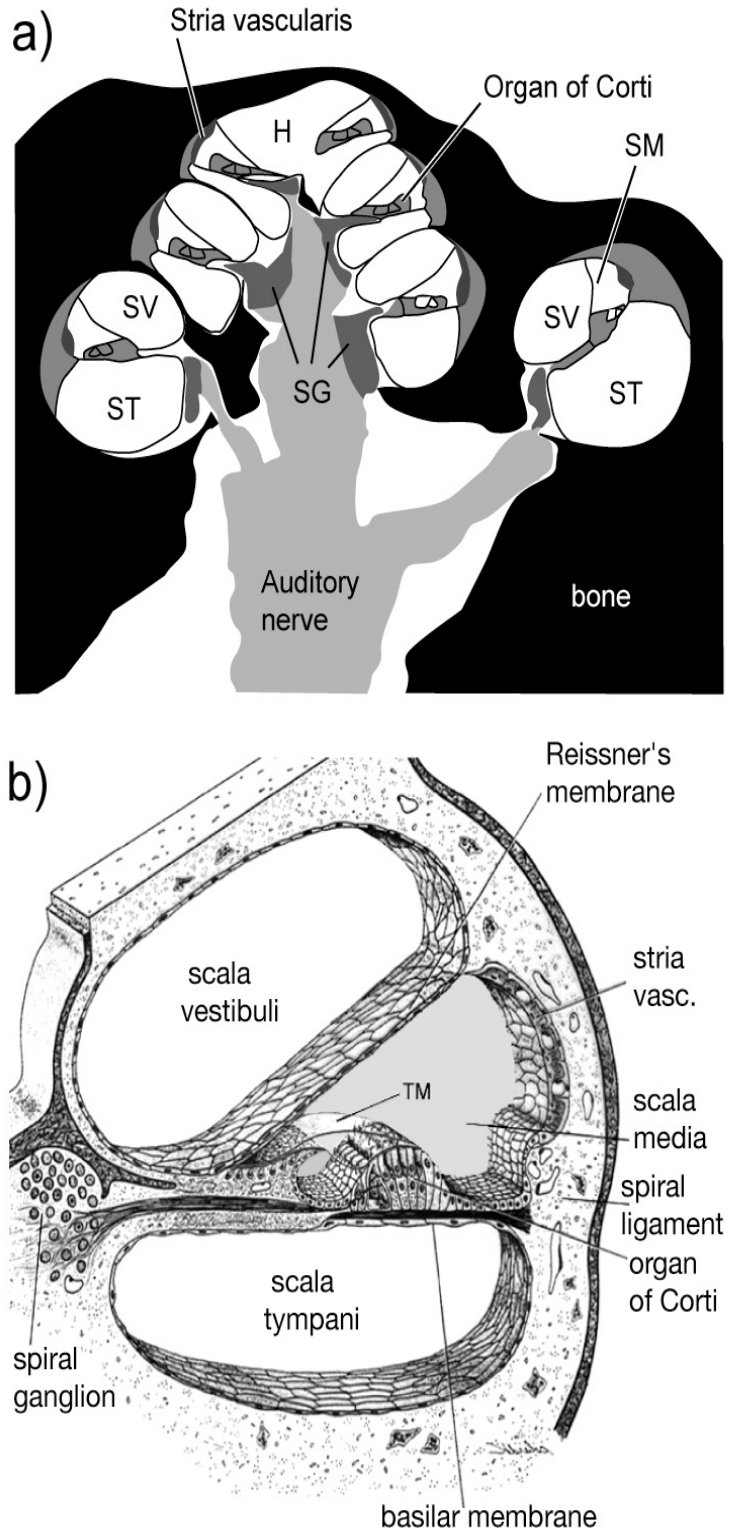

Figure 3.4: a) Sketch of a cross section of cochlea, cut through the center of the coil. The cochlear spirals are cut in cross section, shown at higher resolution in b. b) Cross section of the cochlear spiral showing the three scalae. The scalae are fluid-filled; the SV and ST contain perilymph. The SM contains endolymph which is shaded (Bloom, Fawcett 1975)

3.3 The organ of Corti and auditory hair cells

The hair cells of the cochlear duct are located in a structure called the spiral organ (organ of Corti) (Figure 3.5, 3.6). This sensory structure sits on the basilar membrane, a membrane that separates the cochlear duct from the scala tympani. The hair cells are arranged in a series of longitudinal rows. They lack kinocilia, and their stereocilia are in contact with the overlying *tectorial membrane*. This membrane is firmly attached to the inner wall of the cochlear duct. When a portion of the basilar membrane bounces up and down, the stereocilia of the hair cells are pressed against the tectorial membrane and become distorted. The basilar membrane moves in response to pressure fluctuations within the perilymph. These pressure changes are triggered by sound waves arriving at the tympanic membrane.

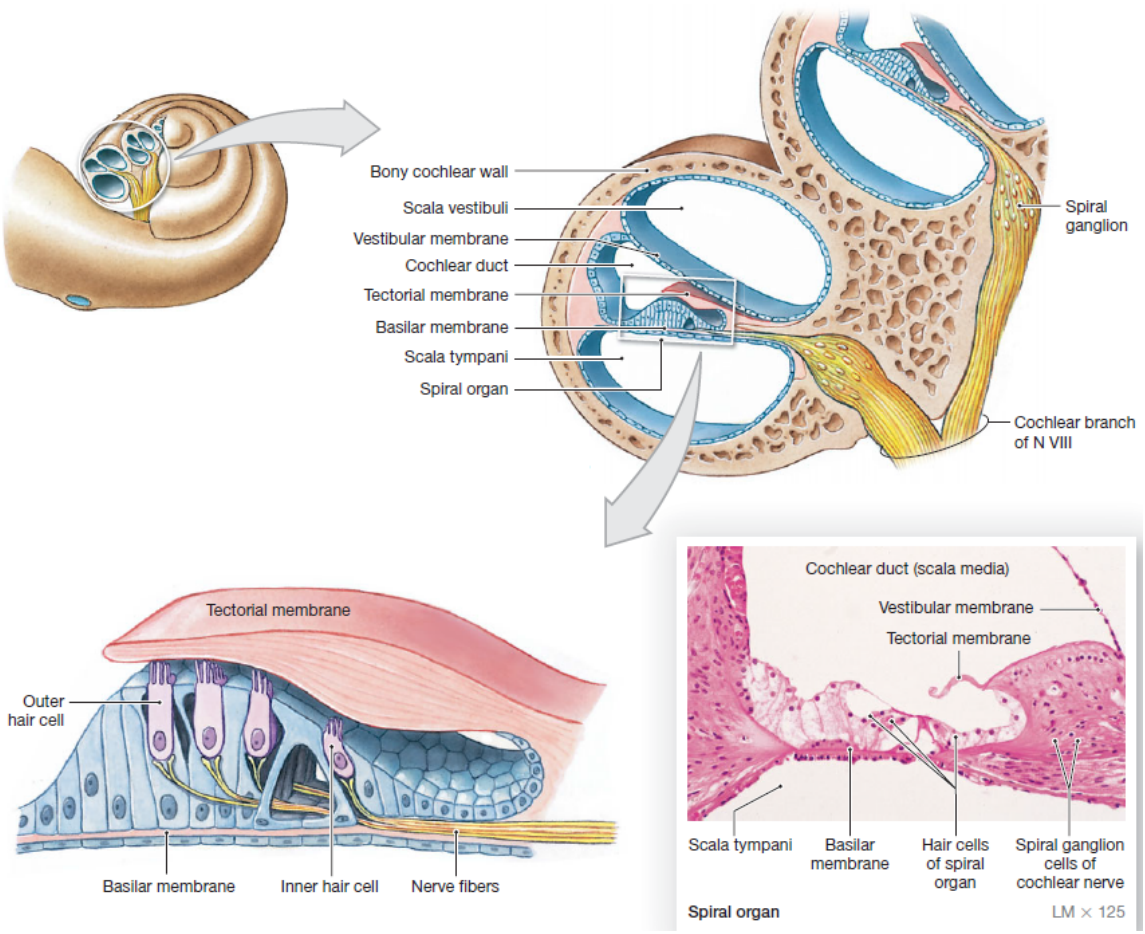

Figure 3.5: Organ of Corti and auditory hair cells (Martini, Nath 2011)

The two types of sensory cells in the organ of Corti are differ in shape and number but have the same functions. With ultrastructural studies on the sensory and supporting cells (Engström

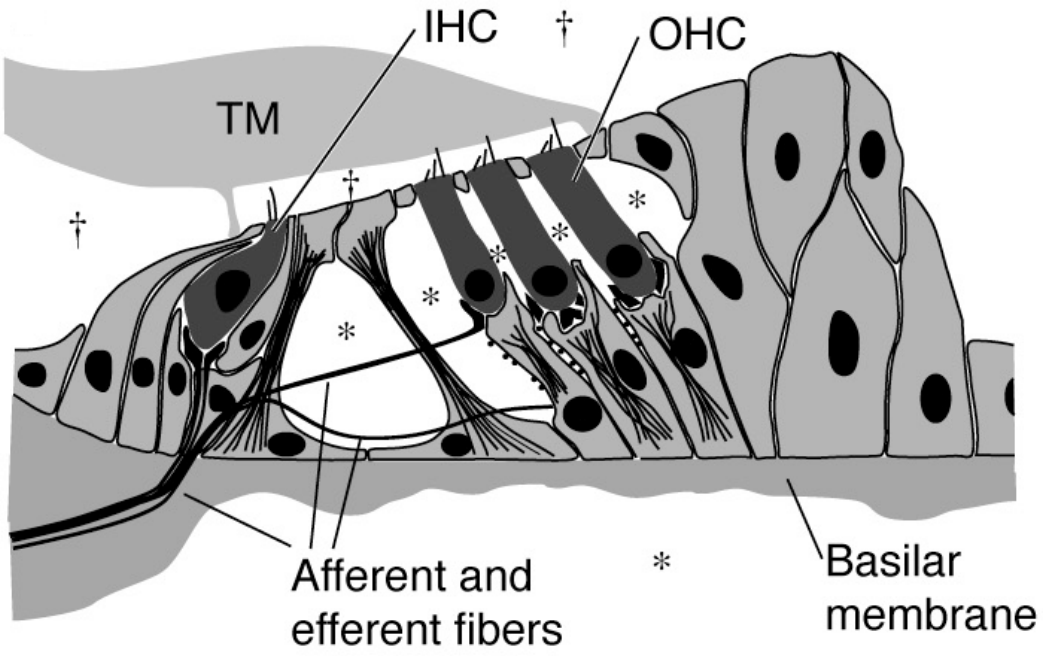

Figure 3.6: Schemtic view of Organ of Corti showing IHC and OHC and several kinds of supporting cells. The spaces with perilymph are marked with (*) and the spaces with endolymph with (†). TM - tectorial membrane, lays on the Organ of Corti (Young 2007)

1958; Kimura 1966; Angelborg and Engström 1973; Lim 1986) and on the innervation (Engström 1958; Smith and Sjostrand 1961a; Spoendlin 1973), it become evident that these two cell types differ dramatically. IHCs play a primarily sensory role in the cochlea, based on the fact that most of the afferent nerve fibers synapse with them. OHCs, although providing some direct sensory input to the central nervous system, more likely modify the mechanical properties of the organ of Corti and the BM.

3.4 Hair Cells

The transduction of basilar-membrane motion into electrical signals goes in IHCs. The OHCs plays in generation of sensitive and sharply-tuned basilar-membrane motion. In this section the review about IHCs and OHCs are presented. Useful literature are available (Dallos Fakler 2002; Eatock Hurley 2003; Fettiplace Hackney 2006; LeMasurier Gillespie 2005).

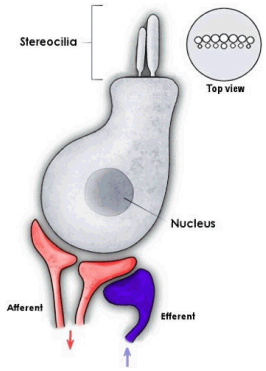

Figure 3.7: The structure of IHC http://www.nano.susx.ac.uk/research/hair-cell.org/Alan_Owen/EDUCATIONPAGE/Education_files/Cochlea_files/Cochlear_cells/CochlearCells_frame.htm

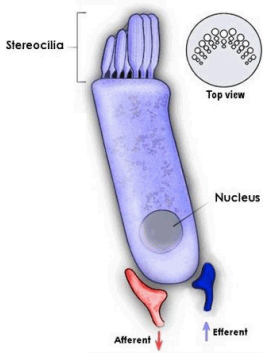

Figure 3.8: The structure of OHC

3.4.1 Inner Hair Cell(IHC)

IHCs are goblet-shaped with a centrally placed nucleus (Figure 3.7) and form on continuous row along the length of the spiraling sensory epithelium. Each IHC has stereocilia arranged in a characteristic flattened "U" shape on its apical surface. The IHC body is filled with round mitochondria, Golgi apparatus multivesicular bodies, lysosomes, and well-developed endoplasmatic reticulum. Lining the plasma membrane by cross-links or pillars (Forge 1987; Furness and Hackley 1990). **The inner hair cells** signal information about the stimulating sound to the brain. There are approximately 3000 inner hair cells which have a pear or flask shape. They mostly send afferent information to the brain via the eights cranial nerve. The IHC are heavily innervated by the afferent fibers that form the auditory nerve, and their main function is to signal the presence of sound to the central nervous system (Spoendlin 1967).

3.4.2 Outer Hair Cell(OHC)

OHCs are long and cylindrical with a more basally placed nucleus. OHCs have a smaller diameter than IHCs, and there are almost four times as many OHCs as IHCs. At the apical surface, the OHCs contact supporting cells with tight junctions and link to them with adherens junctions. Their basal surface is cupped by adjacent supporting cells, but unlike IHCs, in most species they contact only fluid along their lateral surface. (Fay, Popper 1996) . The OHC stereocilia are arranged in a 'W' and although graduated in length, they are longer and thinner than their IHC counter-parts. In most species, they are arranged in three parallel rows; however, some species contain four or five rows (Kimura 1966; Raphael et al. 1991). **The outer hair cell**s are motile, contracting as they depolarise in response to mechanical stimuli. There are approximately 12000 outer hair cells. They have the appearance of test tubes and mostly receive efferent information from the brain. Not only do they react to information received from the brain, but they also receive 'chemical messages' from inside the cochlea which tell them either elongate or to shrink. The OHC receive relatively little afferent innervation, but are the targets of numerous efferent nerve fibers that run from the brainstem to the organ of Corti (Guinan 1996). The main function of the OHCs appears to be to select, amplify, and compress the acoustical signals that actually reach the IHCs. They do this by affecting the mechanics of the cochlear partition.

3.4.3 Type I and type II neurons

The AN fibers lays in the center of the cochlear coil (Figure 3.4a). Spiral ganglion cells have two processes: a distal process that invades the organ of Corti and innervates one IHC and a central process, that travels in the AN to the brain. The arrangement of nerve fibers in the cochlea is shown on Figure 3.9 (Ryugo 1992; Warr 1992).

Considering the afferents firsts, there are two groups of SG (Spiral Ganglion) neurons, called type I and type II neurons. Type I neurons make up about 90-95% the population; their distal processes travel directly to the IHC in the organ of Corti. Each type I neuron innervates one

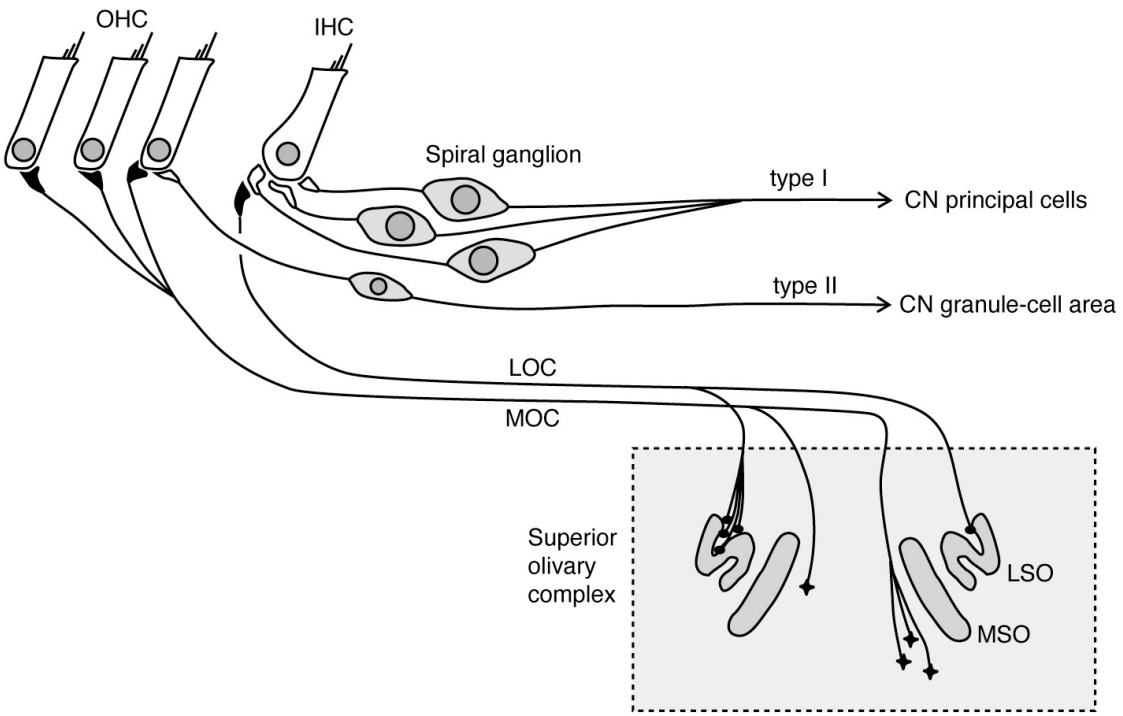

Figure 3.9: Wiring diagram of the Cochlea. The HCs are at left. Afferent terminals on hair cells, those on which HC excites an AN fiber - unfilled; efferent terminals, where an axon from a cell body in the central nervous system contacts a HC or another terminal in the organ of Corti - are filled. IHC are contacted by the distal processes of AN fibers. OHC are innervated by a small population of type II spiral ganglion cells whose axons terminate in the cochlear nucleus (CN). The efferent fibers to the cochlea are called olivocochlear neurons; they originate in the superior olivary complex (SOC). MOC - medial olivocochlear system - near the medial nucleus of the SOC and innervates OHCs. LOC - lateral olivocochlear system is near the lateral nucleus of the SOC and innervates afferent terminals of type I afferent fibers under the IHCs. (Young 2007)

IHC, and each hair cell receives a number of type I fibers; the exact number varies with species and location in the cochlea, but is typically 10-20%. The connection between the IHC and type I hair cells is a standard chemical synapse, by which the hair cell excites the AN (auditory nerve). Type I auditory nerve fibers project into core areas of the cochlea nucleus, the first auditory structure in the brain; type I fibers plus the neurons in the core of cochlear nucleus make up the main pathway for auditory information entering the brain. The remaining 5-10% of the spiral ganglion neurons - type II - innervate OHC. The fibers cross the fluid spaces between the IHC and the OHC and spiral along the basilar membrane beneath the OHCs toward the base of the cochlea innervating a few OHCs along the way. Although the type II fibers are like type I fibers in that they connect hair cells (in this case OHC) to the cochlear nucleus, there are some important differences. The axons of type II SG neurons are unmyelnated, unlike the

type I fibers; their central processes terminate in the granule-cell areas of the cochlear nucleus, where they contact interneurons, meaning neurons that participate in the central circuitry of the nucleus. Finally, type II fibers don‘t seem to respond to sound (Brown 1994; Robertson 1984; Robertson et al. 1999), even though they do propogate APs (Jagger Housley 2003; Reid et al. 2004). It is clear that type I fibers are the main auditory pathway, but the role of the type II fibers is unknown. The term AN (auditory nerve) fiber refer to the type I fibers only. The efferent neurons have cell bodies in brain called the superiorolivary complex; also they called olivocochlear bundle (OCB). There are two groups of OCB neurons. So-called lateral afferents (LOC) travel mainly to the ipsilateral cochlea and make synapses on the dendrites of type I afferents under the IHC. Thus they affect the afferent pathway directly. The second group is MOC, travel to both the ipsilateral and contralateral ears and make synapses on the OHCs (Warr 1992; Guinan 1996). Their effect on the afferent pathway is thus indirect, in that they act through the OHC‘s effects on the transduction process in the cochlea.

3.5 Human Specialities

Many authors have articles about the differences between the human cochleae and those of other mammals (Tylstedt and Rask-Andersen 2001; Tylstedt et al. 1997; Glueckert et al. 2005b). As well (Nadol 1988) reports major differences. In the organ of Corti, the major differences among species are the length and width of the basilar membrane, the number of IHC and OHC, and the length of hairs on both inner and outer hair cells. Significant differences in the innervation pattern of the inner hair cell among these species include the number of afferent nerve terminals per inner hair cell, the degree of branching of afferent fibers, and the number of synapses per afferent nerve terminal. Tylstedt and Rask-Andersen (2001) reported that the cell bodies of the ganglion cells are myelinated in other animals, the spiral ganglion perikarya in humans are unmyelinated (Liu et al. 2012).Rattay et al. (2001a) reported a differences in spiking behavior, e.g. peripherally and centrally evoked spikes arrive with a time difference of about $400\mu s$ in man and $200\mu s$ in cat. Furthermore according to Rattay et al. (2001a) the safety factor for the generation of an AP is reduced by this human peculiarity, i.e., small

changes in certain sensitive parameters cause the absence of AP propagation. Rattay et al. (2001b) reported that in contrast to single fiber experiments with cats, the long peripheral processes in human cochlear neurons cause first excitation in the periphery end, consequently, neurons with lost dendrite need higher stimuli. According to (Rattay et al. 2013) a lack of myelin in the soma regions of human type I neurons causes a large delay in spike conduction in comparison with cat neurons. The absent myelin, in combination with a longer peripheral process, causes quantitative differences of temporal parameters in the electrically stimulated human cochlea compared to the cat cochlea (Figure 3.10).

The results of (Potrusil et al 2012) shows that temporal parameters of the AP are affected by the size of the cell body with stronger variations for spikes induced by cathodic stimulation. Therefore, a more uniform excitation profile of the whole amount of cochlear neurons can be expected for anodic stimulation. Together with morphometric findings, results show a new insight into the unique micro anatomical features of the human spiral ganglion and their impact on AP onset and propagation initiated by micro stimulation. Liu et al. 2014 reported that TEM analyses showed the presence of GJs (Gap Junctions) between SGCs (Spiral Ganglion Cells) surrounding the Type I neurons in humans and guinea pig. Their findings indicated that GJs existed both between SGCs surrounding the same Type I neuron and between neighboring SGNs (Spiral Ganglion Neurons) in humans. They had a length of 4500nm and the intercellular distance approximated 4 nm between adjoining cells. In the guinea pig, the number of SCs that make up the sheath increases proportionately with the volume of the neuron that it surrounds. SGN in guinea pig are smaller and so fewer SCs (Schwann cells) surround an SGN. In guinea pig, they mostly found only one nucleus sitting within the soma. (Figure 3.11).

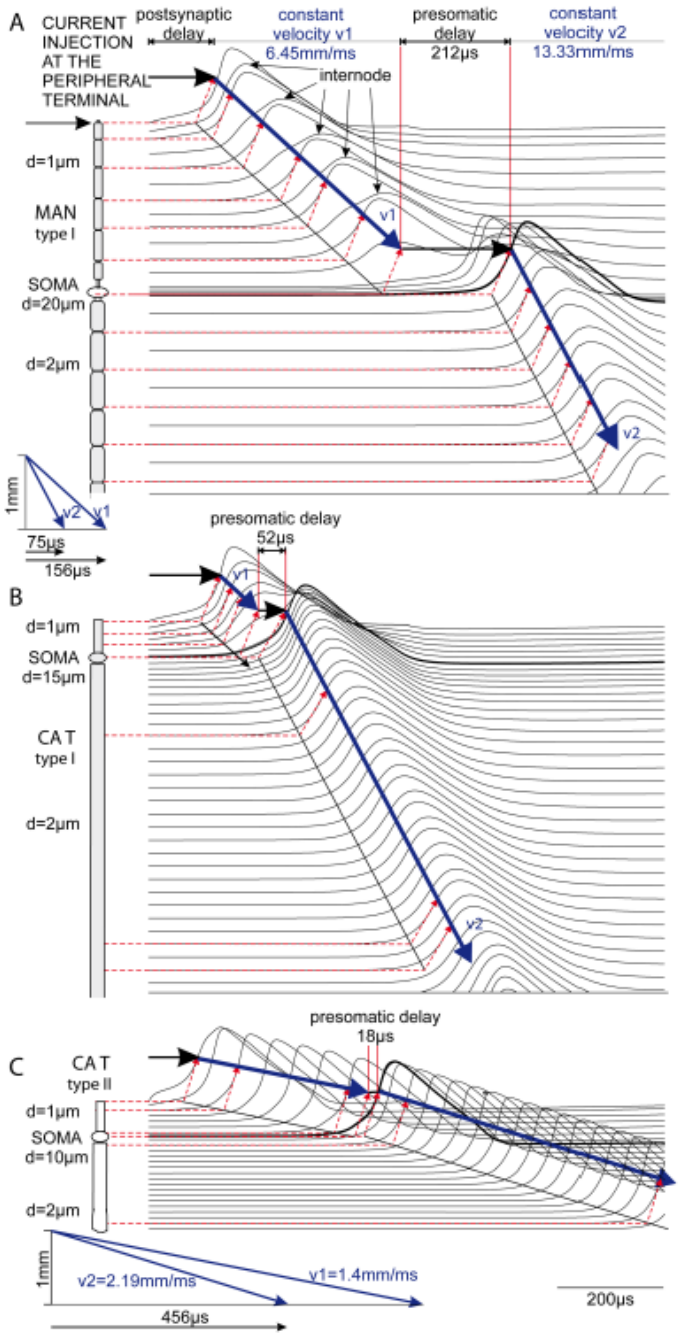

Figure 3.10: Simulated spike transduction in afferent cochlear neurons. Spike initiation by 0.5 ms pulse, 100pA (A and B) and 500 pA for the non-myelinated case (C). (A) shows the spike initiation for afferent cochlear neurons for the Man and (B and C) spike initiation for afferent cochlear neurons for a Cat (Rattay et al 2013)

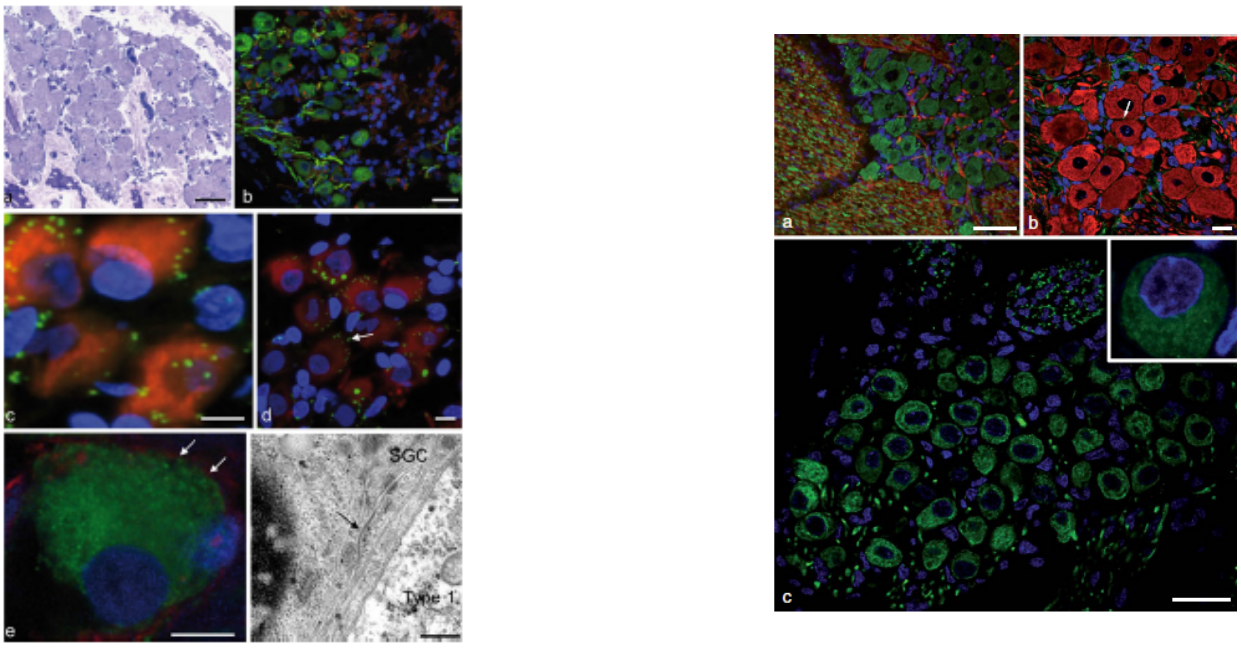

Figure 3.11: Left: Light microscopy, transmission electron microscopy (TEM) and immunofluorescence of human spiral ganglion (SG). Bars 20 μm (a, b), 10 μm (c, d), 5 μm (e), 0.5μm (f) Right: Immunohistochemistry in trigeminal and spiral ganglion of the guinea pig. Bars 100 μm (a), 20 μm (b), 50 μm (c) (Liu et al. 2014)

Chapter 4

Models of human cochler Neurons

4.1 Compartment model

Differences in neural geometry and the fact that the soma of the human cochlear neuron typically is not myelinated are reasons for disagreements between single fiber recordings in animals and the neural code evoked in cochlear implant patients. Authors introduce a compartment model of the human cochlear neuron to study the excitation and propagation process of action potentials. The model can be used to predict (i) the points of spike generation, (ii) the time difference between stimulation and the arrival of a spike at the proximal end of the central axon, (iii) the vanishing of peripherally evoked spikes at the soma region under specific conditions, (iv) the influence of electrode positions on spiking behavior, and (v) consequences of the loss of the peripheral axon. Every subunit of the cochlear neuron is separately modeled. Ion channel dynamics are described by a modified Hodgkin-Huxley model. Influence of membrane noise is taken into account. Here presented a spatial model of the human cochlear neuron that for the first time closely sticks to human morphometric data as known so far. All the neural subunits are individually described by connected electric circuits. Ion channel dynamics are described by the 'warm' HH model. Influence of membrane noise is taken into account. We will compare the reactions of a cat and human cochlear neuron in different case studies (4.1).

A neuron consists of several subunits with individual geometric and electric parameters: the

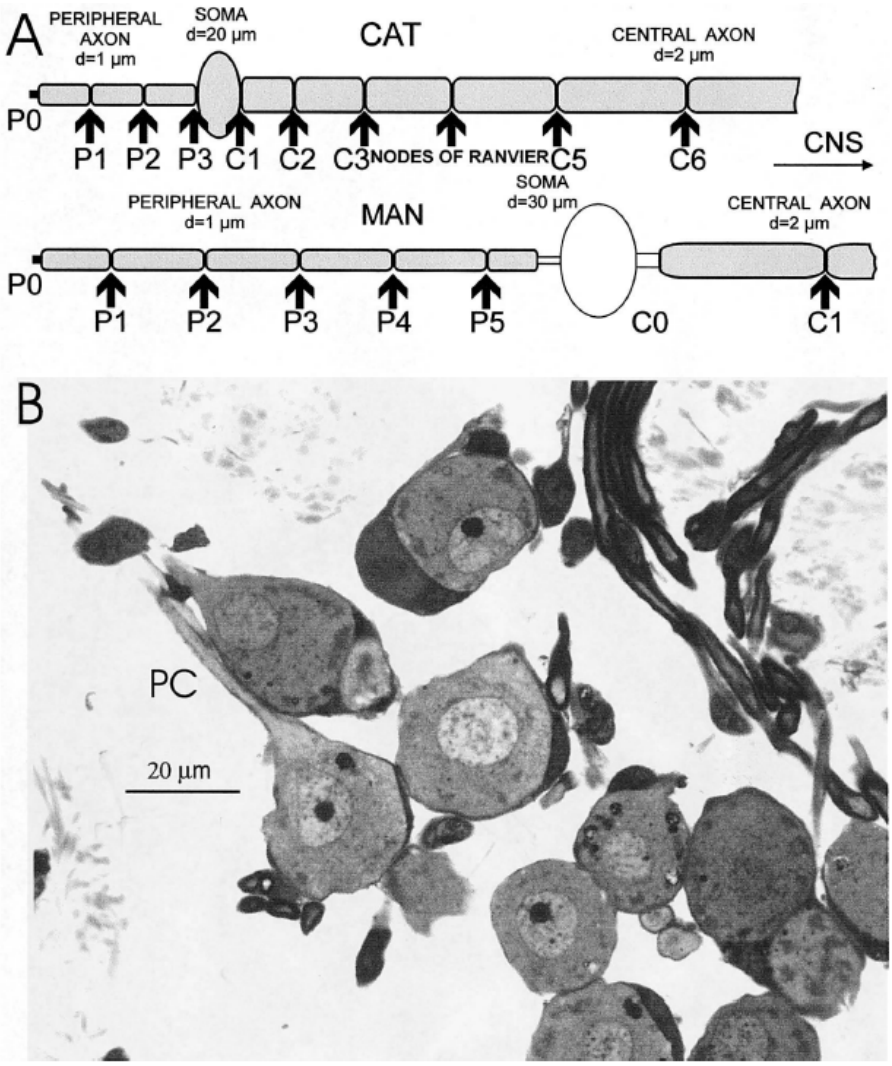

Figure 4.1: Scheme of a cohlear neuron in man and cat. The compartment sequence in MAN is: P0 - first peripheral internode - node - internode -...- internode - presomatic compartment-soma-postsomatic compartment - first central internode - node -..; in CAT there are no specific pre- and postsomatic comartments, the soma is between two nodes of Ranvier.(Rattay et al.2001a).

peripheral terminal, the peripheral nodes and internodes, the presomatic region, the soma, the postsomatic region, and the central nodes and internodes are subunits with different membrane compositions according to their physiological tasks. Usually, every subunit is represented by one compartment, which is modeled by an electric circuit (Fig. 4.2)(Rattay et al.2001a). .

Applying Kirchhoff's law (the sum of all currents at the central point of the n-th compartment is zero) results in:

$$I_{capacitive,n} + I_{ion,n} + I_{ohm,n} = 0 \tag{4.1}$$

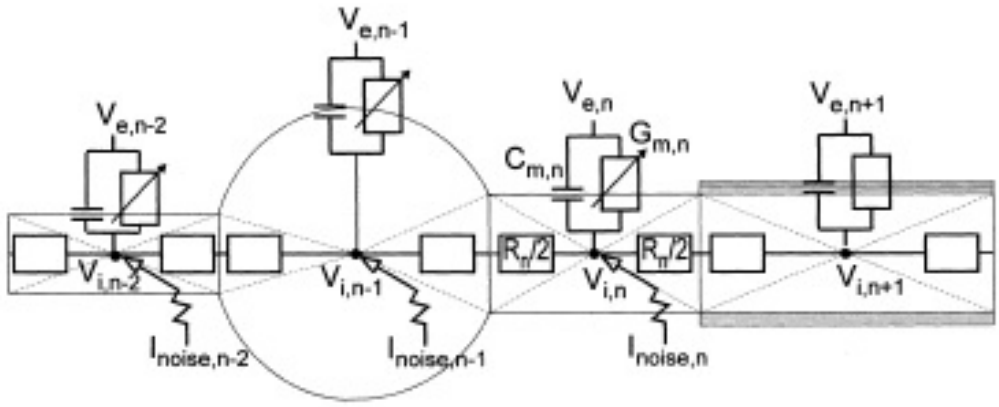

Figure 4.2: Part of the electric network to simulate a cohlear neuron. Examples given describe the pre- and postsomatic compartment, the soma, and the first central internode of a human cohlear neuron.

where $I_{capacitive,n}$ - capacitive current,

$I_{ion,n}$- ionic transmembrane current,

$I_{ohm,n}$- ohmic current.

According to Ohm's Law the voltage between to central points of neighbouring compartments is given as:

$$I_{ohm} = I_{ax} = \frac{V}{R} \tag{4.2}$$

The capacitance is given as $C = \frac{Q}{V}$ and the current can be expressed by means of the charge Q as $I = \frac{dQ}{dt}$. Therefore the general capacitive current is given as:

$$I_{capacitive} = C\frac{dV}{dt} \tag{4.3}$$

$C_{m,n}$ is defined as the membrane capacitance of the n-th compartment and is evaluated by $C_{m,n} = A_n c_{m,n}$, where $c_{m,n}$ denotes the specific membrane capacitance which is reverse proportional to the numbers of myelin layers of the compartment. Denoting $V_{i,n}$ as intracellular potential at the n-th compartment and $V_{e,n}$ respectively as the extracellular potential it follows

that:

$$\frac{d(V_{i,n} - V_{e,n})}{dt} \cdot C_{m,n} + I_{ion,n} + \frac{V_{i,n} - V_{i,n-1}}{R_n/2 + R_{n-1}/2} + \frac{V_{i,n} - V_{i,n+1}}{R_n/2 + R_{n+1}/2} = 0 \tag{4.4}$$

Introducing the reduced membrane voltage $V = V_i - V_e - V_{rest}$ (V_i and V_e represent the intracellular and extracellular potential, respectively ; V_{rest} is the resting potential) leads to the following system of differential equations for calculating the time course of V_n in every compartment:

$$\frac{dV_n}{dt} = \left[-I_{ion,n} + \frac{V_{n-1} - V_n}{R_{n-1}/2 + R_n/2} + \frac{V_{n+1} - V_n}{R_{n+1}/2 + R_n/2} + \frac{V_{e,n-1} - V_{e,n}}{R_{n-1}/2 + R_n/2} + \frac{V_{e,n+1} - V_{e,n}}{R_{n+1}/2 + R_n/2} \right] / C_{m,n} \tag{4.5}$$

If no stimulating electrode and surrounding cluster is present it is assumed that $V_e = 0$ holds and therefore the equation reduces to:

$$\frac{dV_n}{dt} = \left[-I_{ion,n} + \frac{V_{n-1} - V_n}{R_{n-1}/2 + R_n/2} + \frac{V_{n+1} - V_n}{R_{n+1}/2 + R_n/2} \right] / C_{m,n} \tag{4.6}$$

To reduce computational effort authors follow the approach of Rubinstein (1995), who demonstrated that a noise current proportional to the square root of the number of sodium channels within a compartment reflects the main property causing the irregularities in spike generation and timing. Thus, noise term $I_{noise,n}$ in μA becomes:

$$I_{noise,n} = GAUSS \cdot k_{noise} \cdot \sqrt{A_n \cdot g_{Na}} \tag{4.7}$$

GAUSS - Gaussian noise current term, that changes it‘s value every 2.5 μs

k_{noise} - factor common for all compartments

A_n - membrane area in cm^2

g_{Na} - maximum sodium conductance per square unit.

For simulating the spiking behavior of a cochlear neuron a stimulus current needs to be applied to initialize the excitation process. There is a possibility to inject a current at the postsynaptic terminal or directly at soma. To account for this injection this current is substracted from the ionic current, so it will be:

$$I_{ion,n} = I_{ion,n} - I_{inj,n} \tag{4.8}$$

for n equals 1 or represents the soma compartment. $I_{inj,n}$ is about 0.0005 μA for a stimulation of the terminal compartment and approximately 0.005 μA for the soma stimulation.

4.2 Cluster modeling

In order to find the effect of possible clustering neurons, the electrical model has to be done for the soma compartment where neurons are in contact with each other. The adapted circuit is presented in Figure 4.3, where V - potential of the first cell and W - for the second cell. Red arrows are the electrical currents for the first cell and the blue arrows for the second cell accordingly. This figure will help to derive the equations for two and three neuron clustering.

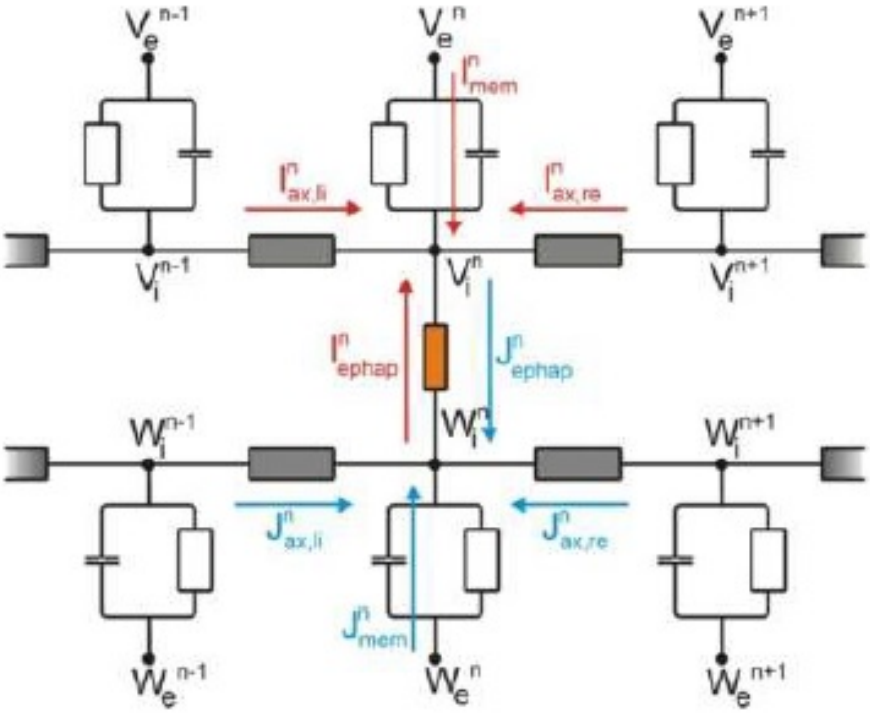

Figure 4.3: The electrical model of two neurons in contact with each other. I currents correspond to cell1 of the bicellular cluster, J currents correspond to cell2 neuron cluster (Wenger C. 2012)

By using Kirchhoff's Law the equations for soma compartments will be deviated. First of all, define the currents that flow in the cells:

I^n_{ephap}– current going from the inside of the first cell with an internal potential V^n_i

J^n_{ephap}– current going from the inside of the second cell with an internal potential W^n_i

By applying Kirchhoff's Law for the node V_i^n we can write the equations as:

$$I_{ephap}^n + I_{ax,r}^n + I_{ax,l}^n + I_{mem}^n = 0 \tag{4.9}$$

$$J_{ephap}^n + J_{ax,r}^n + J_{ax,l}^n + J_{mem}^n = 0 \tag{4.10}$$

If electrical current flow through a resistor from one intracellular compartment to the other intracellular soma compartment then it can be written as:

$$I_{ephap}^n = G_E^n \cdot (V_i^n - W_i^n) \tag{4.11}$$

$$J_{ephap}^n = G_E^n \cdot (W_i^n - V_i^n) = -I_{ephap}^n \tag{4.12}$$

Critical assumptions have to be made for the parameter $G_E^n = g_E^n \cdot A_{contact}^n [mS/cm^2] \cdot [cm^2]$. One layer of membrane is assumed to have a conductance of $g_E = 1mS/cm^2$ (Rattay et. al., 2001). If two cells have direct contact one could assume two layers of membrane (summing up to $g_E = 0.5mS/cm^2$) or also consider possible ionic flow through certain membrane specializations which might increase the value of g_E.

Basically two different neuron clusters are examined, but three neuron clusters should be also take into consideration. For this kind of cluster equations have to be rewritten, where V_n^1- the transmembrane potential at the n-th compartment of cell 1. V_n^2-corresponds for cell 2 and for the cell 3. In the same manner, ephaptic currents are written as: $I_{ephap,n}^1-$ ephaptic current for for the n-th compartment of cell1, the same for cell 2 and cell3. Thus we can derive the ephaptic currents for the special three neuron cluster:

$$I_{ephap,n}^1 = G_{E,n}^1 \cdot (V_{i,n}^1 - V_{i,n}^2) \tag{4.13}$$

$$I_{ephap,n}^2 = G_{E,n}^1 \cdot (V_{i,n}^2 - V_{i,n}^1) + G_{E,n}^2 \cdot (V_{i,n}^2 - V_{i,n}^3) \tag{4.14}$$

$$I_{ephap,n}^3 = G_{E,n}^2 \cdot (V_{i,n}^3 - V_{i,n}^2) \tag{4.15}$$

So, the differential equations have to be adapted according to this equations:

$$I^1_{ephap,n} + I^1_{axR,n} + I^1_{axL,n} + I^1_{mem,n} = 0 \tag{4.16}$$

$$I^2_{ephap,n} + I^2_{axR,n} + I^2_{axL,n} + I^2_{mem,n} = 0 \tag{4.17}$$

$$I^3_{ephap,n} + I^3_{axR,n} + I^3_{axL,n} + I^3_{mem,n} = 0 \tag{4.18}$$

4.2.1 Cluster1

The first cluster consists of two cells - the green cell1 with a diameter of nucleus 17 μm and the yellow cell2 with a diameter of 21.4 μm in diameter. The nuclei are illustrated in blue. The contact area between the cells is 113.7 μm^2 and illustrated in red. Figure 4.4. illustrates the cluster consisting of two cells, green cell1 and yellow cell2.

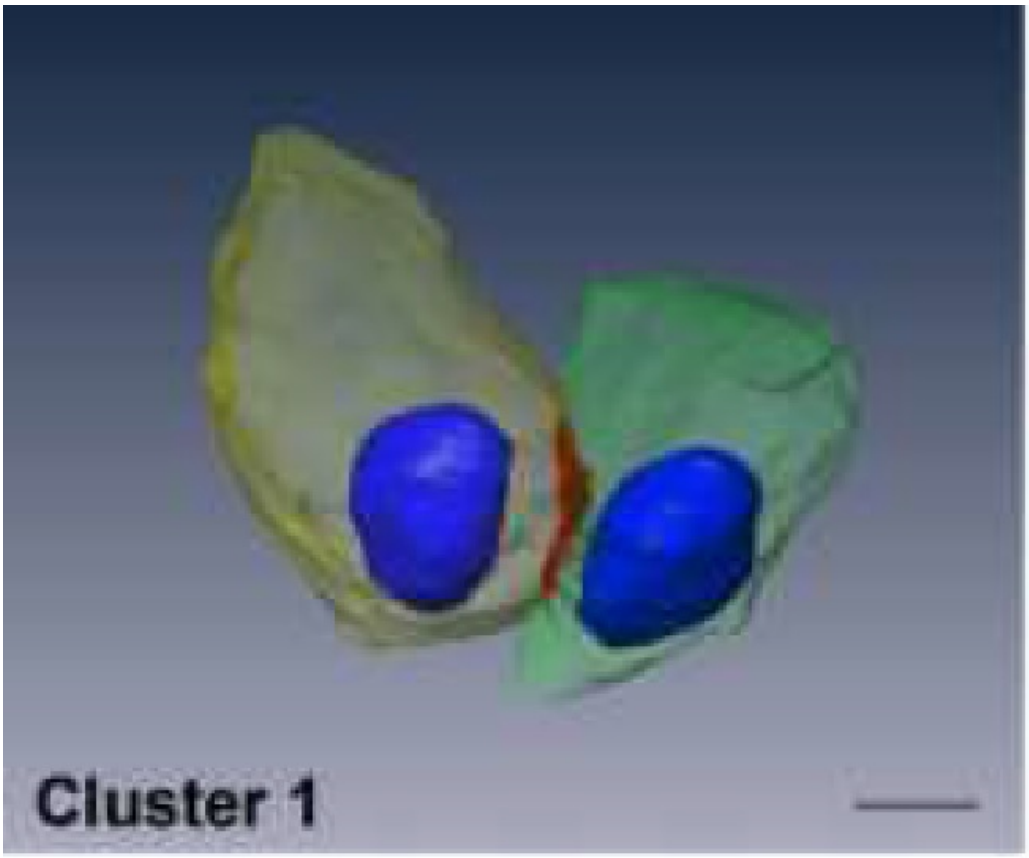

Figure 4.4: Clustering of two neurons (Potrusil(2013))

The calculating area represents 12.52% of the total area of cell1 and 7.9% of the total area of cell2.

In a first experiment the presomatic regions were considered to be very long, 100μm (Rattay et al. 2001). The first cell received current impulse 0nA, whereas the second cell received a current input with a sub threshold amplitude 0.1nA.

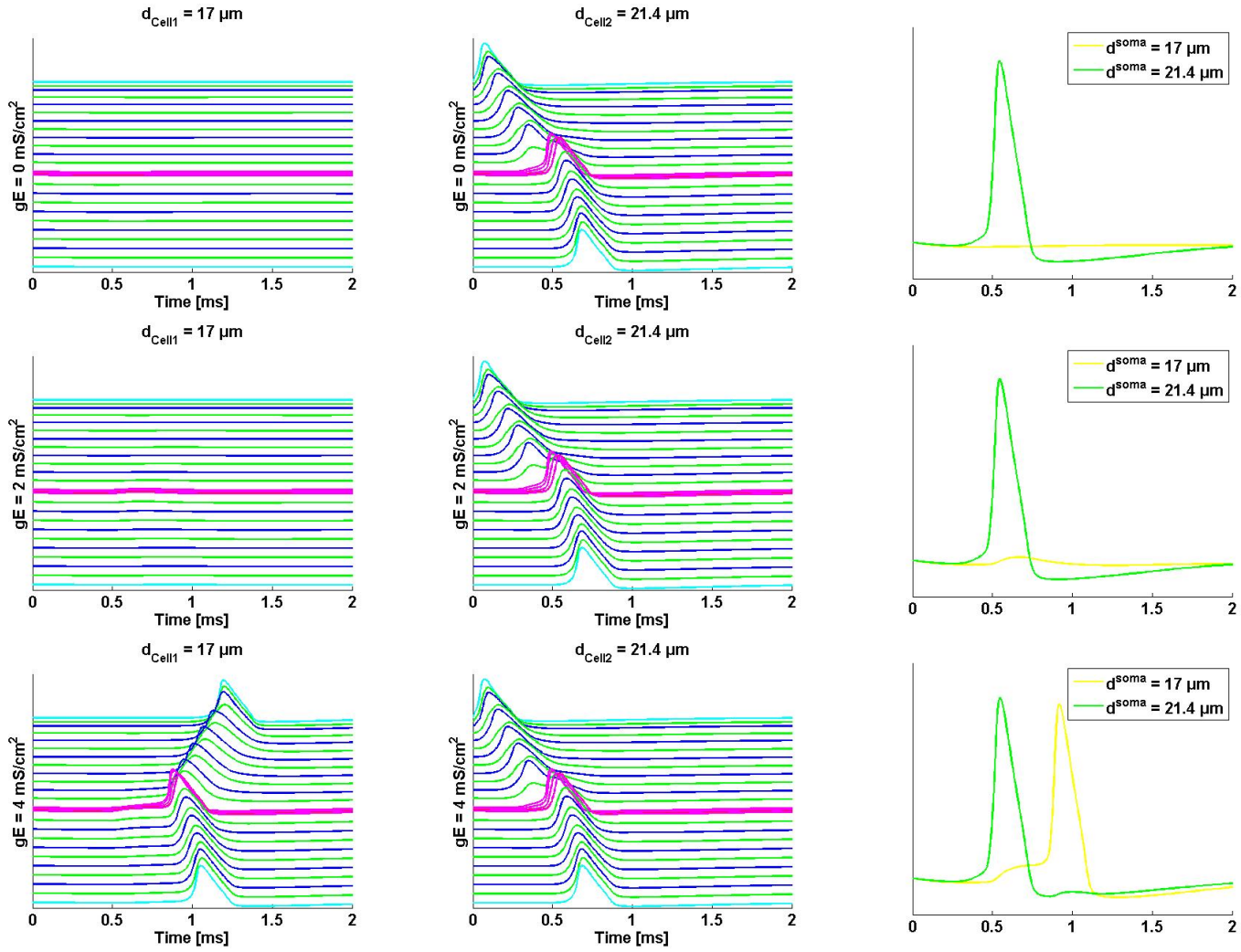

Table 4.1: Using of long presomatic compartment l_{pre}=100μm. Cell1 receives a 0nA subthreshold stimulus, whereas cell2 received a 0.1nA current injection.

The parameter gE was increased from 0 mS/cm^2, which means that there is no connection between two cells till 4 mS/cm^2. For this case the first cell fails to produce a spike. The bigger cell2 initiates a spike at the first compartment, which travels along the dendrite with a certain delay over the soma and then further initiates the spike till the neuron‘s central end. When gE=2 mS/cm^2 the slight depolarization start occur at the cell1, due to the current flow from

the supporting cell2 soma. When the ephaptic conductance is increased to 4 mS/cm^2 cell1 will be excited by the propagating spike of the cell2 and is able to trigger an AP initiation at the soma compartment. Spike 1 appears at 0.879ms, whereas spike 2 appears at 0.486ms, which means of 0.39ms delay. For the second set of experiments all the presomatic were shortened to 50μm and all the cells get the impulse with a sub threshold amplitude 0.1nA. The results with varying parameter gE from 0 till 10 mS/cm^2 are shown in Table 4.2

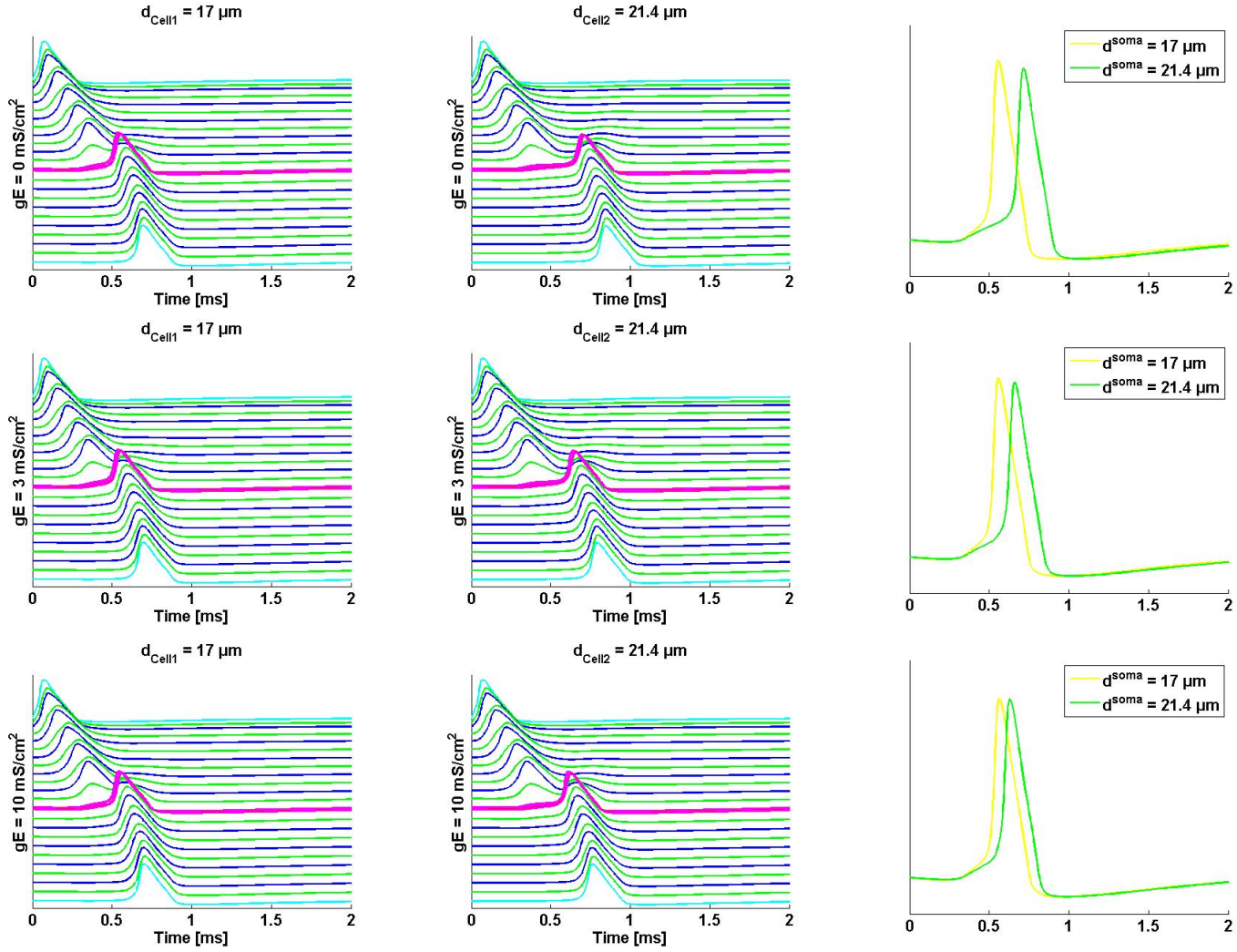

Table 4.2: The both cells are stimulating with 0.1nA current with a short presomatic compartment l_{pre}=50μm. Varying the parameter gE from 0 mS/cm^2 till 10 mS/cm^2

The spike of cell1 appears at 0.557ms, with the AP_{height} at the soma of cell1 is 100.2mV, whereas of cell2 is 95.55mV, with the time delay of 0.162ms. With the increasing parameter gE from 0 till 10 mS/cm^2 we can see that time shift decreases between the cell two spikes (see Table 4.1). Further increase of ephaptic conductance results in increasing spike height of cell2

and decreasing for cell1. For the gE value=10 mS/cm^2 the AP_{height} has almost the same value for cell1 and cell2 as well and also the time shift between the two cells is only 0.063ms apart. Another experiment will be done with stimulating current impulse 0.1nA for the first cell and 0nA for the cell2 with a short presomatic compartment l_{pre}=50μm. This simulation mode fails to initiate AP in a second cell - Table 4.3

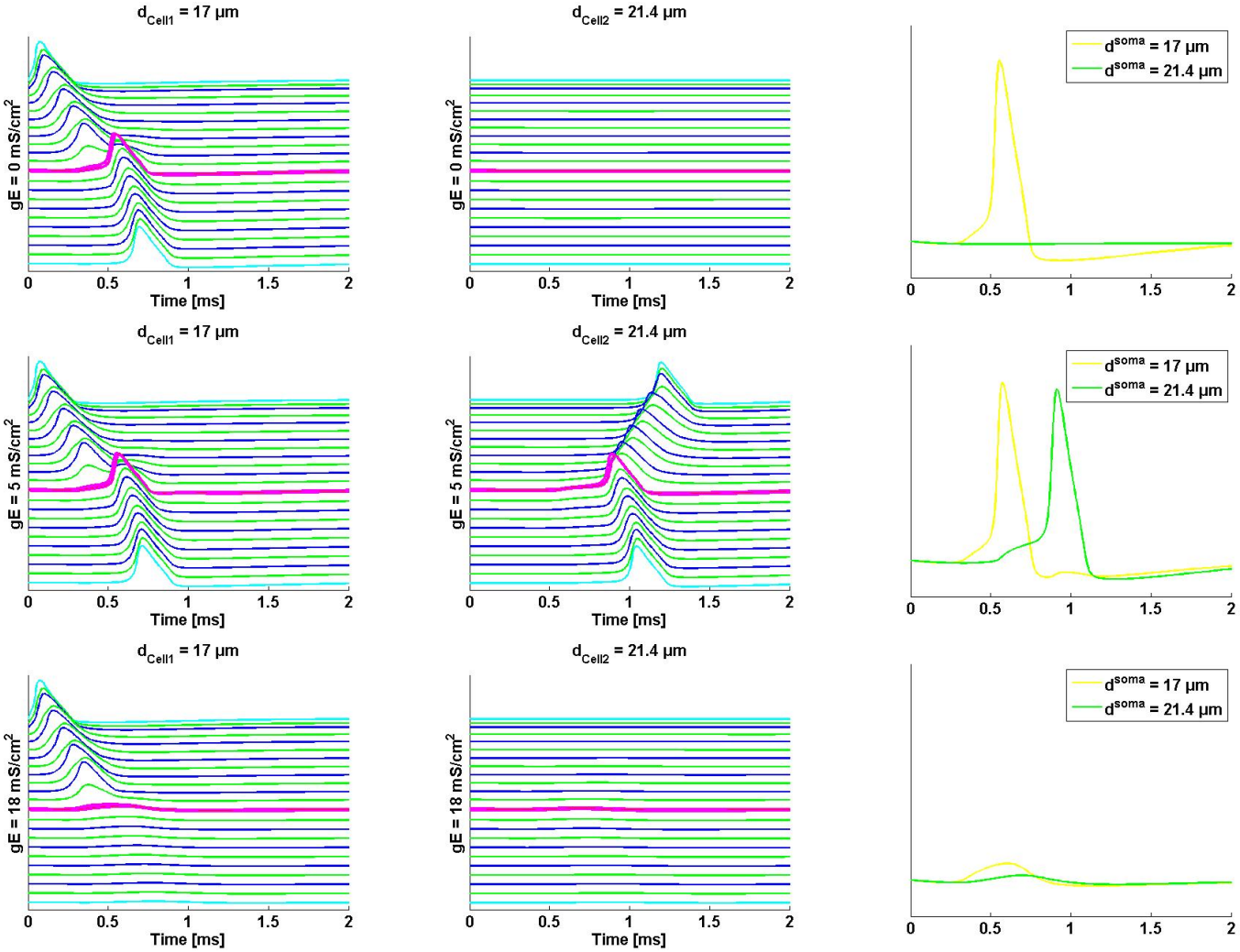

Table 4.3: Using short presomatic compartment l_{pre}=50μm. Cell1 receives a 0.1nA subthreshold stimulus, whereas cell2 received a 0nA current injection.

The parameter gE was increased from 0 mS/cm^2, which means that there is no connection between two cells till 5 mS/cm^2. For this case cell2 fails to produce a spike. The bigger cell2 initiates a spike at the first compartment, which travels along the dendrite with a certain delay over the soma and then further initiates the spike till the neuron‘s central end. When the ephaptic conductance is increased to 5 mS/cm^2 cell2 will be excited by the propagating spike of the cell1 and is able to trigger an AP initiation at the soma compartment. AP_{height} for

the first cell is 98.94mV and quite similar value for cell2 - 95.34mV. When the conductance gets larger then the propagation for both cells breaks down. So the critical values for ephaptic conductance gE is: 5 $\leq$gE$\leq$ 17, if for both cell bodies nm=1.

4.2.2 Cluster2

Now we will consider the cells, which have the same size, cell1 has a soma diameter of 12.03μm, which is displayed in yellow, whereas cell2 has the same value of diameter - 12.53μm and is shown in green at the right side of the Figure 4.5. The contact area between cells was calculated as 74.79μm^2 which represents about 16.5% of the total area of cell1 and 15.6% of cell2. This cluster arrangement has a great influence on each other. The threshold values stay the same 0.1nA.

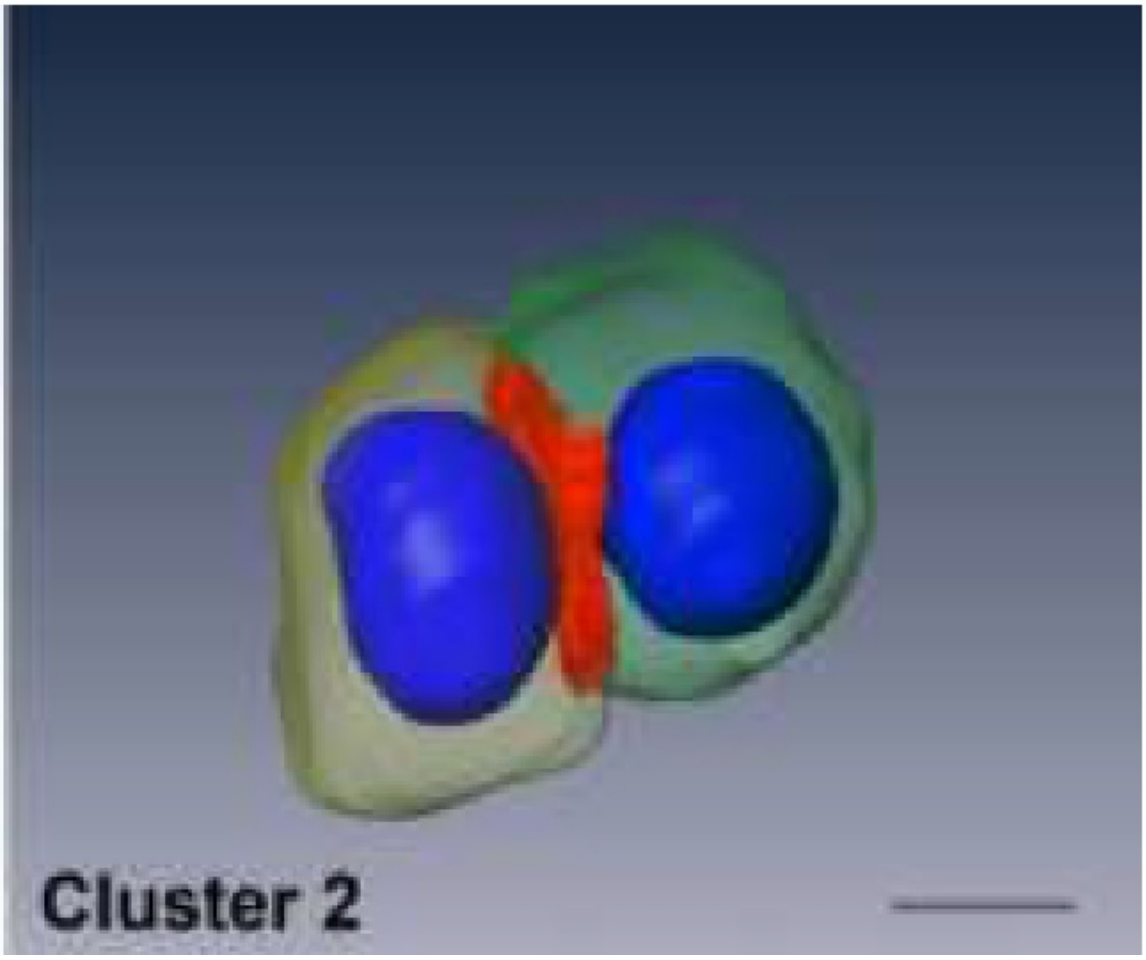

Figure 4.5: The cluster of two cells with a contact area in red (Potrusil (2013))

The simulations were performed for 100μm long presomatic regions of both neurons. Cell2 receives a current injection of 0.1nA, whereas the cell1 gets a 0nA stimulus. Both neurons were modeled with three membrane layers surrounding the somatic region(nm=3) and gE was successfully increased. Table 4.4 shows the synchronization and inhibiting effect of clustering for long presomatic lengths l_{pre}=100μm.

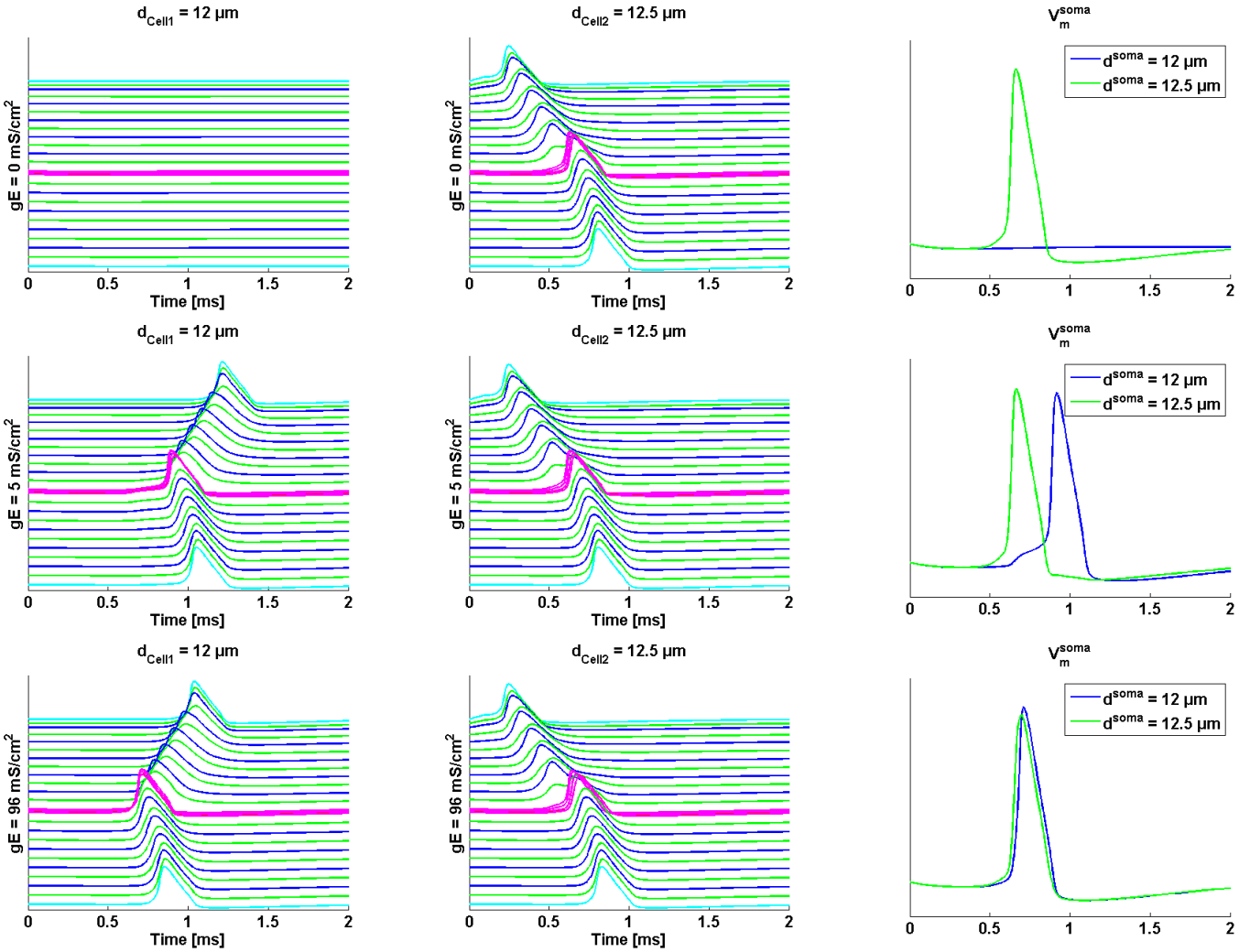

Table 4.4: Neuron2 of cell2 is stimulating with 0.1nA current with a long presomatic compartment l_{pre}=100 μm. Varying the parameter gE from 0 mS/cm^2 till 96 mS/cm^2

For $gE \geq 4$ the unstimulated cell1 initiates a spike at its soma with a height 98.9 mV at 0.91 ms. Compared to cell2 which has an AP_{height} at the soma of 102.1 mV at 0.66ms, so the delay is 0.25msec. When gE is increased this delay rapidly shrinks and also the AP_{height}'s and corresponding peak times in the soma assimilate, i.e, the cells get synchronized. In the next experiment we decrease both length of presomatic compartments to 50μm and stimulate cell1 with 0nA current, whereas cell2 with 0.1nA current. Thus the result is shown on Table 4.5.

We defined the values of gE when begin the break- down of the AP at the soma - 4 $\leq$gE$\leq$ 97, within this range both cells successfully conduct the generated APs to their central model end. Higher gE values show breaking down effect of the AP transmission. Spike onset occurs in cell1 after 0.245ms. The generated AP reaches the central terminal 0.666ms after current injection.

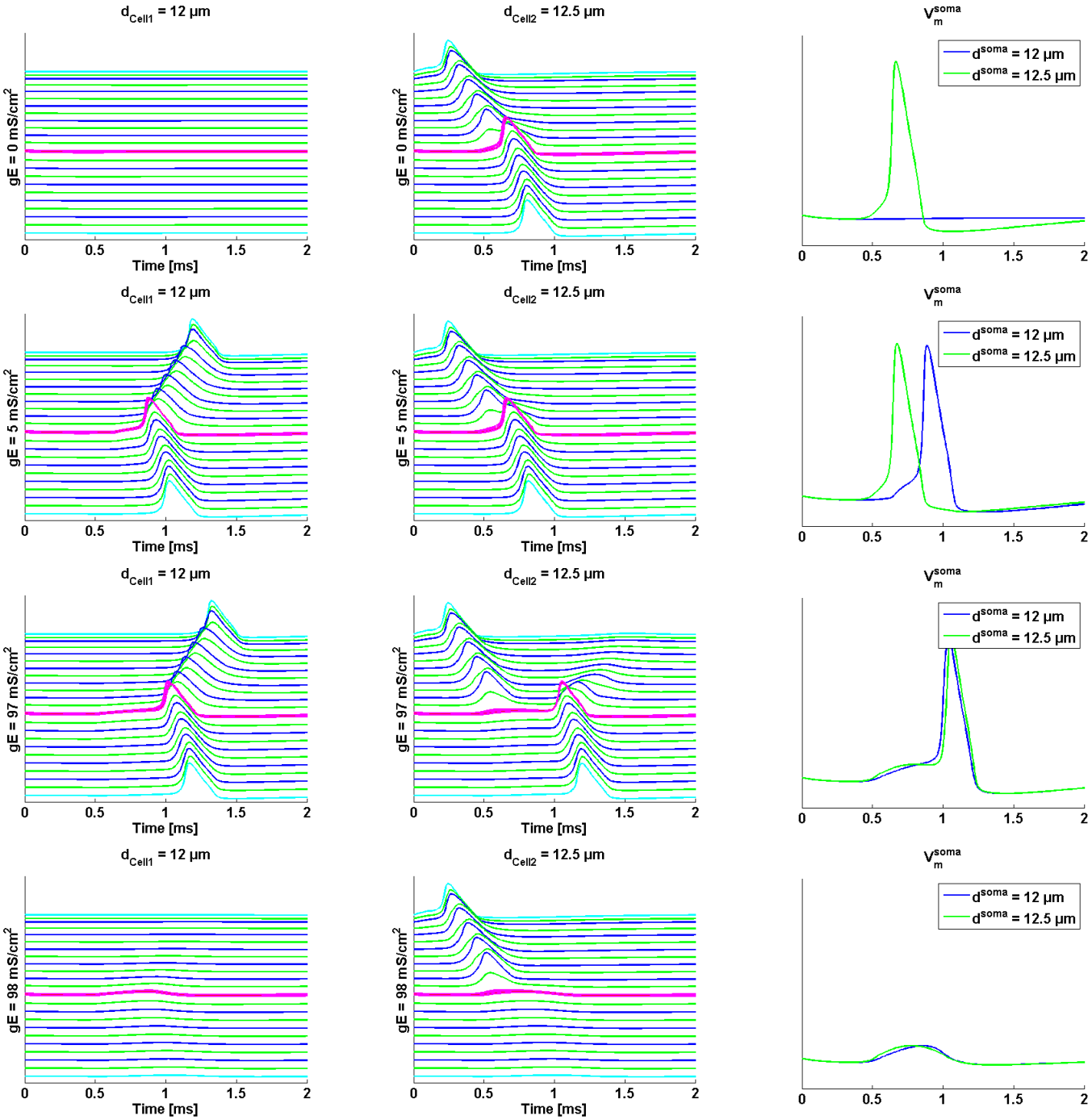

Table 4.5: Neuron2 of cluster2 receives a current injection of 0.1 nA to the peripheral terminal. nm=3 - so three membrane layers surrounding the somatic region. Blue lines - node, while green lines - internodes. The unmyelinated peripheral- and central terminal are presented in cyan while the somatic region is visualized in pink color.

When gE=4 mS/cm^2 cell1 begin to excite, where cell2 has an AP_{height} at the soma of 101.7mV at 0.674ms, leading to AP_{height} of cell1 - 98.29ms at 1.023ms. Further increase of gE makes the signal to be more and more synchronized, thus both generated signals reach the central terminal in a quite the same time. If $gE \geq 97$, both cells are unable to propagate the spike.

When gE=97 mS/cm^2 so the AP conduct spike in both directions for the cell2.

4.2.3 Cluster3

Consider the cells, which have the same size, cell1 has a soma diameter of 18.3μm, which is displayed in yellow, whereas cell2 has the same value of diameter - 18.35μm and is shown in green at the right side of the figure 4.6. The contact area between cells was calculated as 83.41μm^2 which represents about 7.9% of the total area. This cluster arrangement has a great influence on each other. The threshold values stay the same 0.1nA.

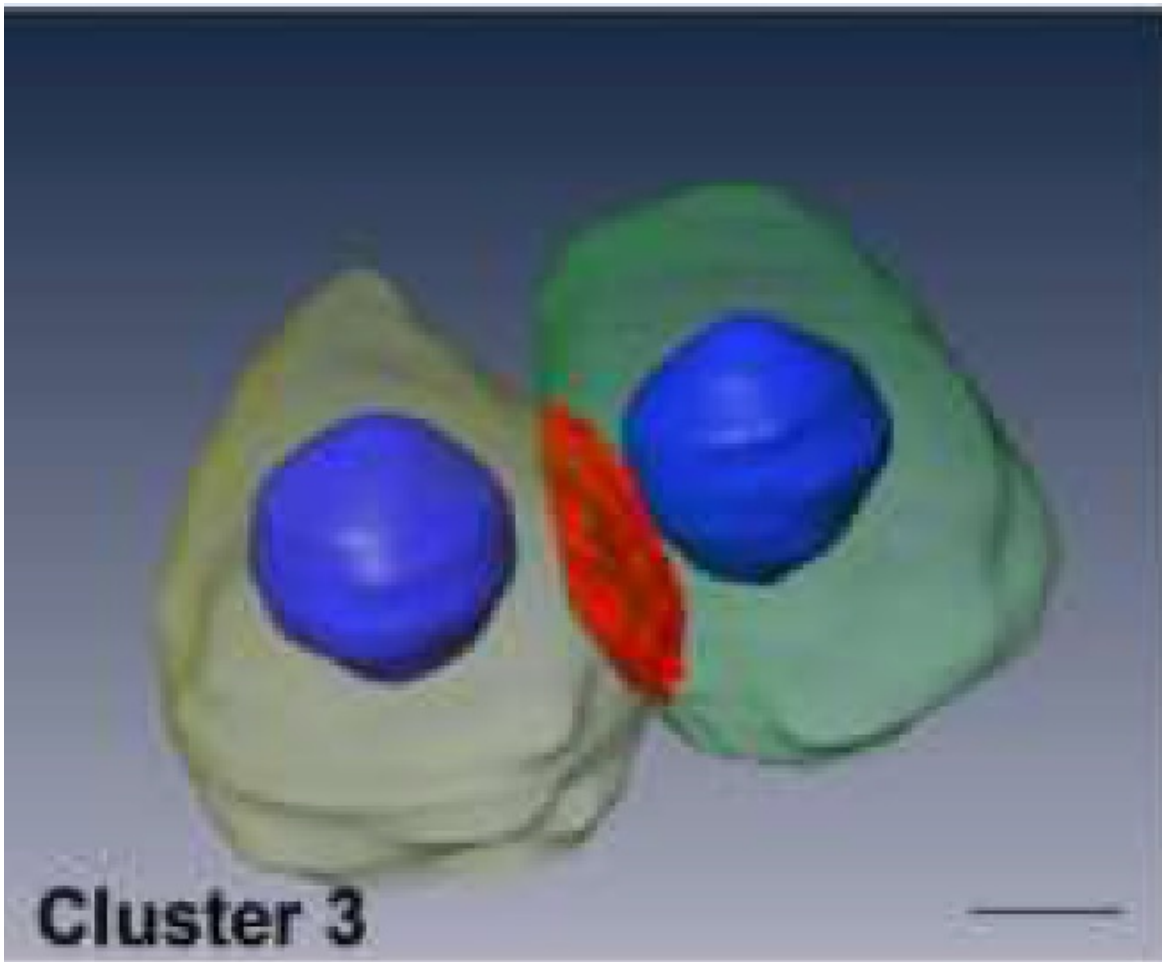

Figure 4.6: Arrangement of the 3 cluster, with the yellow cell1 and green cell2. The nuclei are plotted in blue, the contact area is plotted in red (Potrusil (2013))

Set up the first experiment when only cell2 is stimulated be the current 0,1nA with a long presomatic compartments for both cells. If the ephaptic current is strong enough, the inactive cell1 indicates a spike at its soma with further synchronization according to the spike of cell2 for increasing values gE. The representation of this modeling is shown on Table 4.6.

When gE=0 mS/cm^2 cell1 receives no current input, but the current input to cell2 - 0.01nA

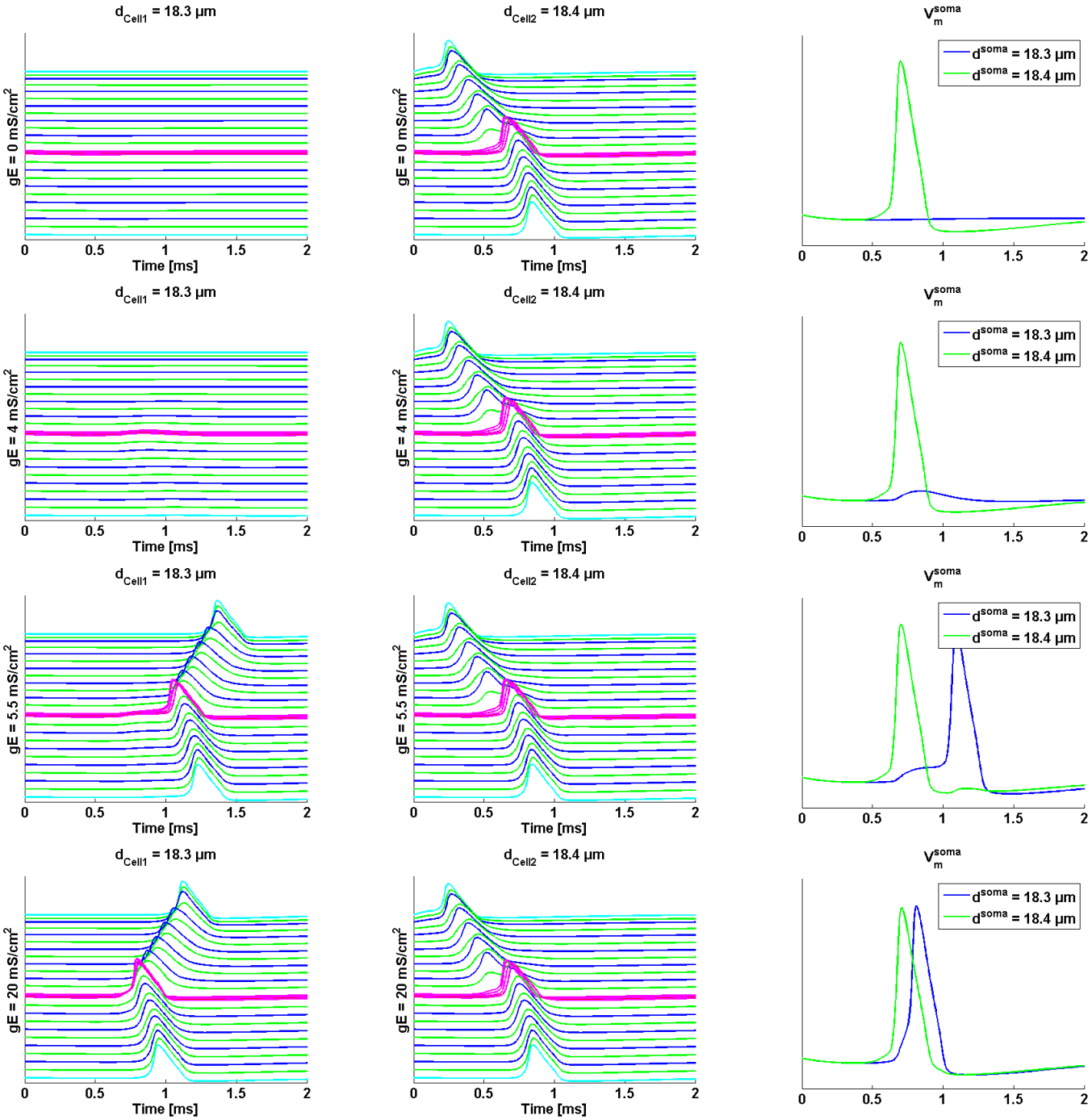

Table 4.6: Neuron2 of cluster3 receives a current injection of 0.1 nA to the peripheral terminal. nm=3 - so three membrane layers surrounding the somatic region. Blue lines depict node, while green lines illustrate internodes. The unmyelinated peripheral- and central terminal are presented in cyan while the somatic region is visualized in pink color.

leads to propagating spike with a AP_{height} at the soma of 102.7 mV which appears at 0.694 ms, and arrives at 0.843 ms at compartment 27. When gE=4 mS/cm^2 the soma of cell1 gets further depolarized. If gE=5.5 mS/cm^2 the AP_{height} of cell1 is 98.18mV which appears 1.092ms after stimulus onset. With the increasing value gE, the spikes of the cells get synchronized. When

gE reach a value 20 mS/cm^2 yellow cell1 gets AP_{height} of 101.7mV at 0.810ms, whereas green cell2 - 100.4mV at 0.709ms. For other experiments both presomatic regions were shortened to 50μm. The cell1 doesn‘t receive a current stimulation, but the cell2 receives a current injection of 0.1nA. For this case cell2 would trigger an AP which then will propagate over the soma region to the central end. Next experiment was done in order to test the influence of myelin layers, three different values of the parameter nm were tested, nm = 2,4,6. Table 4.7 shows three different cases of nm (myelin layers) for a selected values of gE=5 mS/cm^2.

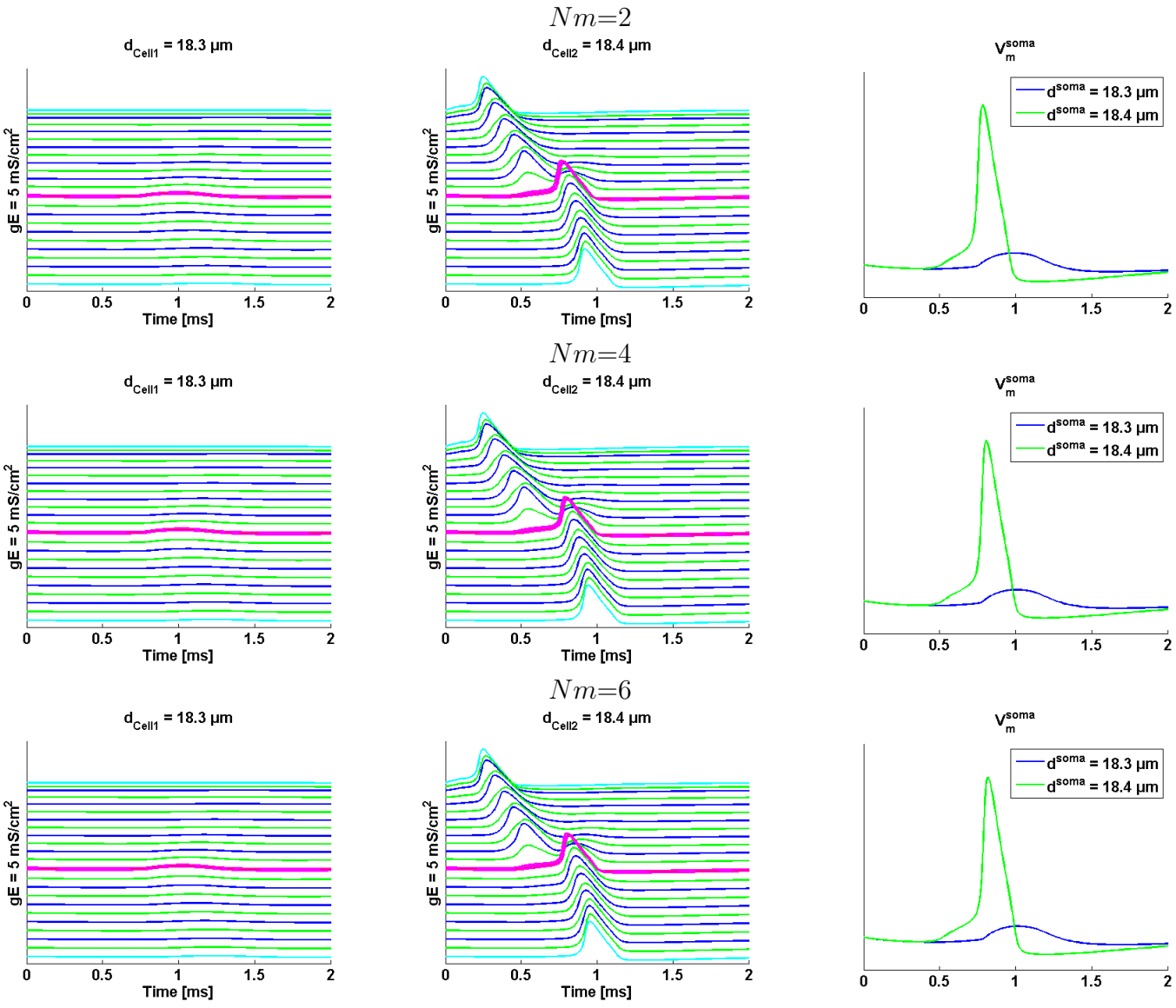

Table 4.7: Short presomatic segments l_{pre}=50μm. Results for varying degree of myelinization with a selected values of gE=3 mS/cm^2.

Table 4.8 shows three different cases of nm for a selected values of gE=11.5 mS/cm^2:

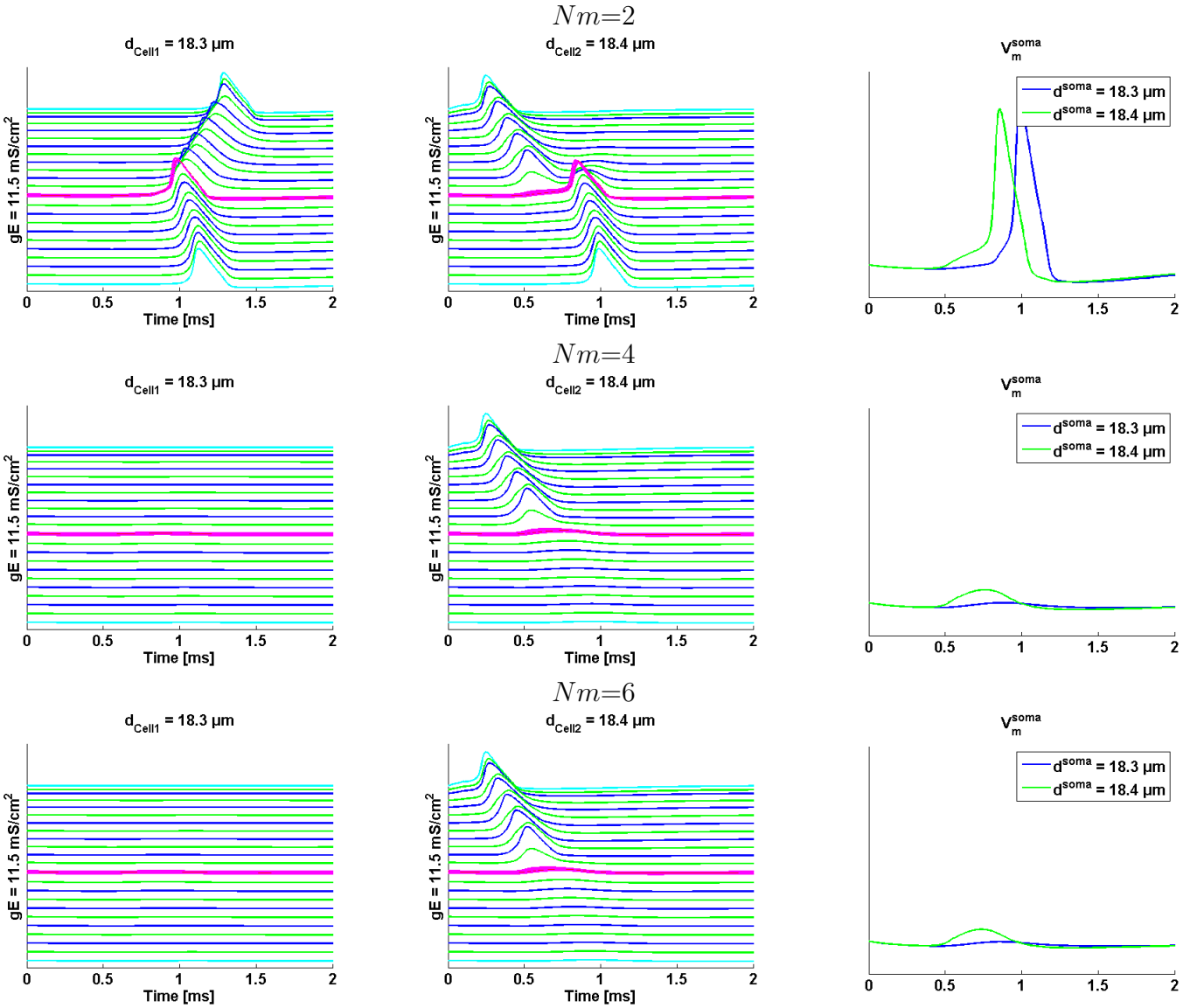

Table 4.8: Short presomatic segments l_{pre}=50μm. Results for varying degree of myelinization with a selected values of gE=11.5 mS/cm^2

For nm=1 the time peak for compartment 27 is 0.875ms, whereas for nm=3 for this compartment is 0.912ms, and for nm=5 the peak time is 0.925ms. If nm=1 holds, for ephaptic conductance values of 5.5 ≤gE≤ 21 mS/cm^2 cell2 is able to depolarize cell1 leading to successful AP transmission while keeping enough current to itself for an ongoing spike conduction. For higher values gE the spike of cell2 is again breaks down and no excitation of cell1 can occur. When nm=3 - no value of gE exists which will normally propagate the AP of cell1 during current supply of cell2. For $gE \geq$ 11.5 mS/cm^2 the spike breaks down at the soma of cell2, so that none of the cells transmit AP. For this case the conductance values is lying in the range of 5.5 ≤gE≤ 11.5 mS/cm^2. For nm=5 break down appears for $gE \geq$ 10 mS/cm^2 spike breaks

down at the soma of cell2, so that none of the cells transmit AP. Table 4.8 illustrates the case of propagation AP for gE=11.5 mS/cm^2. This value has been chosen because it is the value where AP also breaks down at the soma of cell2 for nm=5. It is the first value, where first break-down occur.

4.2.4 Intracellular Spike Trains

In order to analyze behavior of intracellular spike trains make an experiment with different time input, neurons belonging to our standard cluster3 were modeled with long presomatic compartment(100 μm), for three membrane layers surrounding the somatic region(nm=3) for a human cochlear neuron. Table 4.9 shows the spike trains for stimulating cell1 with 0.1nA current every 3ms.

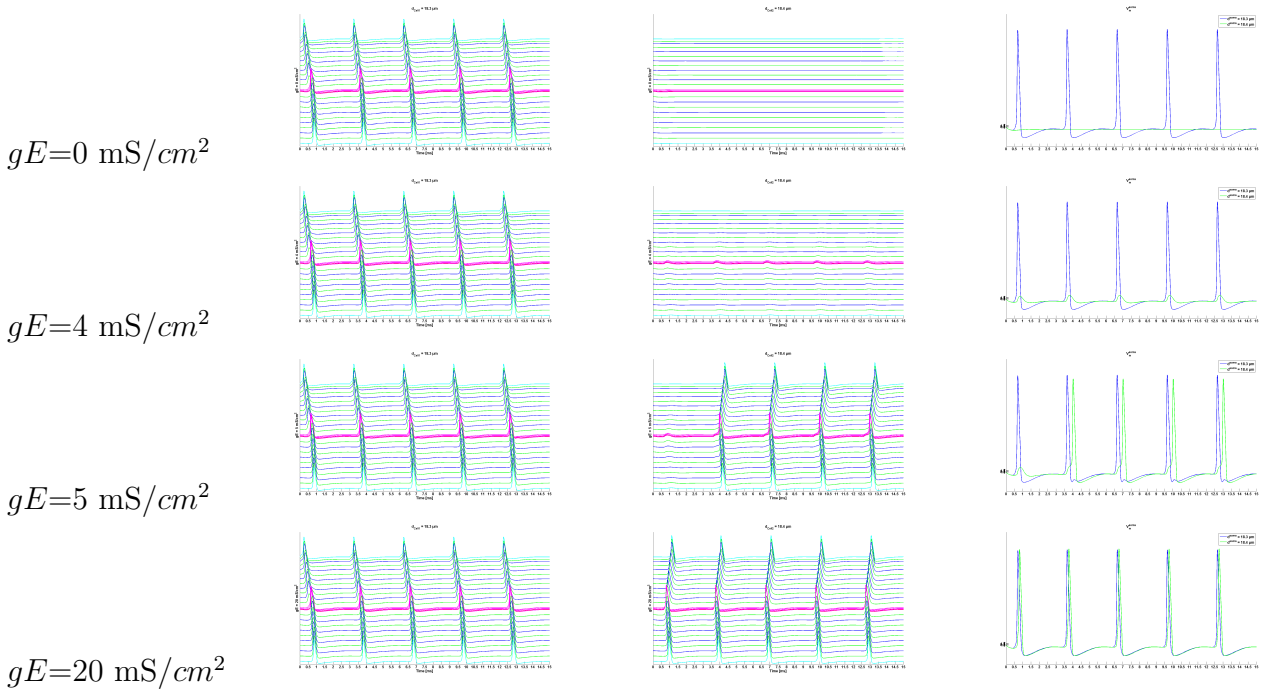

Table 4.9: Synchronization due to ephaptic coupling. Cell1 composing cluster 3 received simultaneously current injection of 0.1nA every 3ms for increasing parameter gE

When gE = 0 mS/cm^2 there is no depolarization of cell2, due to stimulation only cell1 with 0.1nA.The first AP in cell1 is initiated 0.245ms after spike onset and reach the model at 0.832ms. When we increase gE parameter and it becomes gE=4 mS/cm^2 - causes small depolarization of the cell2. With the gE=5 mS/cm^2 it becomes evident the depolarization of cell2 but the first

spike of AP cell2 is not generated. When the conductance is further increased gE=20 mS/cm^2 it can be observed that first AP of cell2 is generated and the induced APs synchronized with the time. Table 4.10 shows the spike trains for stimulating cell2 with 0.1nA current every 5ms.

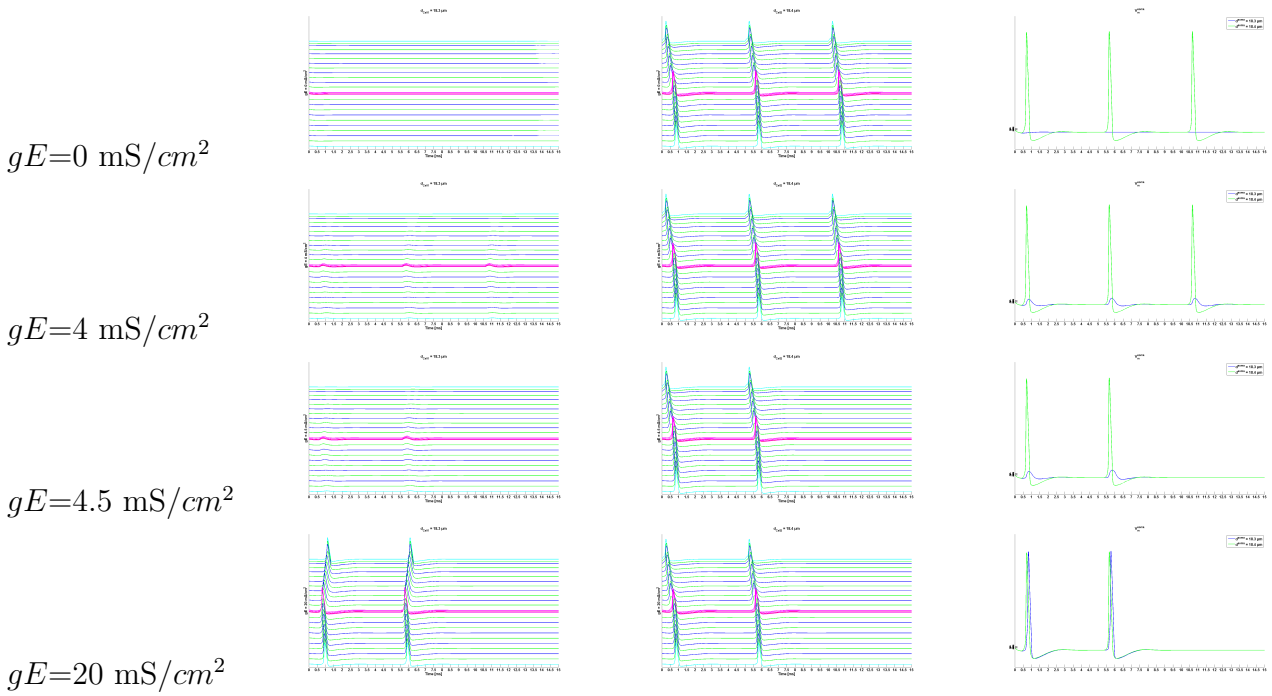

Table 4.10: Synchronization due to ephaptic coupling. Cell2 composing cluster 3 received simultaneously current injection of 0.1nA every 5ms for increasing parameter gE.

When $gE = 0$ mS/cm^2 there is no depolarization of cell1, due to stimulation only cell2 with 0.1nA.The first AP in cell2 is initiated 0.244ms after spike onset and reach the model at 0.829ms. When we increase gE parameter and it becomes $gE = 4$ mS/cm^2 - causes small depolarization of the cell1. With the $gE = 4.5$ mS/cm^2 it becomes evident the depolarization of cell1 but the first spike of AP cell1 is not generated. When the conductance is further increased $gE = 20$ mS/cm^2 it can be observed that first AP of cell1 is generated and the induced APs synchronized with the time. In a next trials we analyze the behavior when both cells are stimulated but with different time delay. We analyze again cluster 3 with current injection 0.1nA every 3ms for cell1 and 5ms for cell2. shows the the spike trains for both cells stimulating cells with 0.1nA current every 3ms for cell1 and 5ms for cell2.

When $gE = 0$ mS/cm^2 both cells transmit normally APs with the distinct simulation rate. For $gE \leq 4$ mS/cm^2 the firing rates remains constant. When $gE = 5$ mS/cm^2 the spiking pattern of the cell2 changes completely, so the resulting AP travels in both directions reaching

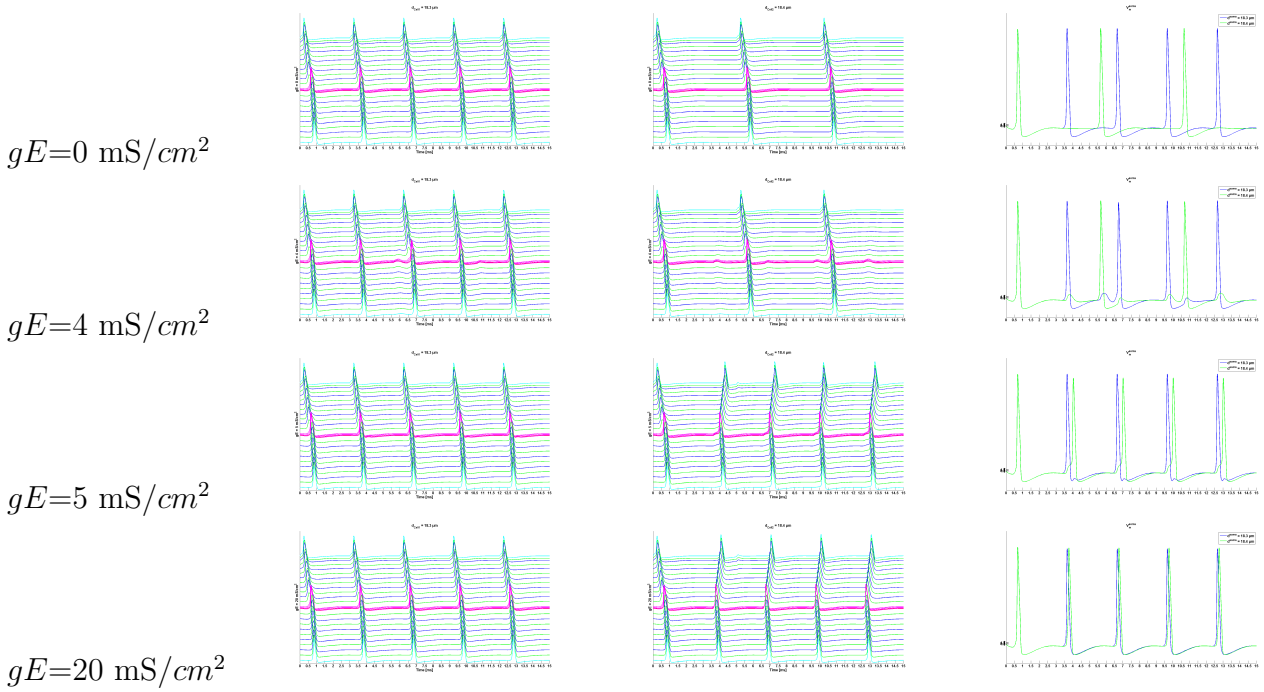

Table 4.11: Synchronization due to ephaptic coupling. Both cells composing cluster 3 received simultaneously current injection of 0.1nA every 3ms for cell1 and 5ms for cell2.$gE \geq 5$ leads to the adaptation of peaks of cell2 and synchronization effects.

the central terminal at 0.656ms after the triggering of cell1. With increasing parameter gE the following spike of cell1 initiate synchronized spikes in cell2 which is consequently adapting the firing rate of cell1. For $gE = 20$ mS/cm^2 the delay between the cell1 and cell2 is reduced to 0.104ms.

4.2.5 Cluster4

Cluster 4 presented as 3-neuron cluster and was systematically tested to detect ephaptic coupling effects. Figure 4.7 illustrates a three-neuron cluster in a cluster arrangement.

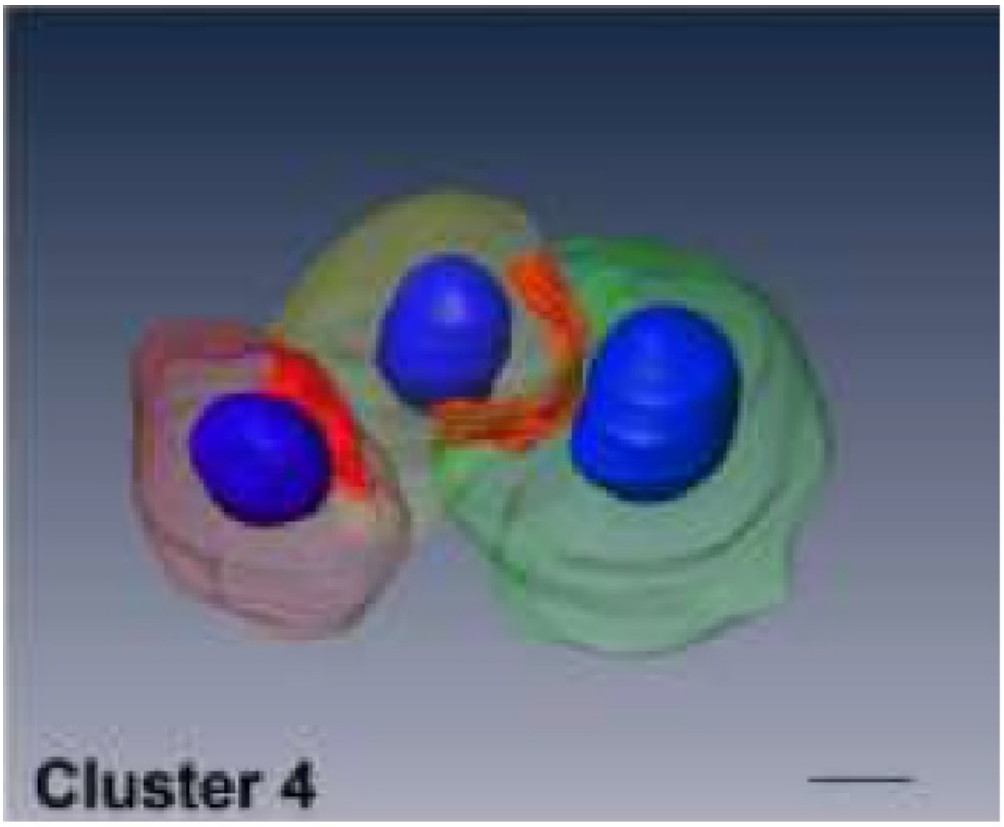

Figure 4.7: Arrangement of three neuron cluster with a three cells (cell1- green cell, cell2 - yellow cell and red cell3) (Potrusil (2013))

The diameter of the cell1 is the biggest $d^1_{soma} = 19.13\mu m$, the middle cell2 - with $d^2_{soma} = 16.17\mu m$ and the smallest one is cell3 - $d^3_{soma} = 14.89\mu m$. The red color - is contact area for two cell1 and cell2, as well as cell2 and cell3. This contact areas have been calculated and between cell1 and cell2 was calculated to be 135.64 μm^2 and the second contact area between cell2 and cell3 is 76.35 μm^2. The cell1 in contact with cell2 represents the 11.8% of the total area and 16.5% of cell2. Cell2 in contact with cell3 at 9.3% of its total surface, whereas for cell3 this contact area represents 11% of total area. The cell2 is connected to other cells and a quarter of it‘s total surface is connected to other somata. The ephaptic coupling was tested as before with current excitation of 0.1nA for the two of cells, when one cell1 stays not stimulated. If only cell2 and cell3 stimulated with 0.1nA and no conductance is considered $gE1$=0 mS/cm^2

and $gE2$=0 mS/cm^2 then the spike height of cell2 is 102.2mV and cell3 is 102.6mV with a delay of 0.648ms for cell2 and 0.636ms for cell3. For $gE1$=3.5 mS/cm^2 and $gE2$=3.5 mS/cm^2 both cells get depolarized and transmit a spike with a delay of 1.116 ms after the current injection of cell2 and cell3. When we will more increase the values $gE1$ and $gE2$ the more synchronized become spikes and the less time delay become between them (see Table 4.12 for $gE1$=6 mS/cm^2 and gE2=6 mS/cm^2). Table 4.12 shows the synchronization of spikes with increasing parameters $gE1$ and $gE2$.

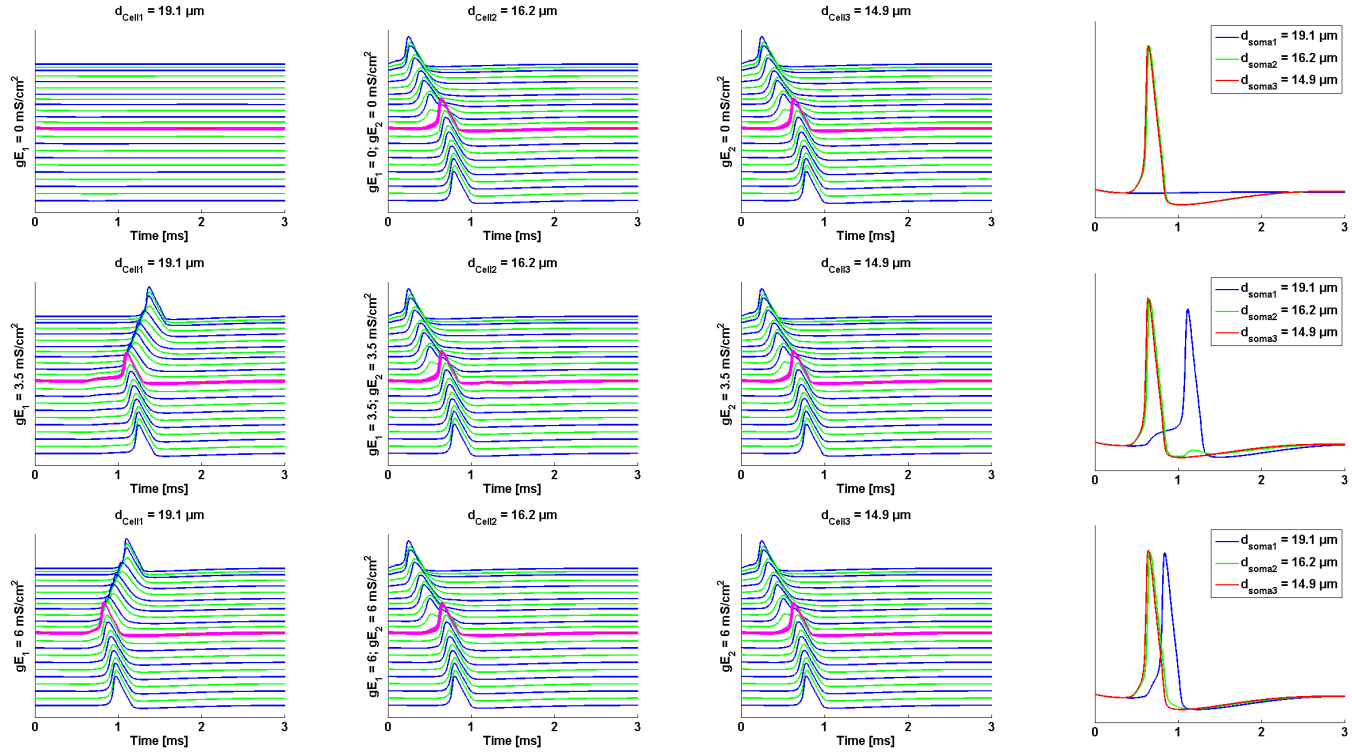

Table 4.12: cell2 and cell3 of the reconstructed tricellular structure are stimulated by 0.1 nA current injection to the peripheral interval. We use a short presomatic compartment (50μm) and their somatic region is surrounded by three membrane layers. Increasing of gE parameter causes synchronization of transmitted signals.

With the long presomatic length, this behavior remains the same. Table 4.13 shows the synchronization of spikes with increasing parameters $gE1$ and $gE2$ for long presomatic length(100μm).

Now make another experiment when the cell1 and cell2 get stimulation of 0.1nA and cell3 doesn‘t receive any stimulating current. The result will be like in a previous experiment, but with no spike for the cell3.

The results for a long presomatic segment(100μm) will be the same as it shown on the Table

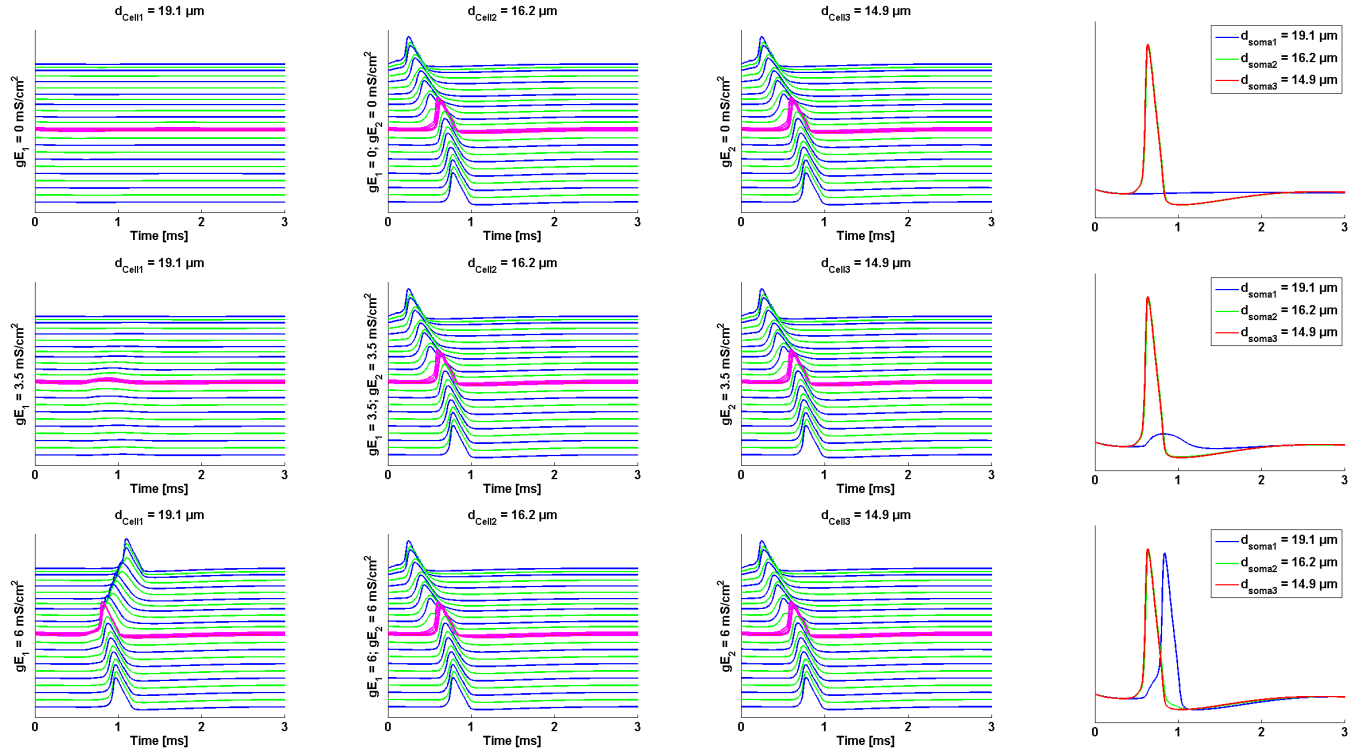

Table 4.13: cell2 and cell3 of the reconstructed tricellular structure are stimulated by 0.1 nA current injection to the peripheral interval. We use a long presomatic compartment ($100\mu m$) and their somatic region is surrounded by three membrane layers. Increasing of gE parameter causes synchronization of transmitted signals.

4.13. and display the same excitation profile as for all three cells when the value of ephaptic conductance increase. If $gE1 > 3.5$ mS/cm^2 and $gE2 > 3.5$ mS/cm^2 will initiate a spike in cell3. When gE1=0 mS/cm^2 and $gE2$=0 mS/cm^2 the spike height for cell1 is 101.6 mV and cell2 is 101.8 mV with a time delay for cell1 0.69ms and 0.68ms for cell2. When $gE1 \geq 3.5$ mS/cm^2 and $gE1 \geq 3.5$ mS/cm^2 the AP_{height} of soma of cell3 is 99.23mV, and it's delayed at the central end since spike arrives at 0.894ms. If we will increase the ephaptic conductance, then more synchronized get cells and the AP of cell3 is increased, whereas the cell2 is decreased and the time delay of the cell3 become less and less in comparison with the cells 1 and 2. Now make another experiment, inject the current 0.1nA for cell1 and cell3, remaining the cell2 with no stimulus. When no ephaptic coupling is considered ($gE1 = 0$ and $gE2 = 0$) and for the short presomatic compartment ($50\mu m$) the difference between the spike of the cell1 and cell3 is greatest, since the soma of cell1 is biggest and the soma of cell3 is smallest. The critical values of $gE1$ and $gE2$ of two cells for tricellular cluster neuron arrangement with the short presomatic compartment ($50\mu m$) were defined from the model as $gE1 \geq 3$ mS/cm^2 and $gE2 \geq 5.5$ mS/cm^2

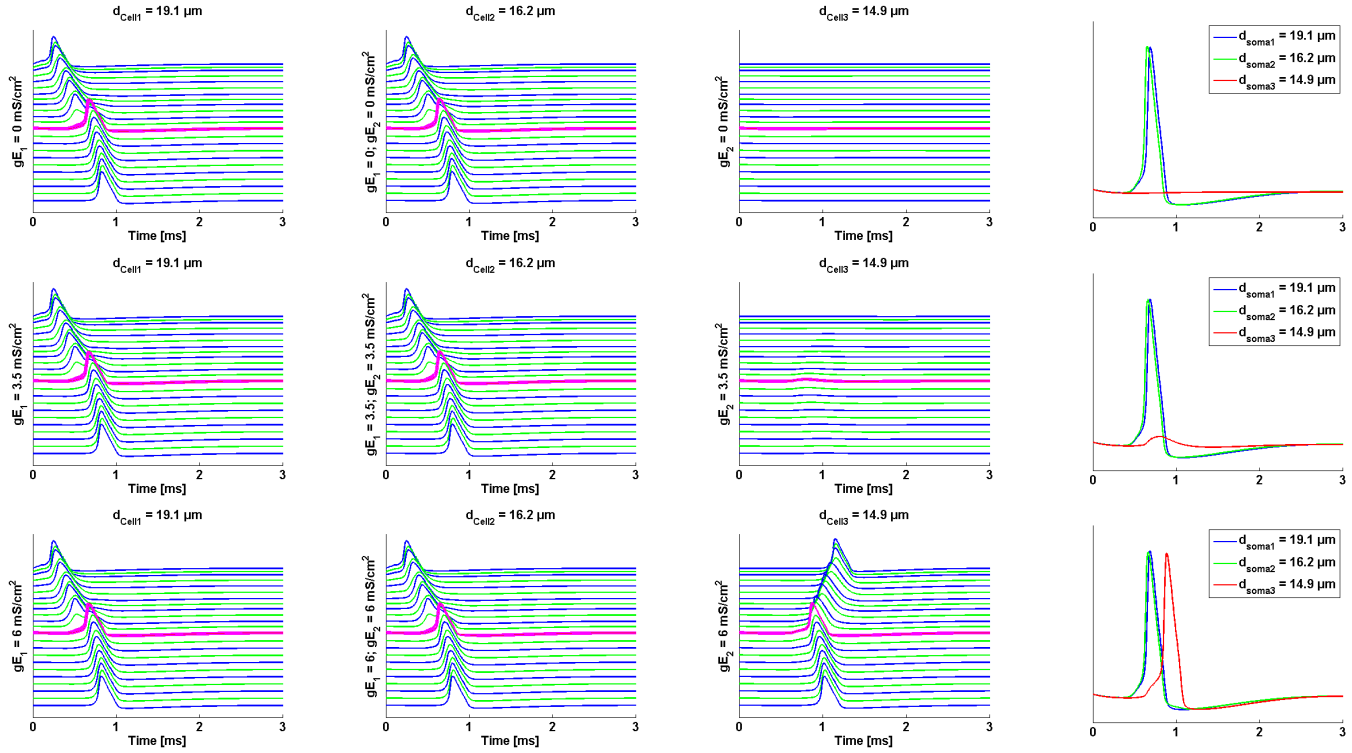

Table 4.14: cell1 and cell2 of the reconstructed tricellular structure are stimulated by 0.1 nA current injection to the peripheral interval. We use a short presomatic compartment($50\mu m$) and their somatic region is surrounded by three membrane layers. Increasing of gE parameter causes synchronization of transmitted signals.

will initiate a spike in cell2 for three membrane layers surrounding the somatic region (nm1=3 and nm2=3).

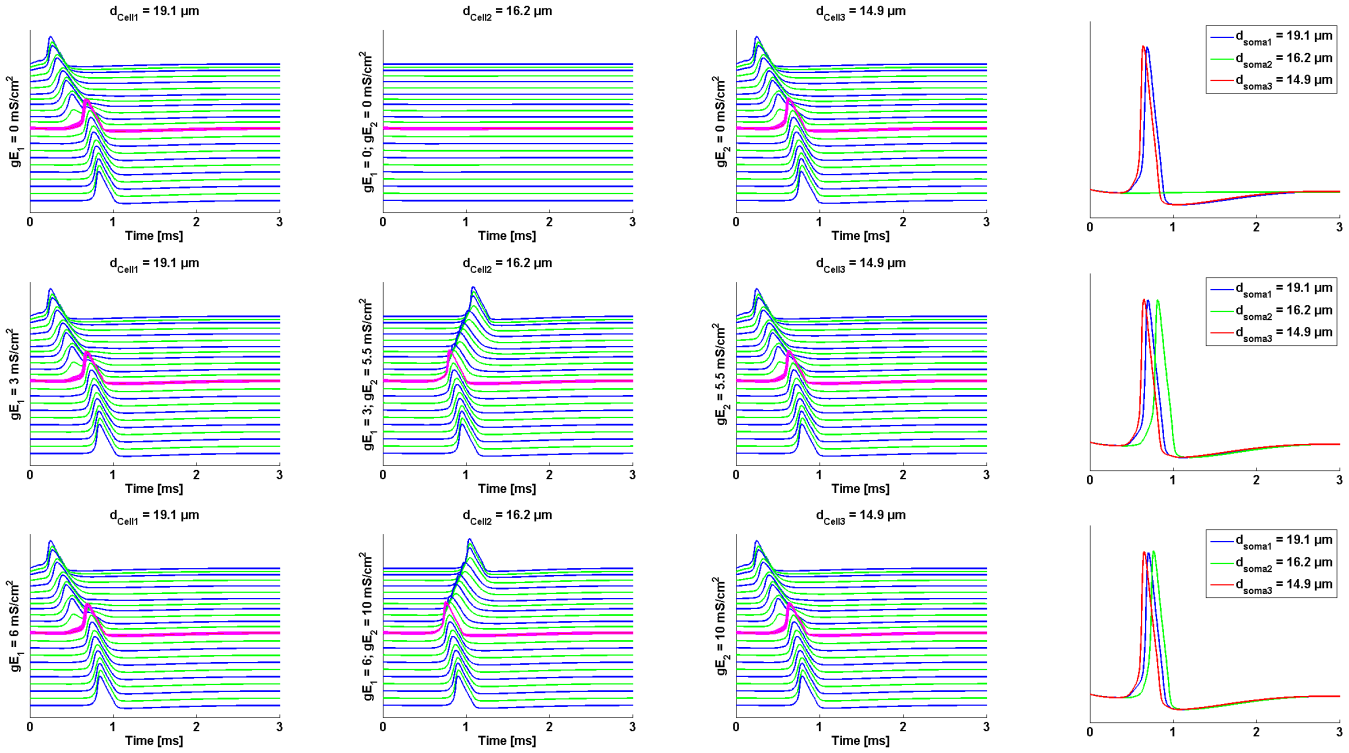

Table 4.15: Short presomatic compartment ($50\mu m$) and the stimulation of cell1 and cell3 by 0.1nA current injection to the peripherial terminal. The values of $gE1$ and $gE2$ are simultaneously raised, different configurations are illustrated above.

Cell2 will be excited by cell3 when $gE1 \geq 3$ mS/cm^2 and $gE2 \geq 5.5$ mS/cm^2. The AP_{height} of cell2 is 101.1mV with a time delay 0.816ms, this is later than for cell1 - 100.6mV with 0.702ms and cell3 - 101.6mV with 0.651ms delay. For $gE1$=6 mS/cm^2 and $gE2$=10 mS/cm^2 can be observed that the spikes get more synchronized in almost equal height of soma and the arrival time as well. For this case illustrated at Table 4.15 (last row) the spike of cell1 arrives at 0.699ms almost at the same time as cell3 - 0.648ms and cell2 - 0.819ms. Now let‘s increase the presomatic compartment to $100\mu m$ and make another experiments for stimulation of cell1 and cell3 by 0.1nA current injection to the peripherial terminal. The critical values of $gE1$ and $gE2$ for tricellular neuron arrangement were found as $gE1 \geq 2$ and $gE2 \geq 2$:

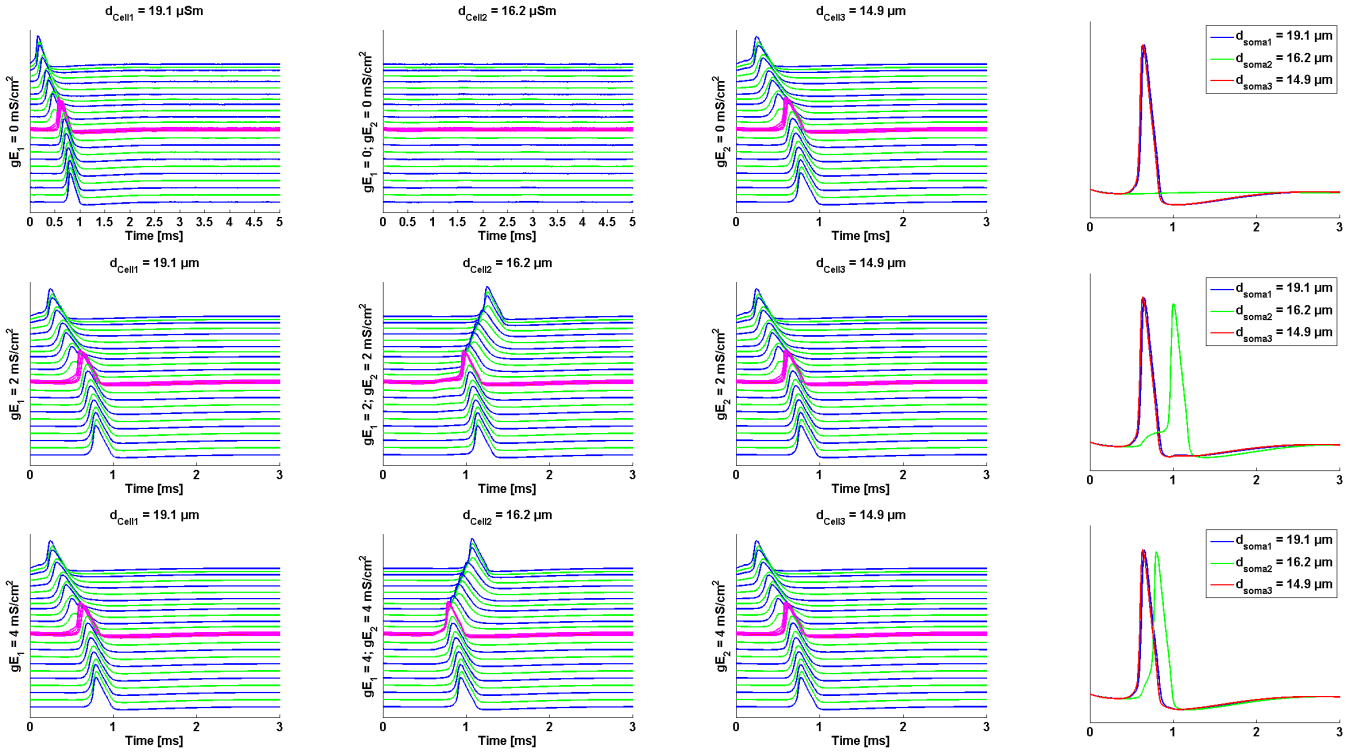

Table 4.16: Long presomatic compartment($100\mu m$) and the stimulation of cell1 and cell3 by 0.1nA current injection to the peripherial terminal. The values of $gE1$ and $gE2$ are simultaneously raised, different configurations are illustrated above.

The critical values of $gE1$ and $gE2$ of two cells for tricellular cluster neuron arrangement with the long presomatic compartment($100\mu m$) were defined from the model as $gE1 \geq 2$ mS/cm^2 and $gE2 \geq 2$ mS/cm^2 will initiate a spike in cell2 for three membrane layers surrounding the somatic region (nm1=3 and nm2=3). When the conductance values are increased cell1 and cell3 are only slightly slower than without ephaptic coupling, but cell2 gets faster and therefore adapts to its companion cells. For this case illustrated at Table 4.16 (last row) the spike of cell1 arrives at 0.654ms almost at the same time as cell3 - 0.633ms and cell2 - 0.801ms. It is necessary to mention that if only ephaptic coupling between cell1 and cell2 is considered, then a combination of conductance values $gE1 \geq 3$ and $gE2$=0 results in successful spike transmission on the cell2. For $gE1$=3 the cell1 and cell3 arrive approximately at the same time - 0.654ms and 0.636ms, whereas the cell2 with a delay of 1.275ms. The next set of experiments consider the case of only stimulating one of three cells with a current injection 0f 0.1nA. Again we varying long and short presomatic compartment as well as current injection into different cells. Firstly, stimulate the cell1 with 0.1nA current injection, with no stimulation for cell2 and cell3 for the

short presomatic compartment ($50\mu m$).

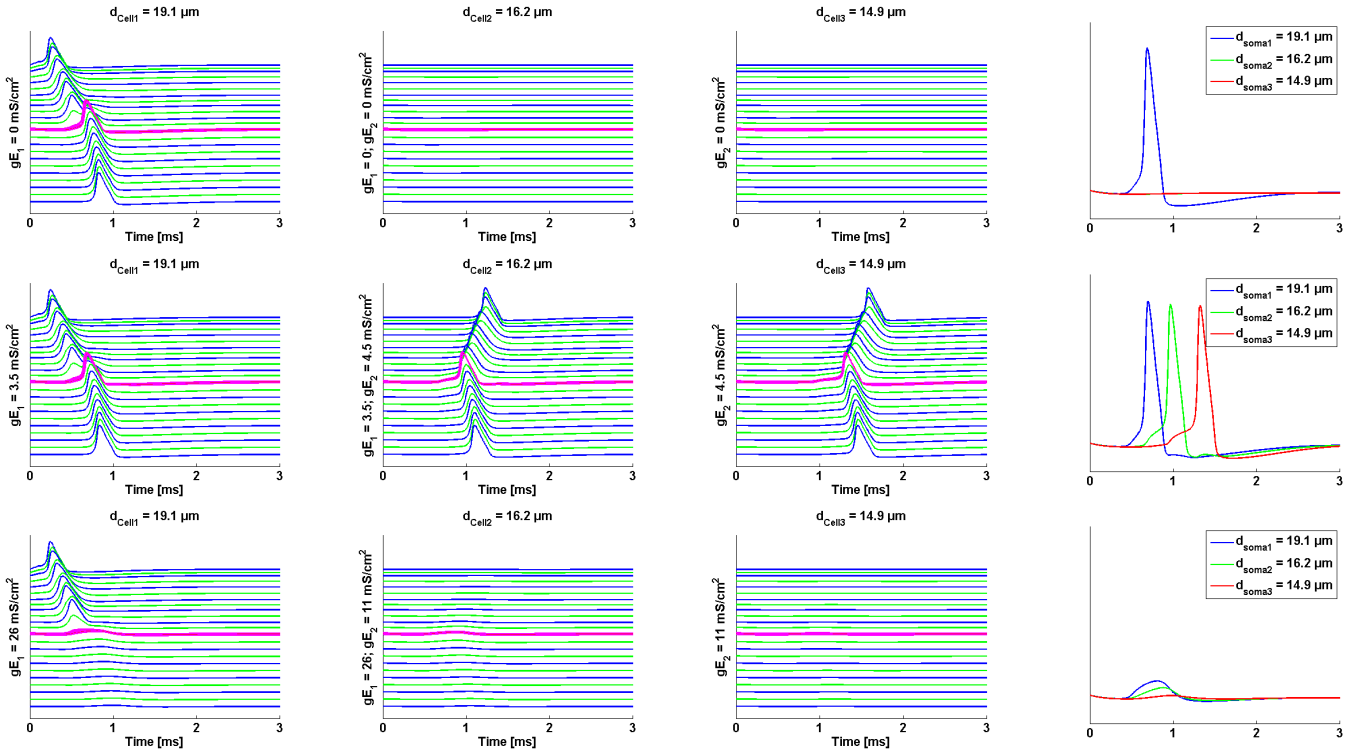

Table 4.17: cell1 of reconstructed tricellular cluster is stimulated by 0.1nA current injection to peripheral interval. The involved neurons feature a short presomatic compartment($50\mu m$) and their somatic region is surrounded by three membrane layers. Ephaptic conductances $gE1$=3.5 mS/cm^2 and $gE2$=4.5 mS/cm^2 ensure aphaptic interaction and successful AP generation at soma of cell2 and cell3.

The critical conductance values for $gE1$ and $gE2$ for a short presomatic compartment($50\mu m$) are 3.5 $\leq$gE1$\leq$ 26 mS/cm^2 and 4.5 $\leq$gE2$\leq$ 11 mS/cm^2. Further increase of $gE1$ and $gE2$ beyond the critical value give no AP in both cells (Table 4.17 - last row). When we change the length of presomatic compartment (now it becomes $100\mu m$). For this case critical values of $gE1$ and $gE2$ lays in the range of $gE1 \geq 3.5$ and 5 $\leq$gE2$\leq$ 21 mS/cm^2. When the values of ephaptic conductances are below this range, then we have only a spike for cell1 with AP_{height} of 103mV and time 0.654ms. If $gE1$= 3.5 mS/cm^2 and $gE2$ =5 mS/cm^2 then the spikes are similar like in Table 4.17 second row, so the both cells are excited by the stimulated cell1. The values of AP_{height} are 101.8mV, 97.36mV, 99.72mV. The spike of cell1 arrives 0.657ms after onset at it's central end, the corresponding values of cell2 and cell3 are 0.957ms and 1.278ms. If we further increase ephaptic conductances $gE1$ and $gE2$ cell2 and cell3 are unable to propagate the spike. The next trials involve current injection of 0.1nA into the other outer cell3 while cell1

and cell2 stay without simulation. For this experiment the length of presomatic compartment doesn‘t change the excitation profiles within the cluster. The results for short length($50\mu m$) are presented on Table 4.18.

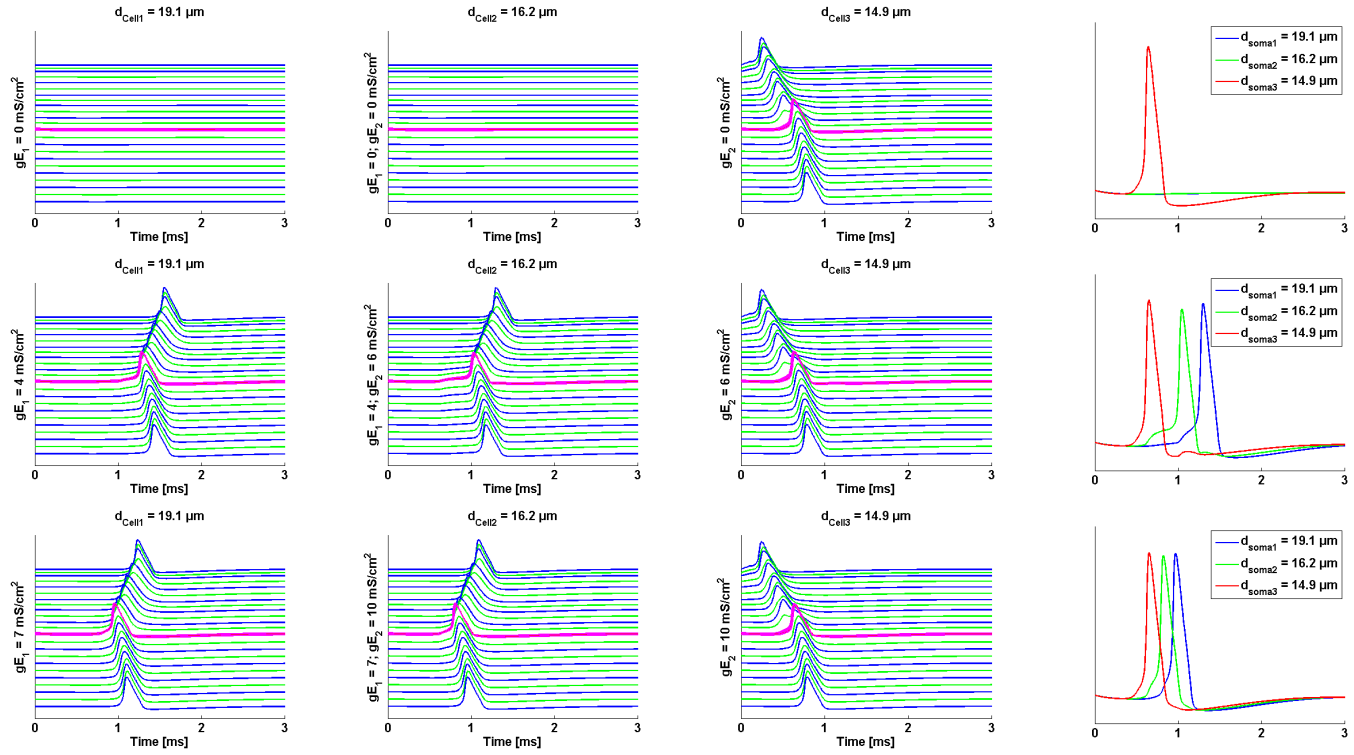

Table 4.18: cell3 of reconstructed tricellular cluster is stimulated by 0.1nA current injection to peripheral interval. The involved neurons feature a short presomatic compartment($50\mu m$) and their somatic region is surrounded by three membrane layers. Ephaptic conductances $gE1$=4 mS/cm^2 and $gE2$=6 mS/cm^2 ensure ephaptic interaction and successful AP generation at soma of cell1 and cell2.

The critical conductance values for $gE1$ and $gE2$ for a short presomatic compartment($50\mu m$) are 3.5 $\leq$gE1$\leq$ 7 and $gE2 \geq 6$.Without ephaptic coupling cell3 produces a spike which has an AP_{height} of 102.2mV at the soma arriving after 0.645ms after spike onset. If $gE1$=4 mS/cm^2 and $gE2$ =6 mS/cm^2 then the spikes are similar like in Table 4.17 second row, so the both cells are excited by the stimulated cell3. The values of AP_{height} are 98.51mV for cell1, 95.02mV for cell2, 101.4mV for cell3. The spike of cell3 arrives 0.651ms after current injection at it‘s central end, the spike of cell2 is the second to arrive at 1.05ms and then cell1 at 1.302ms. If we further increase ephaptic conductances $gE1$ and $gE2$ cell1 and cell3 get more synchronized. These excitation profiles for changing ephaptic conductance values of $gE1$ and $gE2$ are exactly the same as for the long presomatic compartment ($100\mu m$). The critical values for this case a bit

varies 3.5 ≤gE1≤ 6 and $gE2 \geq 6.5$. If $gE1$=4 mS/cm^2 and $gE2$ =6.5 mS/cm^2 then the values of AP_{height} are 100mV for cell1, 96.16mV for cell2, 102.3mV for cell3. The spike of cell3 arrives 0.639ms after current injection at it's central end, the spike of cell2 is the second to arrive at 0.978ms and then cell1 at 1.194ms. If we further increase ephaptic conductances $gE1$ and $gE2$ cell1 and cell3 get more synchronized. The third trial involve current injection of 0.1nA into the other outer cell2 while cell1 and cell3 stay without simulation. For this experiment the length of presomatic compatment doesn't change the excitation profiles within the cluster. The results for long length ($100\mu m$) are presented on Table 4.19.

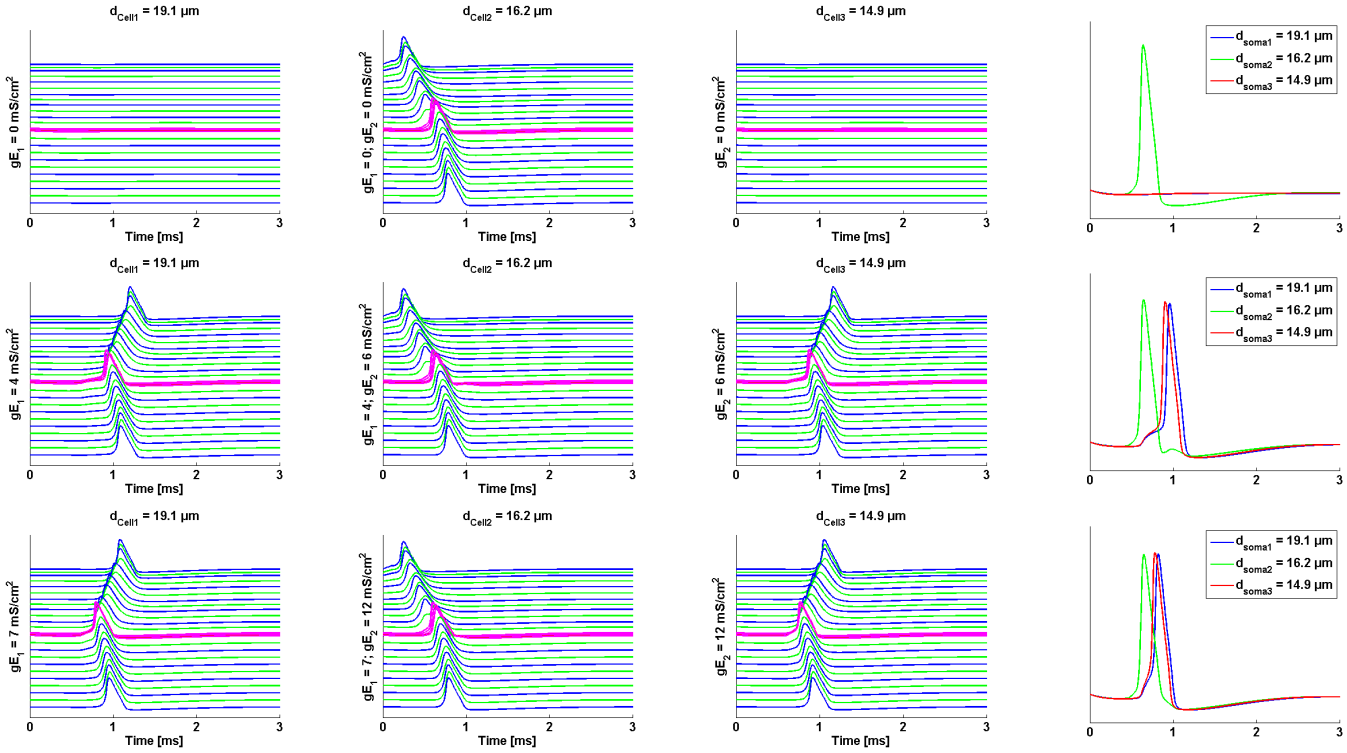

Table 4.19: cell2 of reconstructed tricellular cluster is stimulated by 0.1nA current injection to peripheral interval. The involved neurons feature a long presomatic compartment($100\mu m$) and their somatic region is surrounded by three membrane layers. Ephaptic conductances $gE1$=4 mS/cm^2 and $gE2$=6 mS/cm^2 ensure aphaptic interaction and successful AP generation at soma of cell1 and cell3.

If no ephaptic coupling is considered, cell2 produces a spike with an AP_{height} of 103.2mV at its soma which will arrive after 0.639ms. When $gE1$ and $gE2$ are increased, so the both cells are excited by the stimulated cell2. The values of AP_{height} are 98.87mV for cell1, 101.4mV for cell2, 99.05mV for cell3. The spike of cell2 arrives 0.648ms after current injection at it's central end, the spike of cell3 is the second to arrive at 0.909ms and then cell1 at 0.96ms. If we further

increase ephaptic conductances $gE1$ and $gE2$ leads to further reduction of the spike height of cell2 and faster conduction of cell1 and cell3. The critical conductance values for $gE1$ and $gE2$ for a long presomatic compartment($100\mu m$) are $gE1 \geq 4$ and $gE2 \geq 6$. If the length of presomatic regions are shortened to $50\mu m$ then we have the situation as shown on Table 4.20.

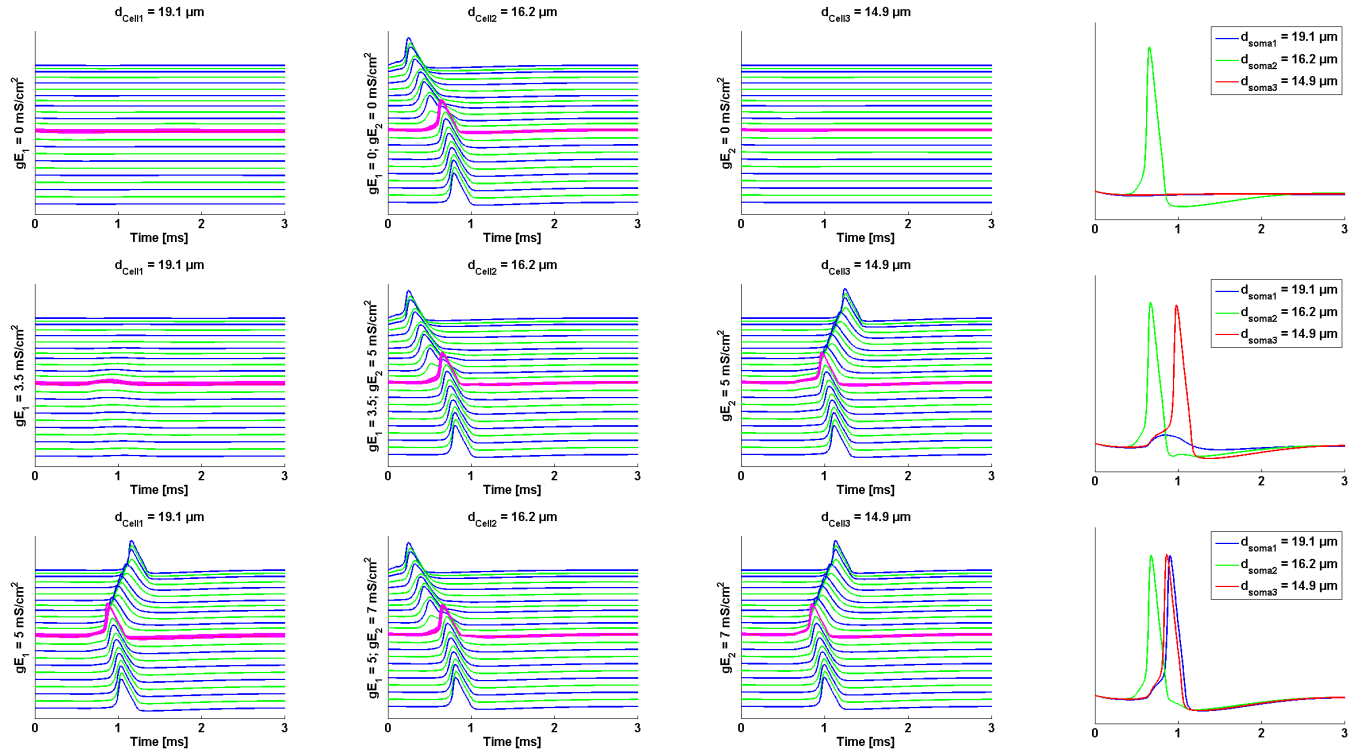

Table 4.20: cell2 of reconstructed tricellular cluster is stimulated by 0.1nA current injection to peripheral interval. The involved neurons feature a short presomatic compartment($50\mu m$) and their somatic region is surrounded by three membrane layers. Ephaptic conductances $gE1$=3.5 cm^2 and $gE2$=5 cm^2 ensure aphaptic interaction and successful AP generation at soma of cell1 and cell3.

The first difference can be seen for the simultaneous increase of the two conductance values, since for $gE1$=3.5 mS/cm^2 and $gE2$=5 mS/cm^2 the spike of cell2 excites the soma3 which successfully transmits a spike to the end, but cell1 still remains silent. When $gE1$ and $gE2$ are increased, so the both cells are excited by the stimulated cell2. The values of AP_{height} are 98.79mV for cell1, 100.4mV for cell2, 100.1mV for cell3. The spike of cell2 arrives 0.678ms after current injection at it's central end, the spike of cell3 is the second to arrive at 0.9ms and then cell1 at 0.984ms. If we further increase ephaptic conductances $gE1$ and $gE2$ leads to further reduction of the spike height of cell2 and faster conduction of cell1 and cell3.

Chapter 5

Cell Synchronization

The origin of the term synchronization comes from the Greek and it means ‘occurring in the common time‘ (Pikovsky et al. 2001). The original meaning of the synchronization has been maintained up to now in the colloquial use if the word, as the capacity of the objects of different nature to acquire a common regime. Synchronization phenomena are abundant in science, nature engineering and social life. Systems are diverse as firing neurons and applauding audiences exhibit a tendency to operate in synchrony. In case two cells, which are coupled with each other and the coupling factor induces an adjustment of the rhythms leading to a mutual synchronization. In this case we have a *bidirectional coupling*. Another situation is described by a u*unidirectional coupling*. Here one system evolves freely and drives the evolution of the other, so the response system is slaved to follow the dynamics of the driver system which acts as an external forcing.

5.1 Noise Effects

Now we will include noise:

$$I_{noise,n} = GAUSS \cdot k_{noise}\sqrt{A_n \cdot g_{Na}} \tag{5.1}$$

where GAUSS is a Gaussian noise current term(mean=0, S.D.=1) that changes it's value every $2.5\mu s$, k_{noise}= 0.05 $\mu A \mathrm{mS}^{-1/2}$ - factor common to all compartments, A_n denotes membrane area in cm^2 and g_{Na} is the maximum sodium conductance per square unit.(Rattay et al. 2001a). In our experiments we will increase the maximum sodium conductance per square unit(g_{Na}) , and meanwhile increase the noise current, which depends on the g_{Na}. In each case parameter g_{Na} for human soma will be increased from 140mS cm^{-2} till 240mS cm^{-2}as well as for the regions simulated with a 10-fold channel density the maximum sodium conductance per square unit will be simulated from 1400mS cm^{-2} till 2400mS cm^{-2}.

5.2 Unidirectional Coupling

The ephaptic coupling was tested with current excitation of 0.1nA for only one of two cells(Figure 5.1), when only cell1 stay stimulated.

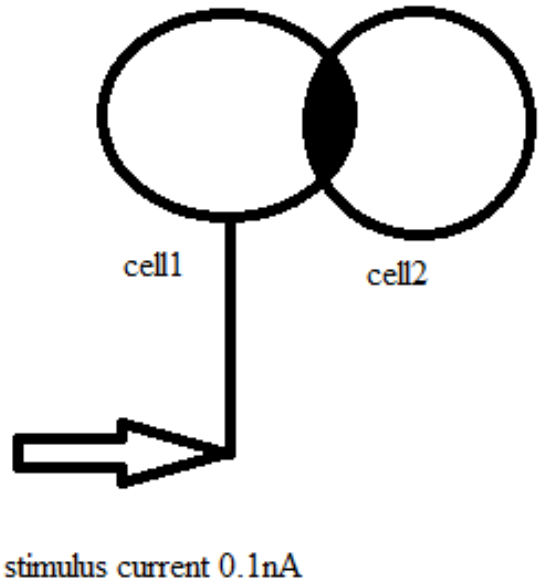

Figure 5.1: The stimulation of only cell1 in a cluster

5.2.1 Cluster1

Make the experiment for the first cluster when the first cell received current impulse 0.1nA, including noise factor k_{noise}=0.05 $\mu A\text{mS}^{-1/2}$, when the conductance parameter gE=0 mS/cm^2:

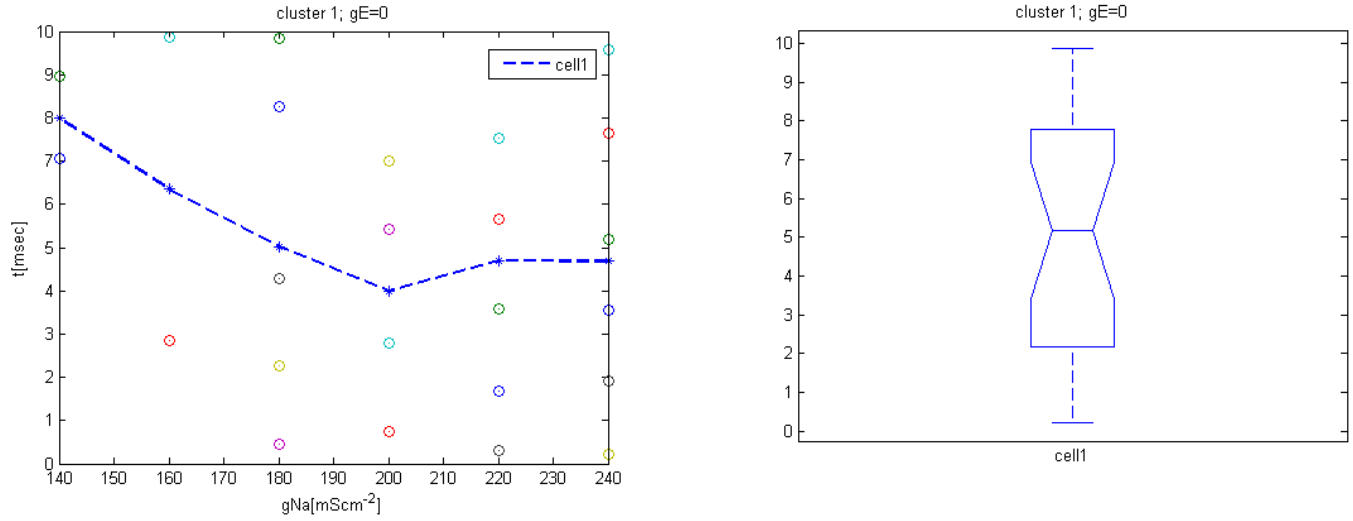

Table 5.1: cell1 of the reconstructed bicellular structure are stimulated by 0.1 nA current injection to the peripheral interval with using noise factor k_{noise}= 0.05 $\mu A\text{mS}^{-1/2}$ and increasing parameter gNa from 140-240 mS cm^{-2} for gE=0 mS/cm^2

Another experiments will be done also for the first cluster for the increasing parameter gE=2

mS/cm^2 including noise factor k_{noise}= 0.05 $\mu A \mathrm{mS}^{-1/2}$:

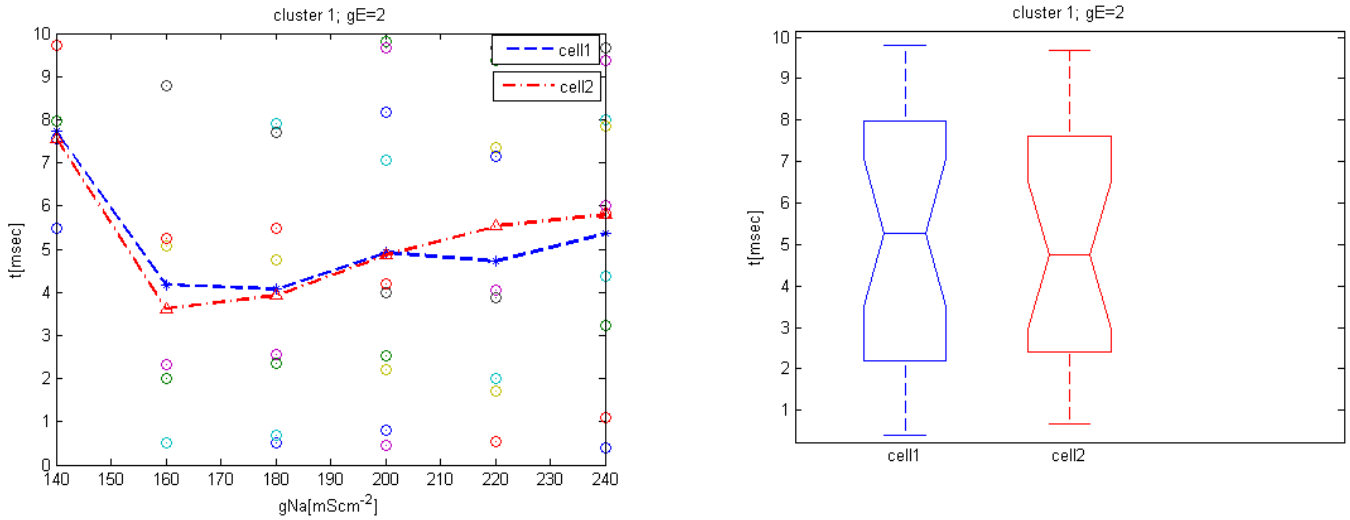

Table 5.2: cell1 of the reconstructed bicellular structure are stimulated by 0.1 nA current injection to the peripheral interval with using noise factor k_{noise}= 0.05 $\mu A \mathrm{mS}^{-1/2}$ and increasing parameter gNa from 140-240 mS cm^{-2} for gE=2 mS/cm^2

Now increase parameter gE=4 mS/cm^2 including noise factor k_{noise}= 0.05 $\mu A \mathrm{mS}^{-1/2}$:

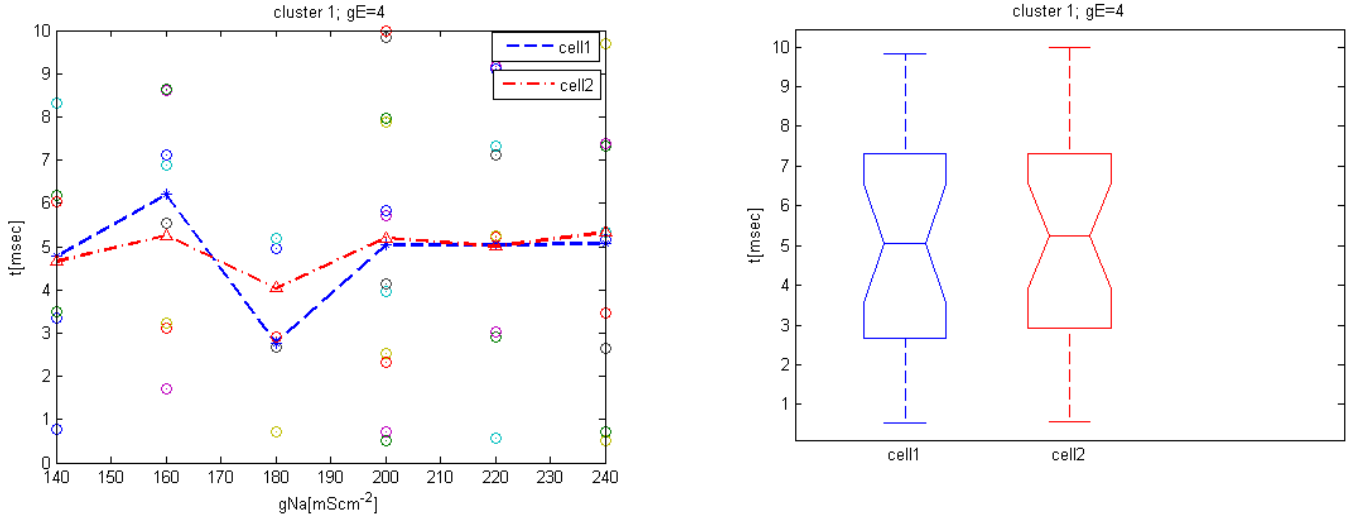

Table 5.3: cell1 of the reconstructed bicellular structure are stimulated by 0.1 nA current injection to the peripheral interval with using noise factor k_{noise}= 0.05 $\mu A \mathrm{mS}^{-1/2}$ and increasing parameter gNa from 140-240 mS cm^{-2} for gE=4 mS/cm^2

Conclusion: As we can see for the first cluster with the increasing parameter gE=0 mS/cm^2 till gE=4 mS/cm^2 signal becomes more and more synchronized, the maximum and minimum values of two cells becomes closer and the effect of synchronization occur.

5.2.2 Cluster2

Make the experiment for the second cluster when the first and second cells received current impulse 0.1nA, including noise factor k_{noise}= 0.05 $\mu A \mathrm{mS}^{-1/2}$, when the conductance parameter gE=0 mS/cm^2:

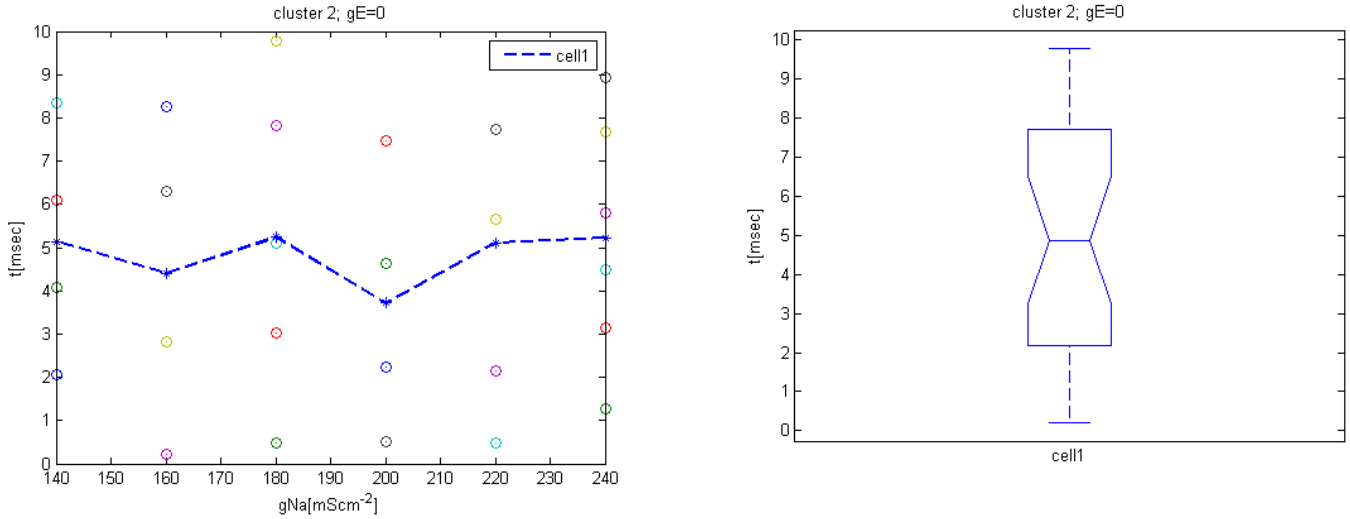

Table 5.4: cell1 of the reconstructed bicellular structure are stimulated by 0.1 nA current injection to the peripheral interval with using noise factor k_{noise}= 0.05 $\mu A \mathrm{mS}^{-1/2}$ and increasing parameter gNa from 140-240 mS cm^{-2} for gE=0 mS/cm^2

Another experiments will be done for the second cluster for the increasing parameter gE=2 mS/$cm^2$2 including noise factor k_{noise}= 0.05 $\mu A \mathrm{mS}^{-1/2}$:

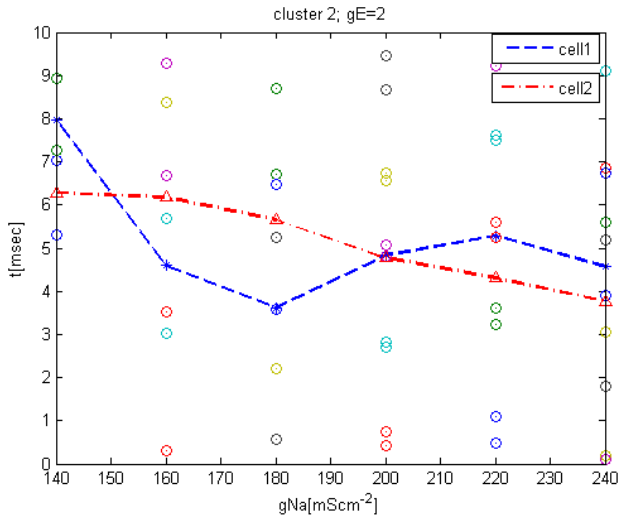

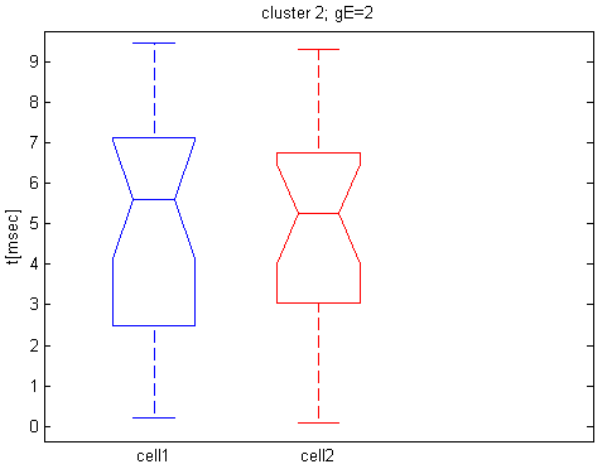

Table 5.5: cell1 of the reconstructed bicellular structure are stimulated by 0.1 nA current injection to the peripheral interval with using noise factor k_{noise}= 0.05 $\mu A\text{mS}^{-1/2}$ and increasing parameter gNa from 140-240 mS cm^{-2} for gE=2 mS/cm^2

Now increase parameter gE=4mS/cm^2 including noise factor k_{noise}= 0.05 $\mu A\text{mS}^{-1/2}$:

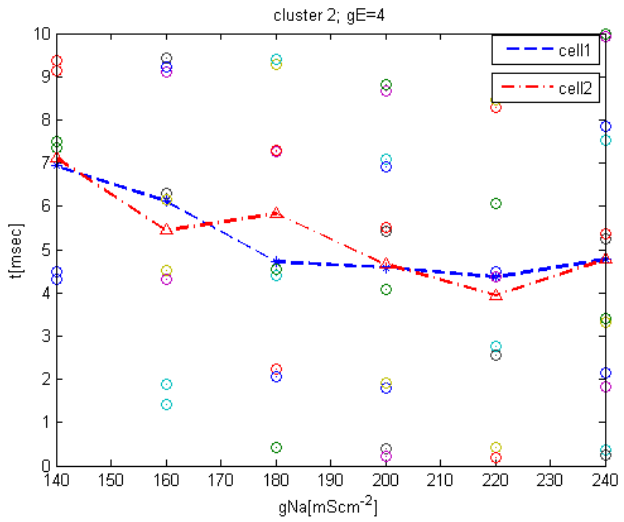

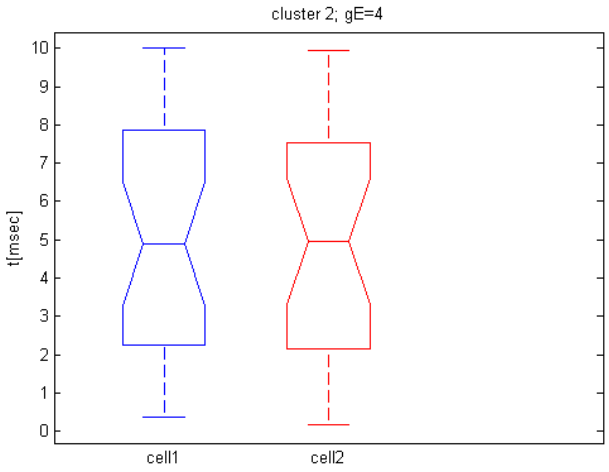

Table 5.6: cell1 of the reconstructed bicellular structure are stimulated by 0.1 nA current injection to the peripheral interval with using noise factor k_{noise}= 0.05 $\mu A\text{mS}^{-1/2}$ and increasing parameter gNa from 140-240 mS cm^{-2} for gE=4 mS/cm^2

Conclusion: As we can see for the second cluster with the increasing parameter gE=0mS/cm^2 till gE=4 mS/cm^2 signal becomes more and more synchronized, thus the mean values of two cells becomes closer and the effect of synchronization between two cells become more evident.

5.2.3 Cluster3

Make the experiment for the cluster3 when the first and second cells received current impulse 0.1nA, including noise factor k_{noise}= 0.05 $\mu A \mathrm{mS}^{-1/2}$, when the conductance parameter gE=0 mS/cm^2:

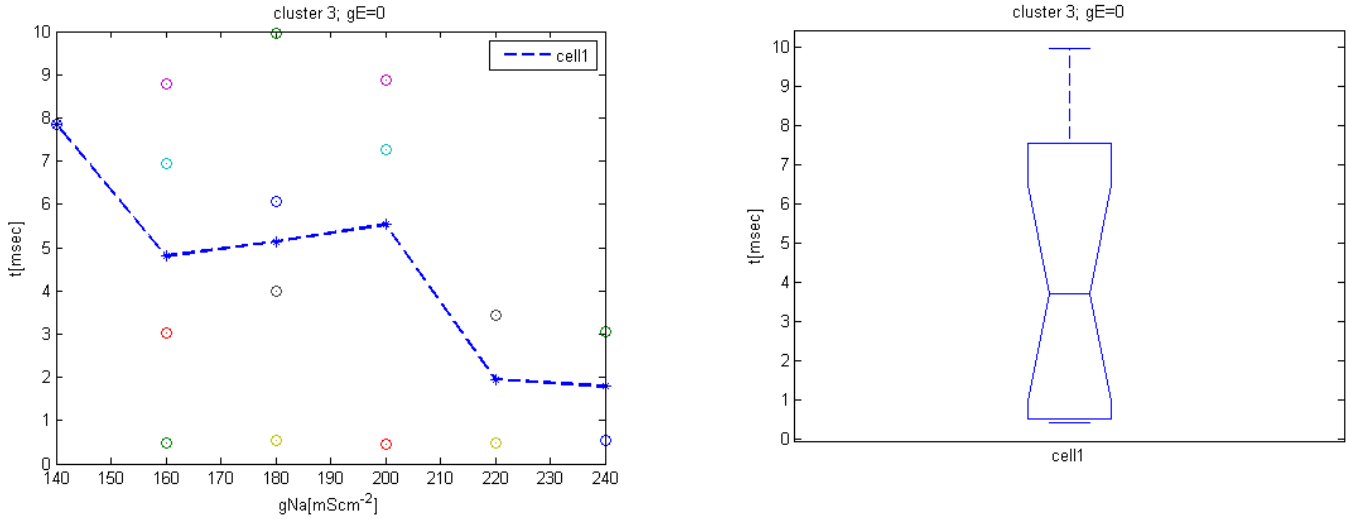

Table 5.7: cell1 of the reconstructed bicellular structure are stimulated by 0.1 nA current injection to the peripheral interval with using noise factor k_{noise}= 0.05 $\mu A \mathrm{mS}^{-1/2}$ and increasing parameter gNa from 140-240 mS cm^{-2} for gE=0 mS/cm^2

Another experiments will be done for the third cluster for the increasing parameter gE=2 mS/cm^2 including noise factor k_{noise}= 0.05 $\mu A \mathrm{mS}^{-1/2}$:

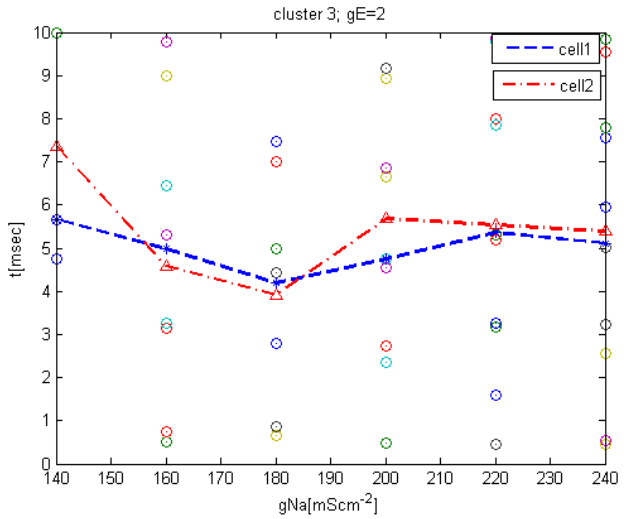

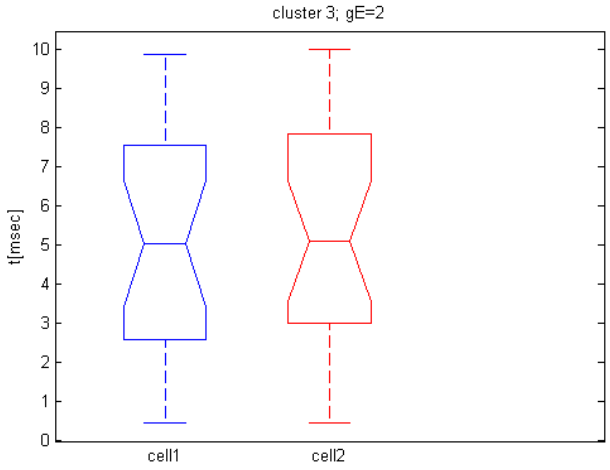

Table 5.8: cell1 of the reconstructed bicellular structure are stimulated by 0.1 nA current injection to the peripheral interval with using noise factor k_{noise}= 0.05 $\mu A \mathrm{mS}^{-1/2}$ and increasing parameter gNa from 140-240 mS cm^{-2} for gE=2 mS/cm^2

Now increase parameter gE=4 mS/cm^2 including noise factor k_{noise} for the second cluster= 0.05 $\mu A \mathrm{mS}^{-1/2}$:

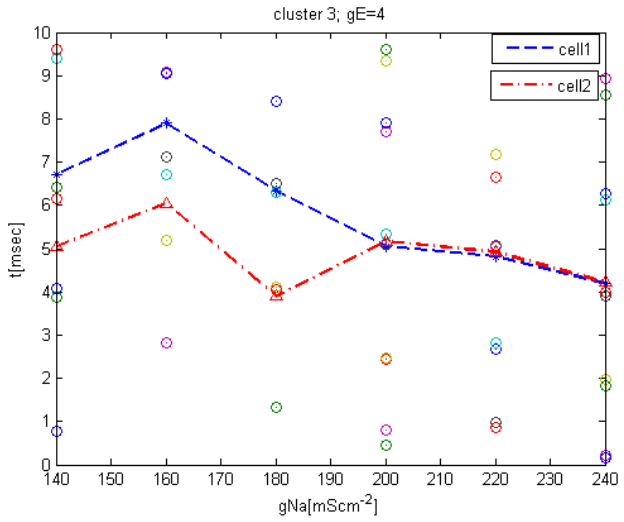

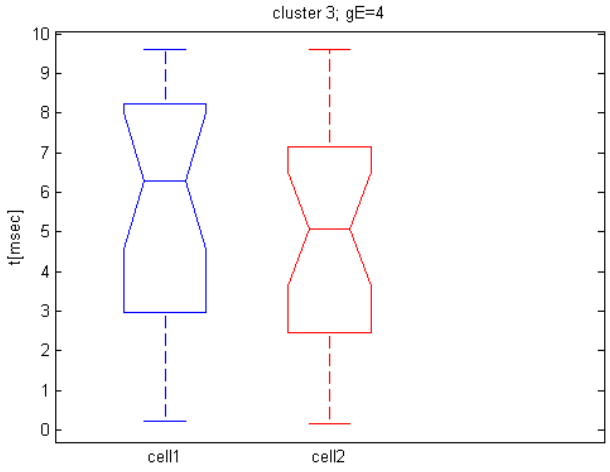

Table 5.9: cell1 of the reconstructed bicellular structure are stimulated by 0.1 nA current injection to the peripheral interval with using noise factor k_{noise}= 0.05 $\mu A \mathrm{mS}^{-1/2}$ and increasing parameter gNa from 140-240 mS cm^{-2} for gE=4 mS/cm^2

5.2.4 Cluster4

The ephaptic coupling was tested as before with current excitation of 0.1nA for the three of cells(Figure 5.2)

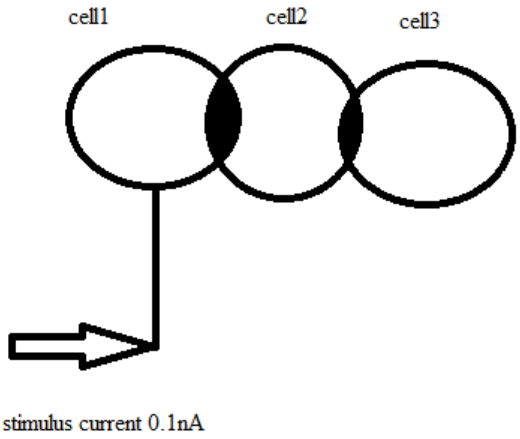

Figure 5.2: The stimulation of only cell1 in a cluster

When all the cells stay stimulated and conductance is considered $gE1$=0 mS/cm^2 and $gE2$=0 mS/cm^2:

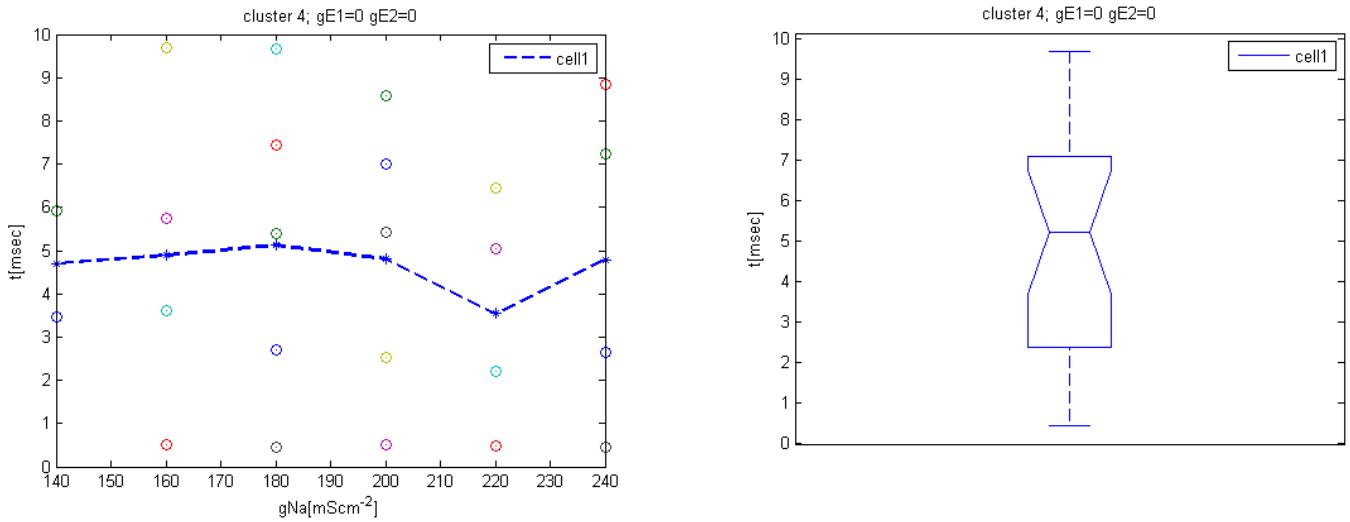

Table 5.10: cell1 of the reconstructed tricellular structure are stimulated by 0.1 nA current injection to the peripheral interval with using noise factor k_{noise}= 0.05 $\mu A \mathrm{mS}^{-1/2}$ and increasing parameter gNa from 140-240 mS cm^{-2} for $gE1$=0 mS/cm^2 and $gE2$=0 mS/cm^2.

In the next experiment the current excitation of 0.1nA for the three of cells, when all the cells stay stimulated and conductance is considered $gE1$=0 mS/cm^2 and $gE2$=2 mS/cm^2:

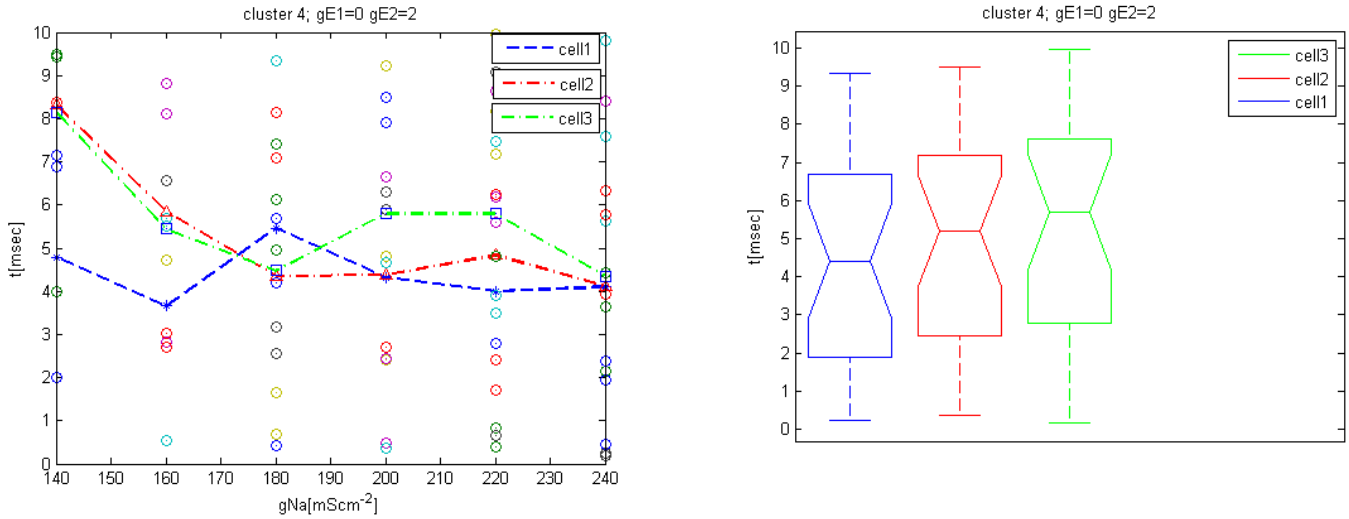

Table 5.11: cell1 of the reconstructed tricellular structure are stimulated by 0.1 nA current injection to the peripheral interval with using noise factor k_{noise}= 0.05 $\mu A\text{mS}^{-1/2}$ and increasing parameter gNa from 140-240 mS cm^{-2} for $gE1$=0 mS/cm^2 and $gE2$=2 mS/cm^2.

Another experiments will be done for the fourth cluster for the increasing parameter $gE1$=2 mS/cm^2 and $gE2$=0 mS/cm^2 including noise factor k_{noise}= 0.05 $\mu A\text{mS}^{-1/2}$:

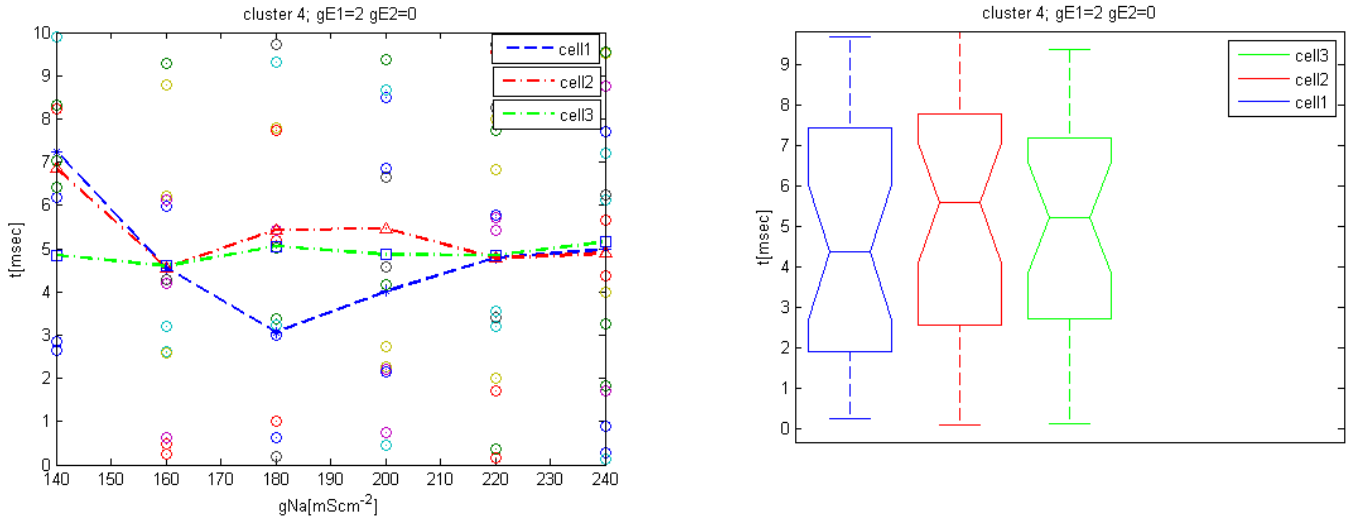

Table 5.12: cell1 of the reconstructed tricellular structure are stimulated by 0.1 nA current injection to the peripheral interval with using noise factor k_{noise}= 0.05 $\mu A\text{mS}^{-1/2}$ and increasing parameter gNa from 140-240 mS cm^{-2} for $gE1$=2 mS/cm^2 and $gE2$=0 mS/cm^2.

Another experiments will be done for the increasing parameter $gE1$=2 mS/cm^2 and $gE2$=2 mS/cm^2 including noise factor k_{noise}= 0.05 $\mu A\text{mS}^{-1/2}$:

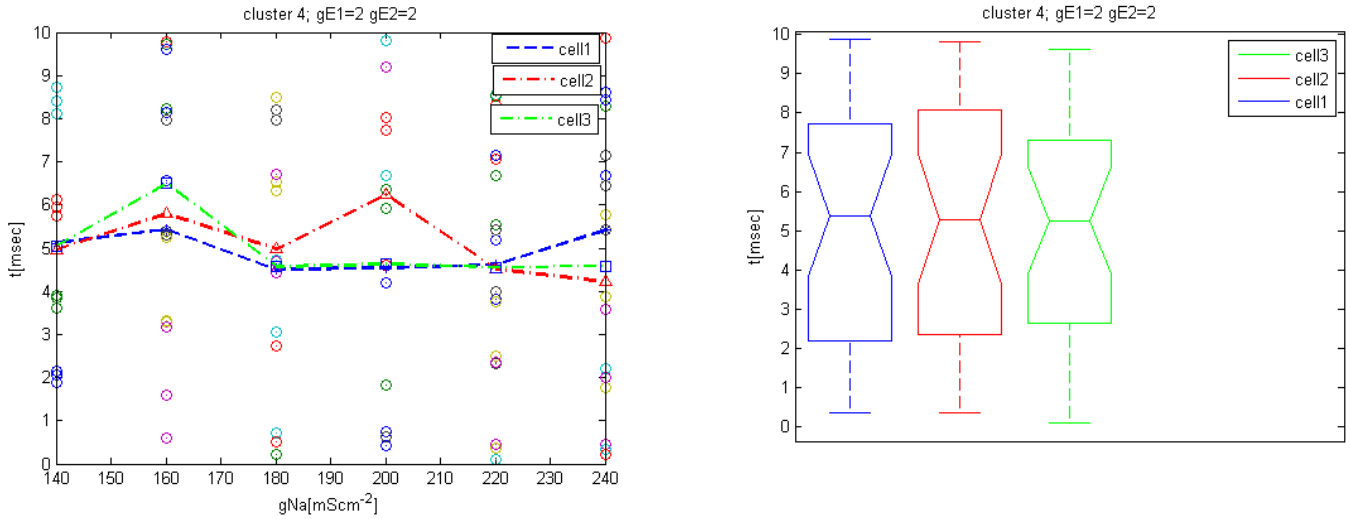

Table 5.13: cell1 of the reconstructed tricellular structure are stimulated by 0.1 nA current injection to the peripheral interval with using noise factor k_{noise}= 0.05 $\mu A \mathrm{mS}^{-1/2}$ and increasing parameter gNa from 140-240 mS cm^{-2} for $gE1$=2 mS/cm^2 and $gE2$=2 mS/cm^2.

In the next experiment the current excitation of 0.1nA for the three of cells, when all the cells stay stimulated and conductance is considered $gE1$=0 mS/cm^2,$gE2$=4 mS/cm^2 :

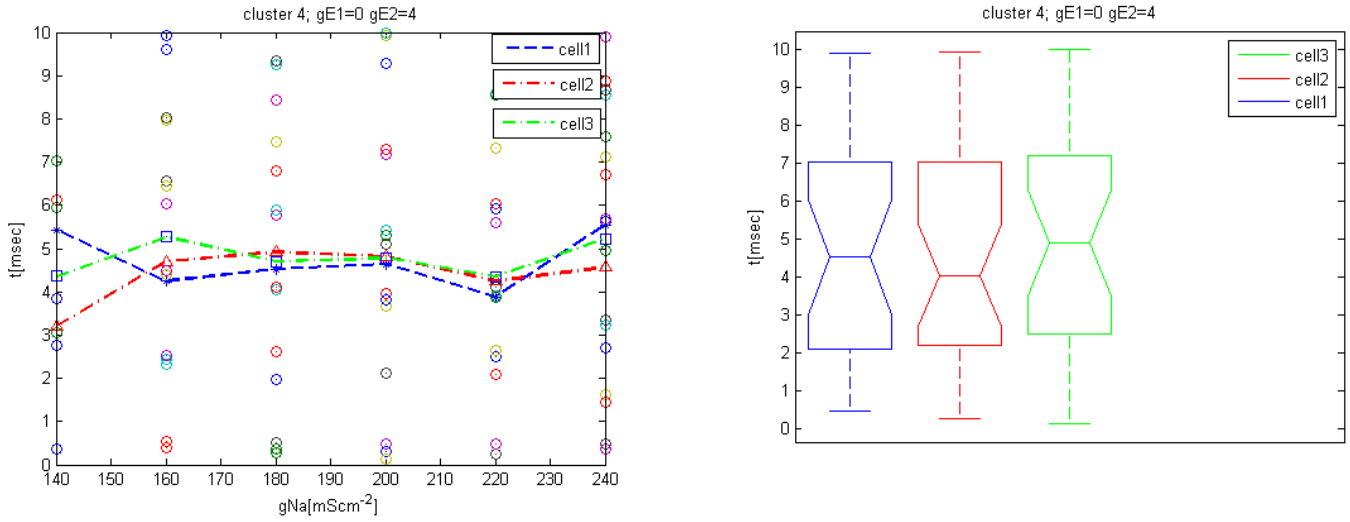

Table 5.14: cell1 of the reconstructed tricellular structure are stimulated by 0.1 nA current injection to the peripheral interval with using noise factor k_{noise}= 0.05 $\mu A \mathrm{mS}^{-1/2}$ and increasing parameter gNa from 140-240 mS cm^{-2} for $gE1$=0 mS/cm^2 and $gE2$=4 mS/cm^2.

Another experiments will be done for the increasing parameter $gE1$=4 mS/cm^2,$gE2$=0 mS/cm^2 including noise factor k_{noise}= 0.05 $\mu A \mathrm{mS}^{-1/2}$:

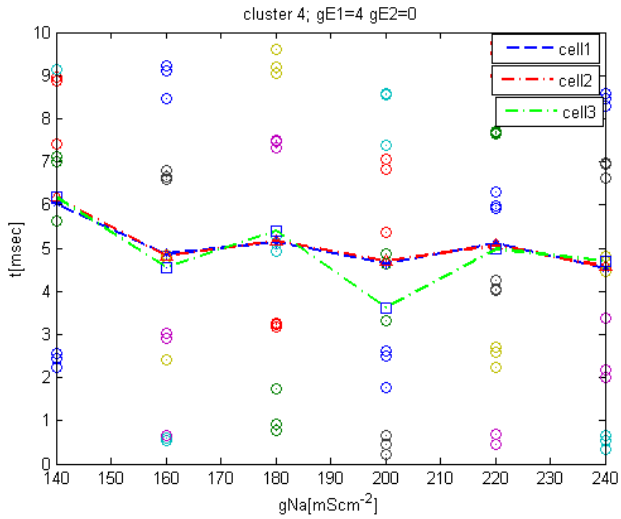

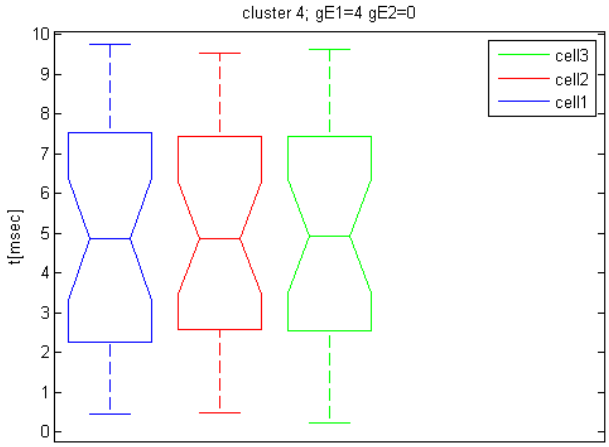

Table 5.15: cell1 of the reconstructed tricellular structure are stimulated by 0.1 nA current injection to the peripheral interval with using noise factor k_{noise}= 0.05 $\mu A \mathrm{mS}^{-1/2}$ and increasing parameter gNa from 140-240 mS cm^{-2} for $gE1$=4 mS/cm^2 and $gE2$=0 mS/cm^2.

At the end when $gE1$=4 mS/cm^2,$gE2$=4 mS/cm^2 including noise factor k_{noise}= 0.05 $\mu A \mathrm{mS}^{-1/2}$

:

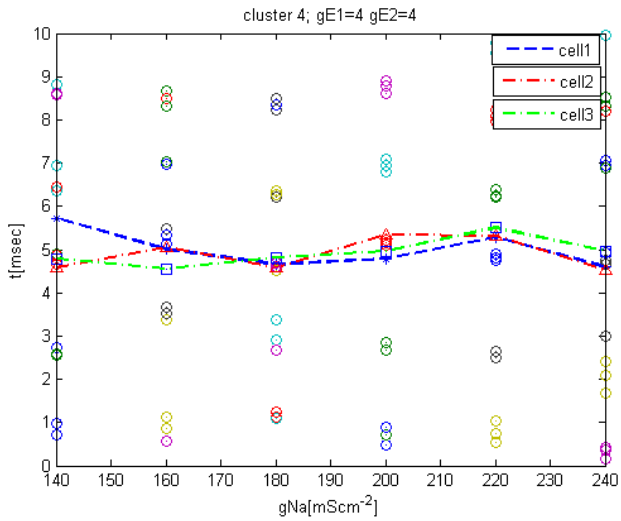

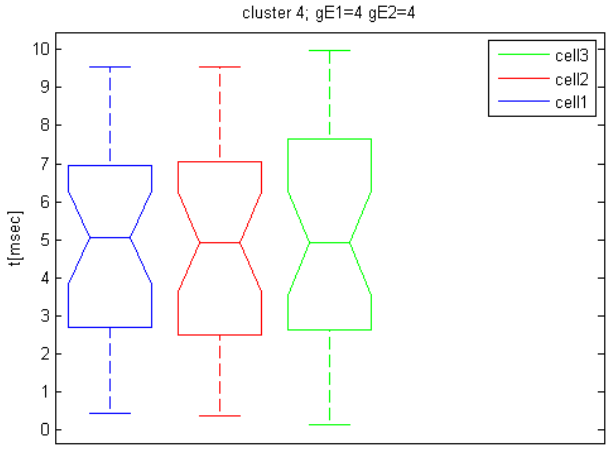

Table 5.16: cell1 of the reconstructed tricellular structure are stimulated by 0.1 nA current injection to the peripheral interval with using noise factor k_{noise}= 0.05 $\mu A \mathrm{mS}^{-1/2}$ and increasing parameter gNa from 140-240 mS cm^{-2} for $gE1$=4 mS/cm^2 and $gE2$=4 mS/cm^2.

Conclusion: As we can see for the fourth cluster with the increasing parameter $gE1$=0 mS/cm^2 and $gE2$=0 mS/cm^2 till $gE1$=4 mS/cm^2 and $gE2$=4 mS/cm^2 signal becomes more and more synchronized, thus the mean values, max and min values of two cells becomes closer and the effect of synchronization between two cells occur.

5.3 Bidirectional Coupling

The ephaptic coupling was tested with current excitation of 0.1nA for the two of cells(Figure 5.3), when all the cells stay stimulated.

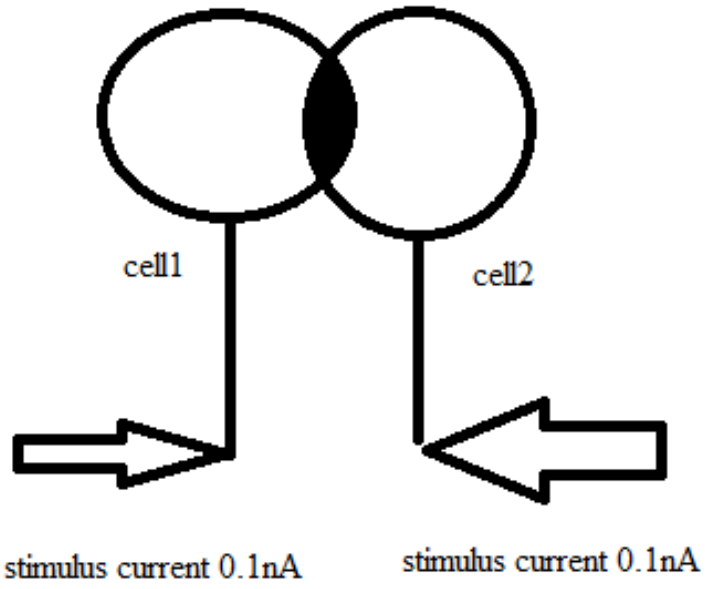

Figure 5.3: The stimulation of two cells in a cluster

5.3.1 Cluster1

Make the experiment for the first cluster when the first and second cells received current impulse 0.1nA, including noise factor k_{noise}= 0.05 $\mu A \mathrm{mS}^{-1/2}$, when the conductance parameter gE=0 mS/cm^2:

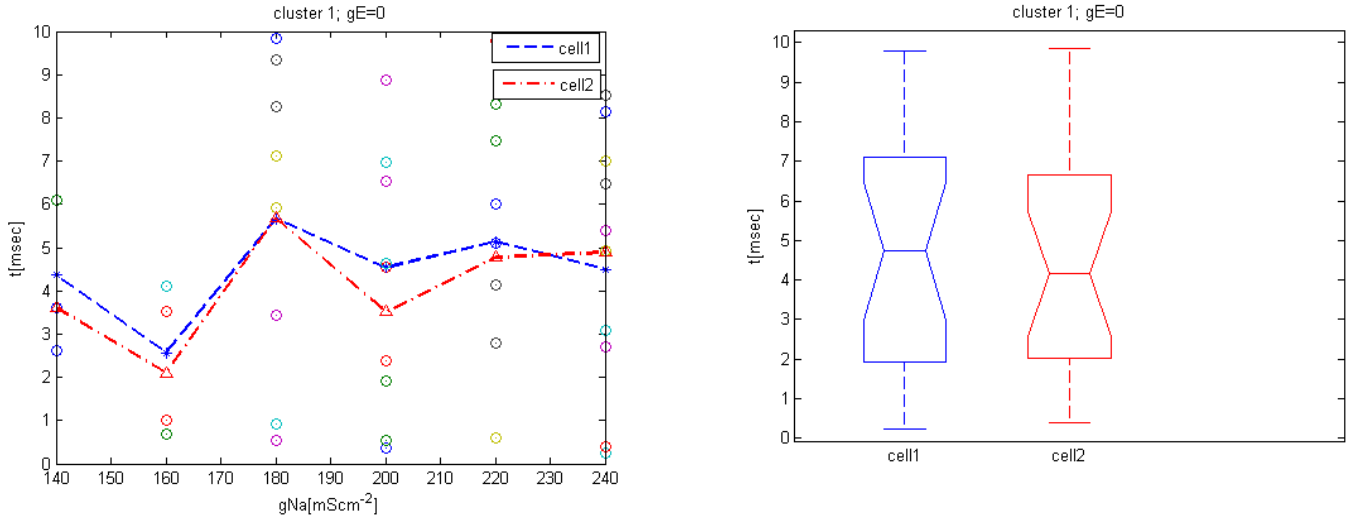

Table 5.17: cell1 and cell2 of the reconstructed bicellular structure are stimulated by 0.1 nA current injection to the peripheral interval with using noise factor k_{noise}= 0.05 $\mu A \mathrm{mS}^{-1/2}$ and increasing parameter gNa from 140-240 mS cm^{-2} for gE=0 mS/cm^2

Another experiments will be done also for the first cluster for the increasing parameter gE=2 mS/cm^2including noise factor k_{noise}= 0.05 $\mu A \mathrm{mS}^{-1/2}$:

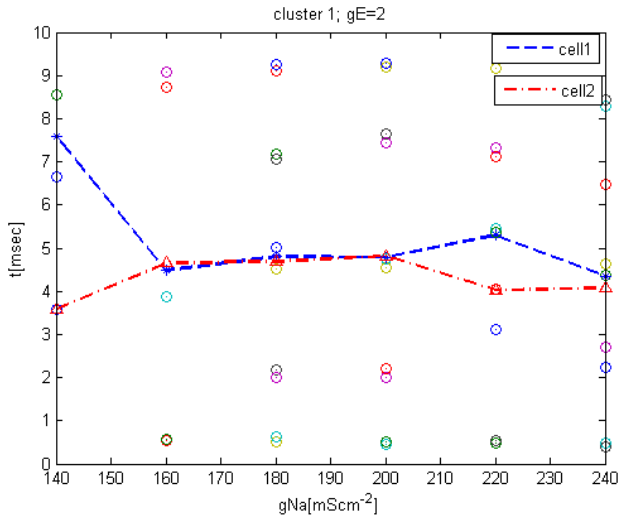

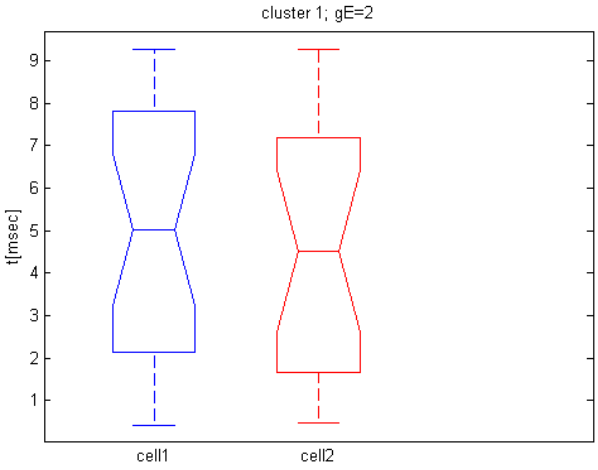

Table 5.18: cell1 and cell2 of the reconstructed bicellular structure are stimulated by 0.1 nA current injection to the peripheral interval with using noise factor k_{noise}= 0.05 $\mu A \mathrm{mS}^{-1/2}$ and increasing parameter gNa from 140-240 mS cm^{-2} for gE=2 mS/cm^2

Now increase parameter gE=4 mS/cm^2 including noise factor k_{noise}= 0.05 $\mu A \mathrm{mS}^{-1/2}$:

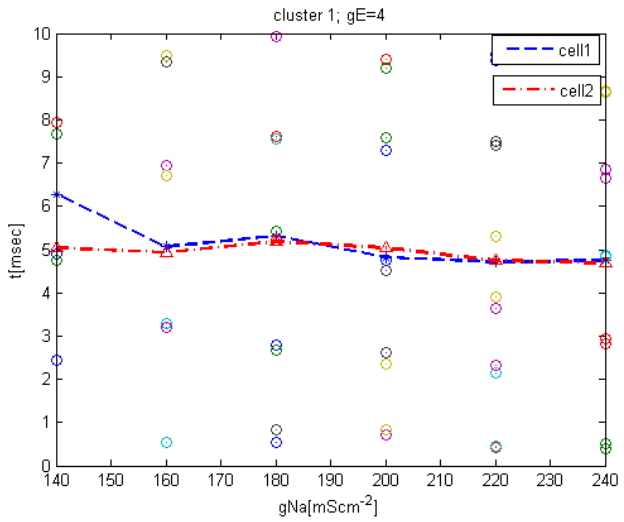

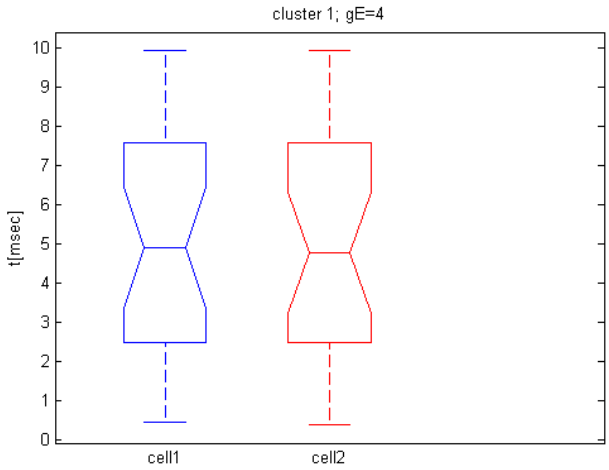

Table 5.19: cell1 and cell2 of the reconstructed bicellular structure are stimulated by 0.1 nA current injection to the peripheral interval with using noise factor k_{noise}= 0.05 $\mu A \mathrm{mS}^{-1/2}$ and increasing parameter gNa from 140-240 mS cm^{-2} for gE=4 mS/cm^2

Conclusion: As we can see for the first cluster with the increasing parameter gE=0 mS/cm^2 till gE=4 mS/cm^2 signal becomes more and more synchronized, thus the mean values of two cells becomes closer and the effect of synchronization between two cells become more evident.

5.3.2 Cluster2

Make the experiment for the second cluster when the first and second cells received current impulse 0.1nA, including noise factor k_{noise}= 0.05 $\mu A \mathrm{mS}^{-1/2}$, when the conductance parameter gE=0 mS/cm^2:

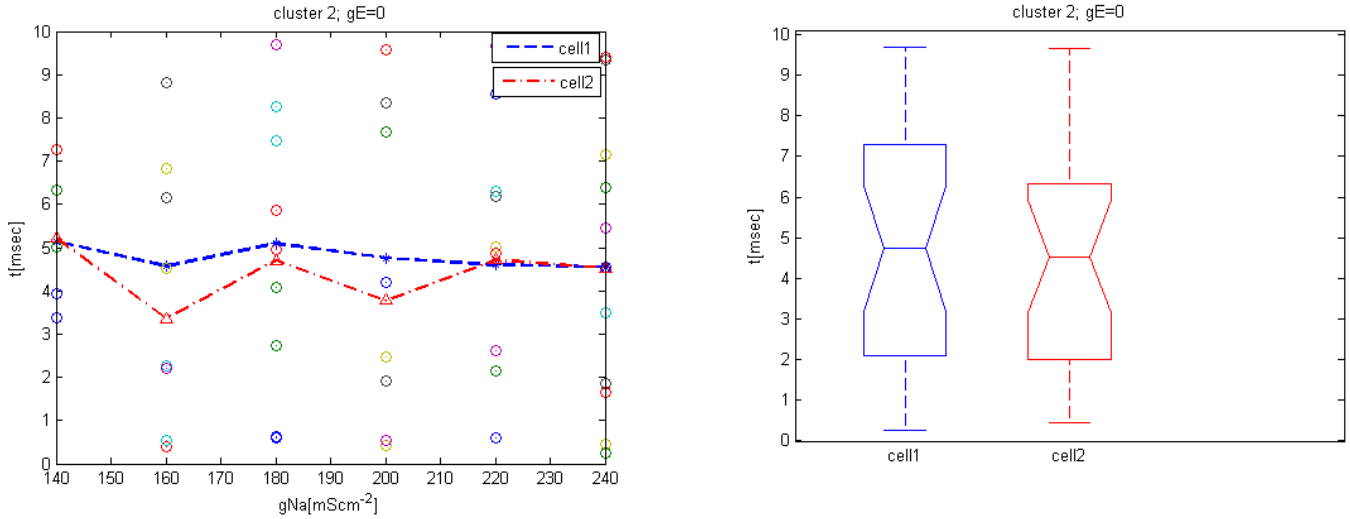

Table 5.20: cell1 and cell2 of the reconstructed bicellular structure are stimulated by 0.1 nA current injection to the peripheral interval with using noise factor k_{noise}= 0.05 $\mu A \mathrm{mS}^{-1/2}$ and increasing parameter gNa from 140-240 mS cm^{-2} for gE=0 mS/cm^2

Another experiments will be done for the second cluster for the increasing parameter gE=2 mS/cm^2including noise factor k_{noise}= 0.05 $\mu A\text{mS}^{-1/2}$:

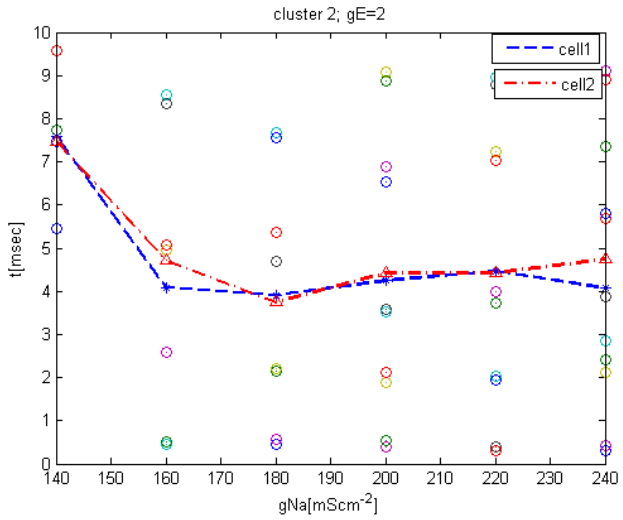

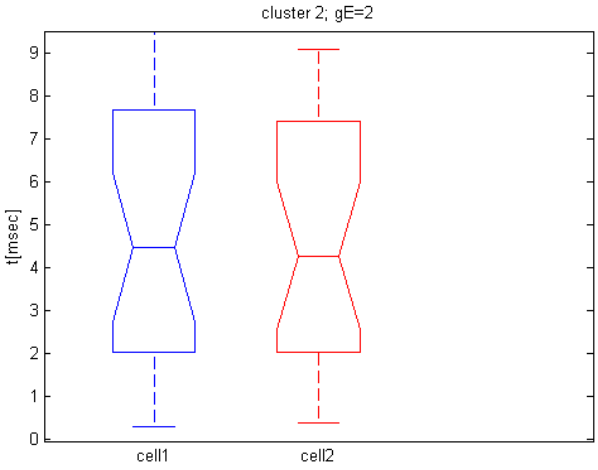

Table 5.21: cell1 and cell2 of the reconstructed bicellular structure are stimulated by 0.1 nA current injection to the peripheral interval with using noise factor k_{noise}= 0.05 $\mu A\text{mS}^{-1/2}$ and increasing parameter gNa from 140-240 mS cm^{-2} for gE=2 mS/cm^2

Now increase parameter gE=4 mS/cm^2 including noise factor k_{noise} for the second cluster= 0.05 $\mu A\text{mS}^{-1/2}$:

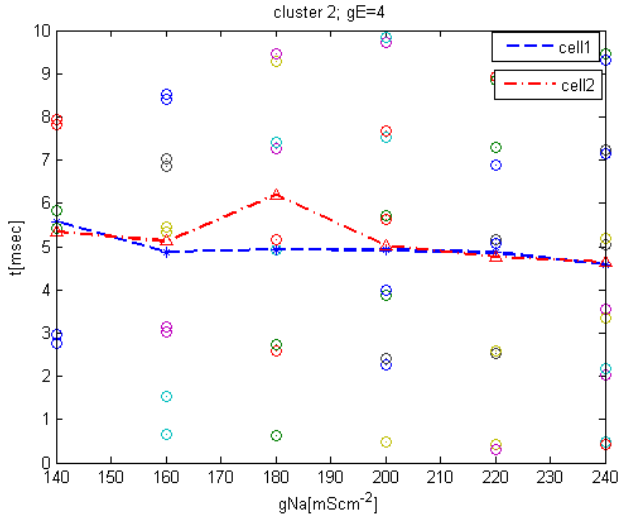

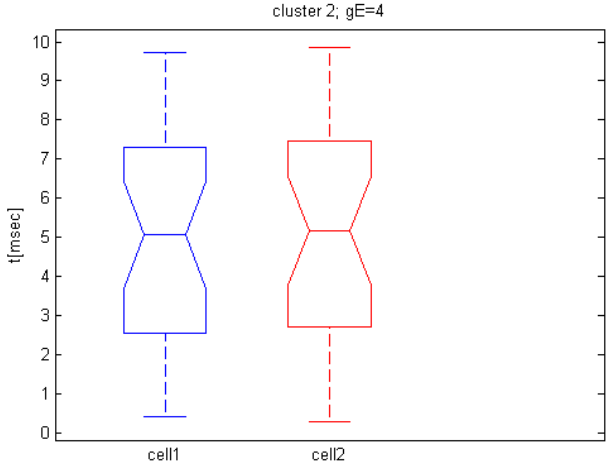

Table 5.22: cell1 and cell2 of the reconstructed bicellular structure are stimulated by 0.1 nA current injection to the peripheral interval with using noise factor k_{noise}= 0.05 $\mu A\text{mS}^{-1/2}$ and increasing parameter gNa from 140-240 mS cm^{-2} for gE=4 mS/cm^2

Conclusion: As we can see for the second cluster with the increasing parameter gE signal becomes more and more synchronized, as it was written before.

5.3.3 Cluster3

Make the experiment for the cluster3 when the first and second cells received current impulse 0.1nA, including noise factor k_{noise}= 0.05 $\mu A \mathrm{mS}^{-1/2}$, when the conductance parameter gE=0 mS/cm^2:

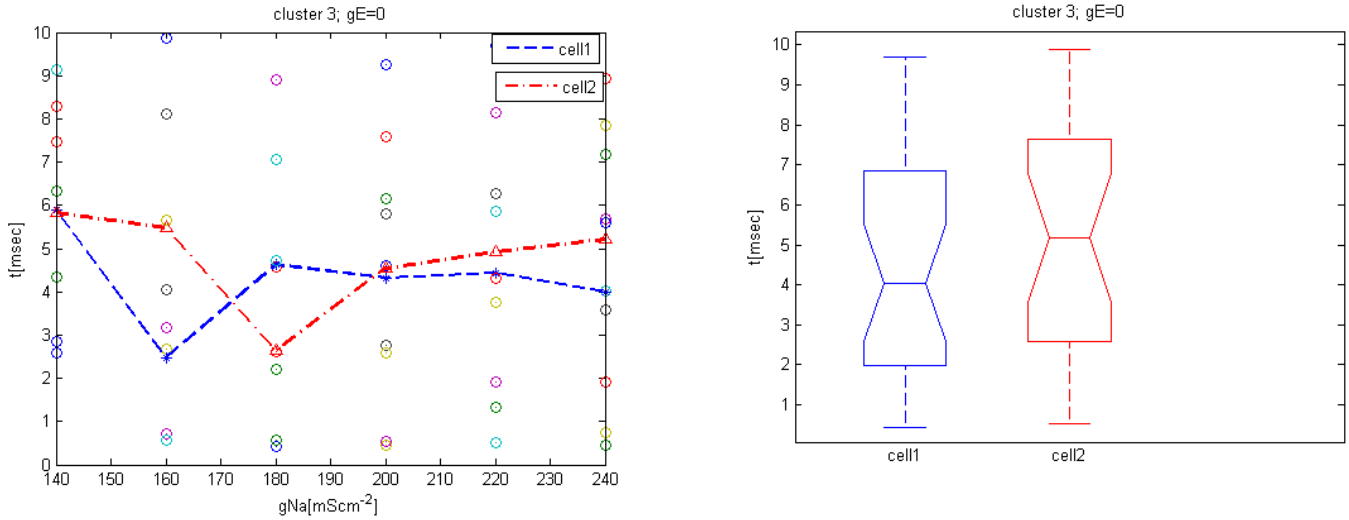

Table 5.23: cell1 and cell2 of the reconstructed bicellular structure are stimulated by 0.1 nA current injection to the peripheral interval with using noise factor k_{noise}= 0.05 $\mu A \mathrm{mS}^{-1/2}$ and increasing parameter gNa from 140-240 mS cm^{-2} for gE=0 mS/cm^2

Another experiments will be done for the third cluster for the increasing parameter gE=2 mS/cm^2 including noise factor k_{noise}= 0.05 $\mu A \mathrm{mS}^{-1/2}$:

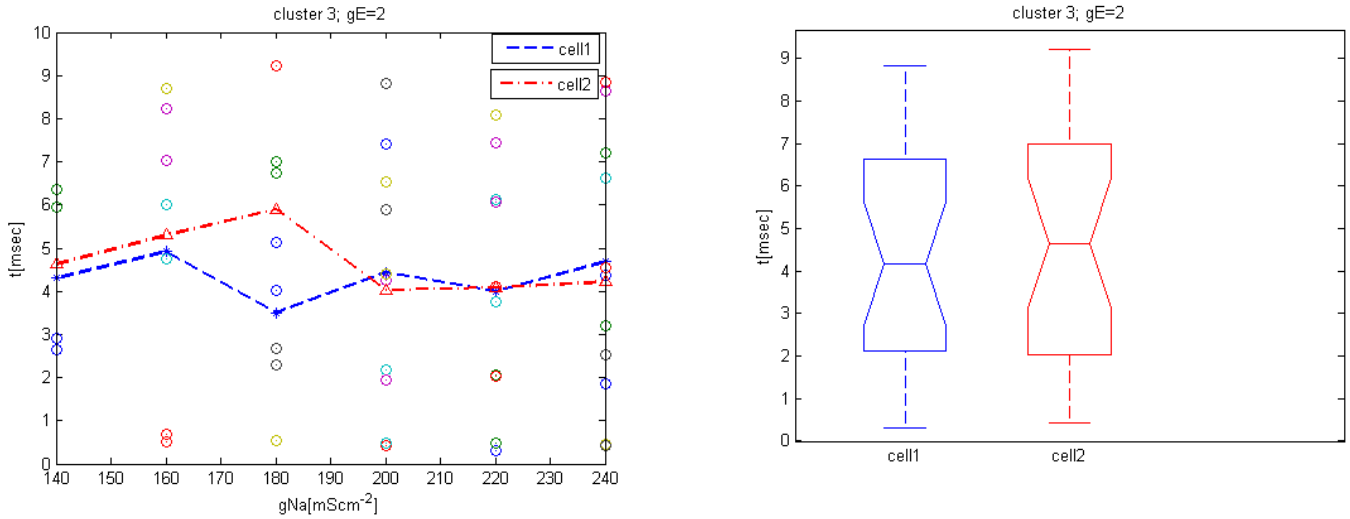

Table 5.24: cell1 and cell2 of the reconstructed bicellular structure are stimulated by 0.1 nA current injection to the peripheral interval with using noise factor k_{noise}= 0.05 $\mu A \mathrm{mS}^{-1/2}$ and increasing parameter gNa from 140-240 mS cm^{-2} for gE=2 mS/cm^2

Now increase parameter gE=4 mS/cm^2 including noise factor k_{noise} for the second cluster= 0.05 $\mu A \mathrm{mS}^{-1/2}$:

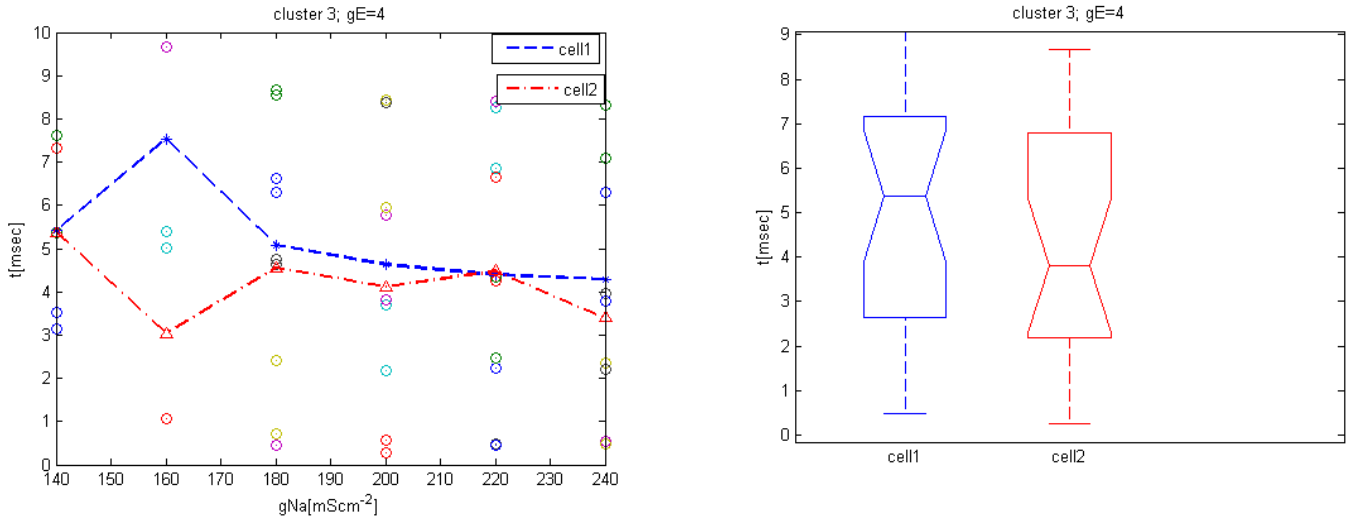

Table 5.25: cell1 and cell2 of the reconstructed bicellular structure are stimulated by 0.1 nA current injection to the peripheral interval with using noise factor k_{noise}= 0.05 $\mu A \mathrm{mS}^{-1/2}$ and increasing parameter gNa from 140-240 mS cm^{-2} for gE=4 mS/cm^2

Conclusion: As we can see for the third cluster with the increasing parameter gE=0 mS/cm^2 till gE=4 mS/cm^2 signal becomes more and more synchronized, thus the mean values of two cells becomes closer and the effect of synchronization between two cells become more evident.

5.3.4 Cluster4

The ephaptic coupling was tested as before with current excitation of 0.1nA for the three of cells(Figure 5.4)

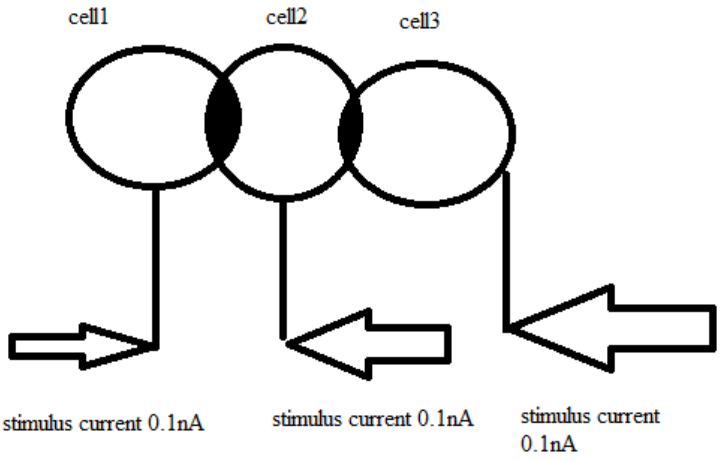

Figure 5.4: The stimulation of three cells in a cluster

When all the cells stay stimulated and conductance is considered $gE1$=0 mS/cm^2 and $gE2$=0 mS/cm^2:

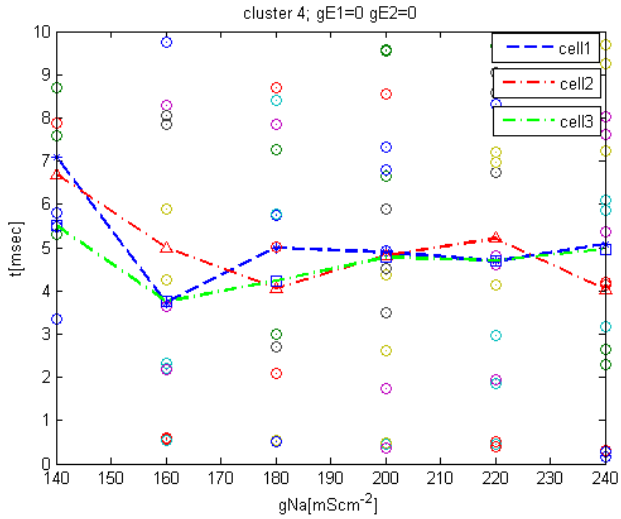

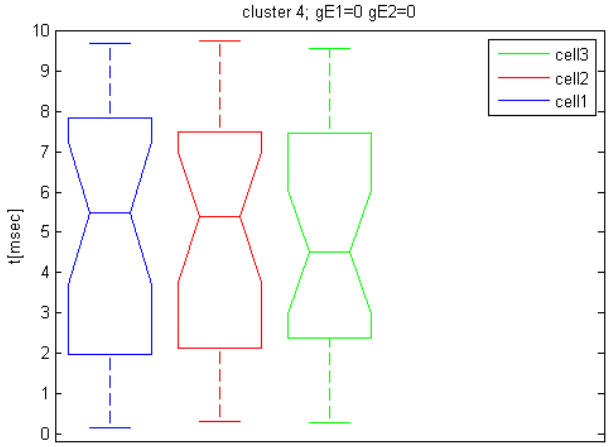

Table 5.26: cell1, cell2 and cell3 of the reconstructed tricellular structure are stimulated by 0.1 nA current injection to the peripheral interval with using noise factor k_{noise}= 0.05 $\mu A \mathrm{mS}^{-1/2}$ and increasing parameter gNa from 140-240 mS cm^{-2} for $gE1$=0 mS/cm^2 and $gE2$=0 mS/cm^2.

In the next experiment the current excitation of 0.1nA for the three of cells, when all the cells stay stimulated and conductance is considered $gE1$=0 mS/cm^2 and $gE2$=2 mS/cm^2:

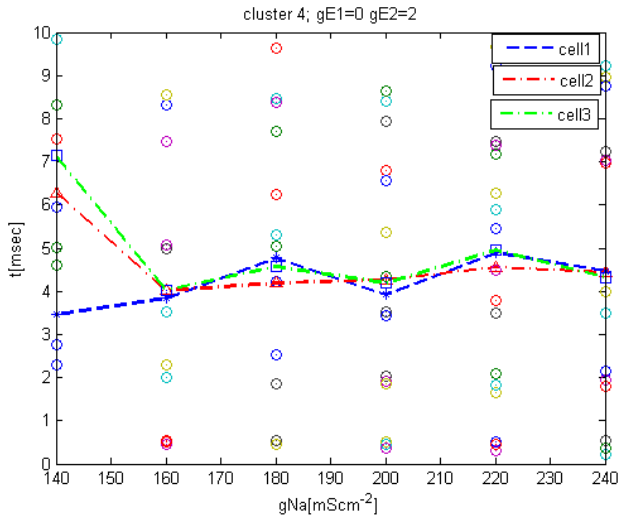

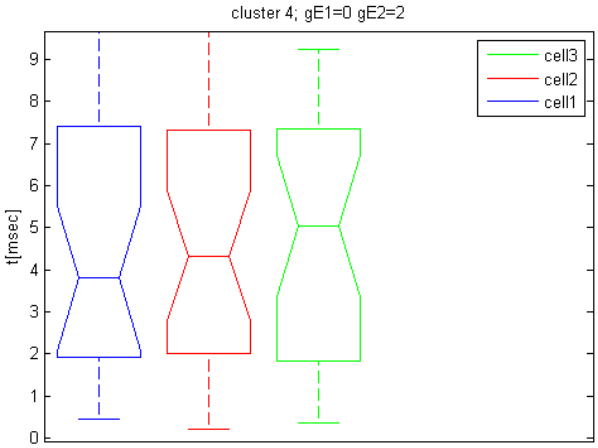

Table 5.27: cell1, cell2 and cell3 of the reconstructed tricellular structure are stimulated by 0.1 nA current injection to the peripheral interval with using noise factor k_{noise}= 0.05 $\mu A \mathrm{mS}^{-1/2}$ and increasing parameter gNa from 140-240 mS cm^{-2} for $gE1$=0 mS/cm^2 and $gE2$=2 mS/cm^2.

Another experiments will be done for the fourth cluster for the increasing parameter $gE1$=2 mS/cm^2 and $gE2$=0 mS/cm^2 including noise factor k_{noise}= 0.05 $\mu A \mathrm{mS}^{-1/2}$:

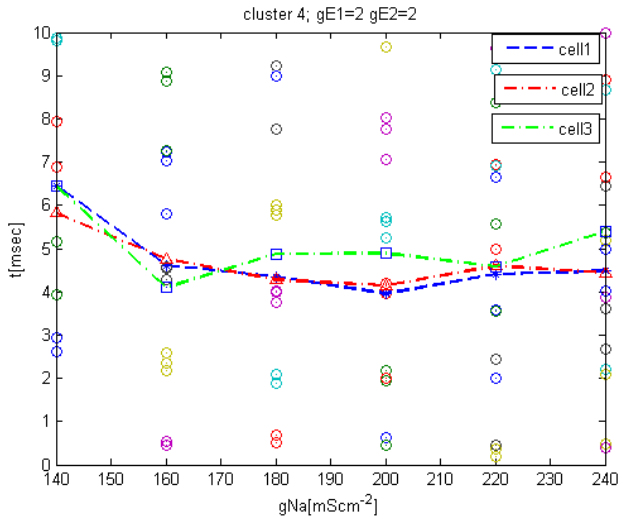

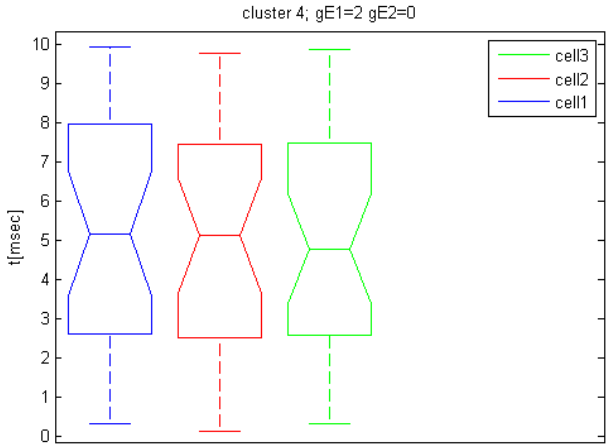

Table 5.28: cell1, cell2 and cell3 of the reconstructed tricellular structure are stimulated by 0.1 nA current injection to the peripheral interval with using noise factor k_{noise}= 0.05 $\mu A \mathrm{mS}^{-1/2}$ and increasing parameter gNa from 140-240 mS cm^{-2} for $gE1$=2 mS/cm^2 and $gE2$=0 mS/cm^2.

Another experiments will be done for the increasing parameter $gE1$=2 mS/cm^2 and $gE2$=2 mS/cm^2 including noise factor k_{noise}= 0.05 $\mu A \mathrm{mS}^{-1/2}$:

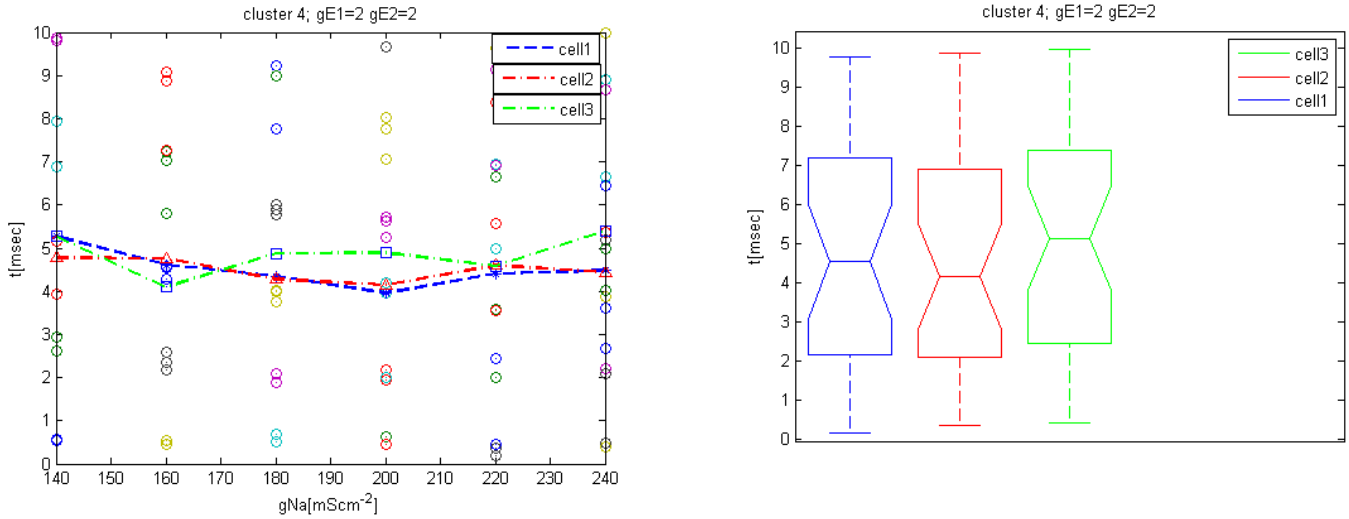

Table 5.29: cell1, cell2 and cell3 of the reconstructed tricellular structure are stimulated by 0.1 nA current injection to the peripheral interval with using noise factor k_{noise}= 0.05 $\mu A\text{mS}^{-1/2}$ and increasing parameter gNa from 140-240 mS cm^{-2} for $gE1$=2 mS/cm^2 and $gE2$=2 mS/cm^2.

In the next experiment the current excitation of 0.1nA for the three of cells, when all the cells stay stimulated and conductance is considered $gE1$=0 mS/cm^2 and $gE2$=4 mS/cm^2:

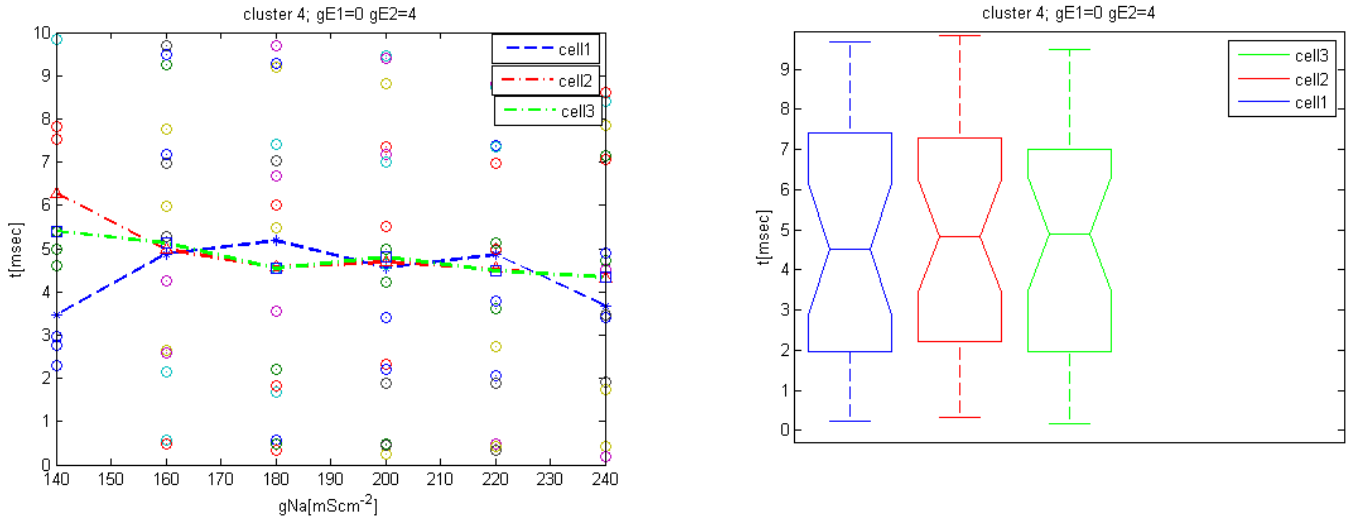

Table 5.30: cell1, cell2 and cell3 of the reconstructed tricellular structure are stimulated by 0.1 nA current injection to the peripheral interval with using noise factor k_{noise}= 0.05 $\mu A\text{mS}^{-1/2}$ and increasing parameter gNa from 140-240 mS cm^{-2} for $gE1$=0 mS/cm^2 and $gE2$=4 mS/cm^2.

Another experiments will be done for the increasing parameter $gE1$=4 mS/cm^2 and $gE2$=0 mS/cm^2 including noise factor k_{noise}= 0.05 $\mu A\text{mS}^{-1/2}$:

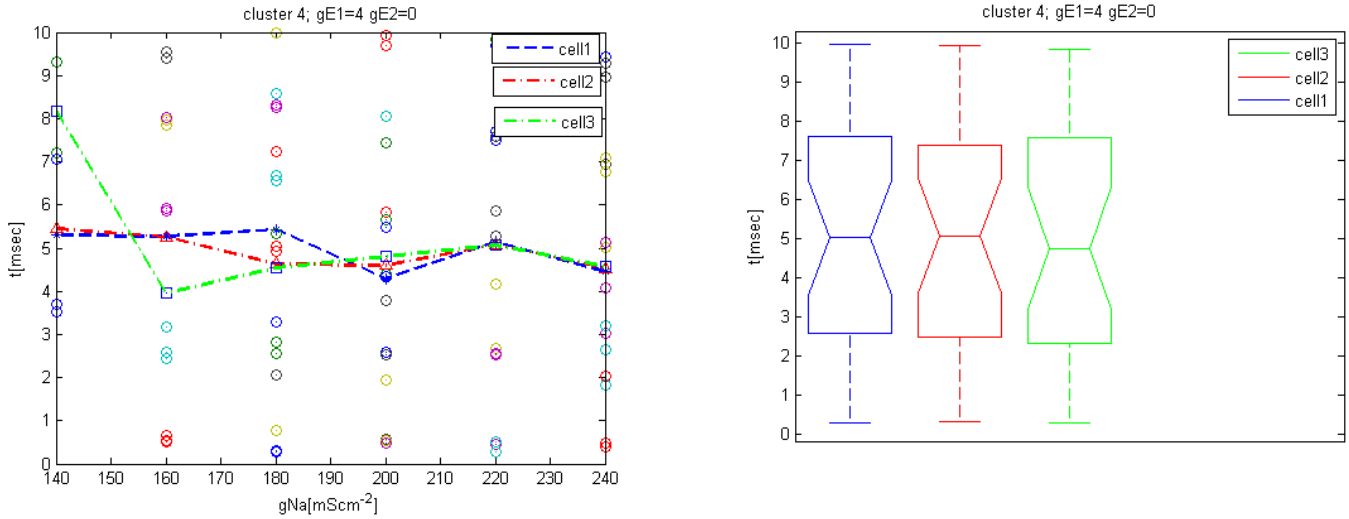

Table 5.31: cell1, cell2 and cell3 of the reconstructed tricellular structure are stimulated by 0.1 nA current injection to the peripheral interval with using noise factor k_{noise}= 0.05 $\mu A\text{mS}^{-1/2}$ and increasing parameter gNa from 140-240 mS cm^{-2} for $gE1$=4 mS/cm^2 and $gE2$=0 mS/cm^2.

At the end when $gE1$=4 mS/cm^2 and $gE2$=4 mS/cm^2 including noise factor k_{noise}= 0.05 $\mu A\text{mS}^{-1/2}$:

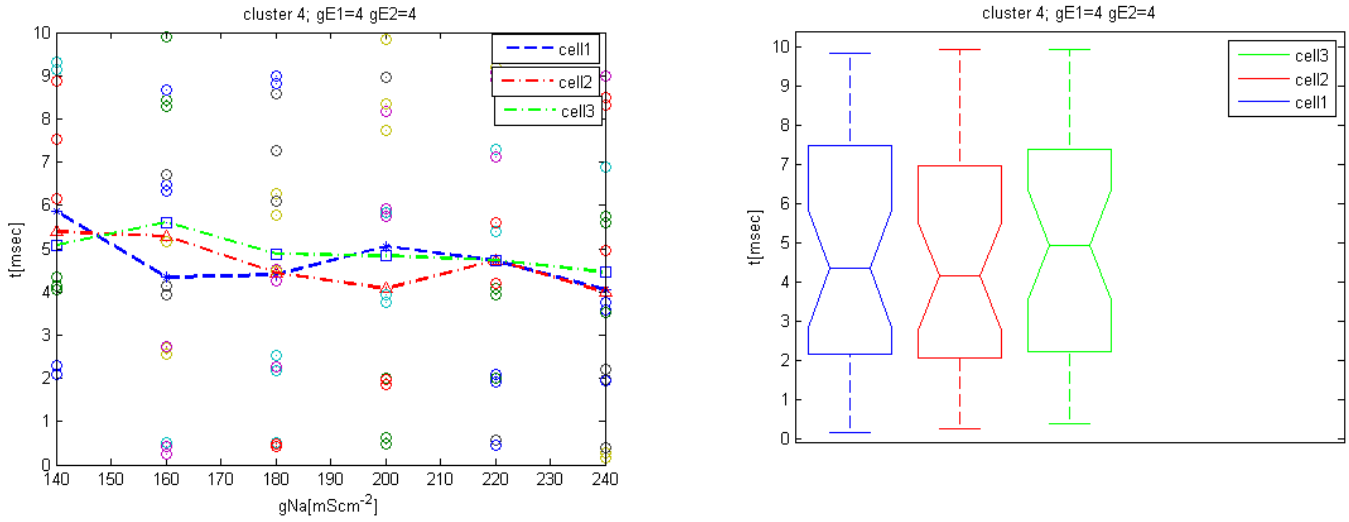

Table 5.32: cell1, cell2 and cell3 of the reconstructed tricellular structure are stimulated by 0.1 nA current injection to the peripheral interval with using noise factor k_{noise}= 0.05 $\mu A\text{mS}^{-1/2}$ and increasing parameter gNa from 140-240 mS cm^{-2} for $gE1$=4 mS/cm^2 and $gE2$=4 mS/cm^2.

Conclusion: As we can see for the fourth cluster with the increasing parameter $gE1$=0 mS/cm^2 and $gE2$=0 mS/cm^2 till $gE1$=4 mS/cm^2 and $gE2$=4 mS/cm^2 signal becomes more and more synchronized and synchronization between two cells become more evident.

Chapter 6

Conclusion

The results presented obtained by computer simulation should be analyzed from a critical point of view since the mathematical model used in this thesis underlies some limitations. These restrictions and the chosen parameters of the model should be kept in mind, while discussing the investigations. So this paragraph should summarize the findings and point out the arising questions which remain to be answered in the future by examination of further tests, comparison results and possible changes in the mathematical model.

Firstly, it should be reminded that the used models refer to a simplified geometry of the cochlear neurons by spherical compartments (soma) and cylindrical compartments (other parts). A lot of simulations were done with changing different parameters. It should be mentioned, that only the HH-model was used. Although the accelerated, warmed HH-model was used for all compartments, further models should be investigated in the future. The two main problems are the geometrical as well as the electrical properties of the cluster. On the other hand the description of the physical interaction between the cluster and the included neurons predicted by the mathematical model might be simulated by further tests. Nevertheless, the results demonstrated a strong interaction between neurons bounded together through a cluster. Also it should be mentioned that current fluctuations represented by the are presented in this thesis. With the current fluctuations these revealed differences in the spiking behavior can be explained in this work.

Secondly, when we increase conductance of Na-channels, it causes more noise (equation 5.1). In the simulations and therefore increase the number of activating spikes and the channel density. Consequently, it become a reason of spontaneous activity .This needs more energy, as the result producing false data and information.

Thirdly, with the increasing noise (conductance of Na-channels) the time shift between the first AP-spikes become less and less, that‘s proves that our simulation with noise artifacts are made correctly.

Finally, we should mention, that the standard conductance value for HH-model is, with the increasing conductance parameter from till the number of spikes are increased and, in reality, this spiking pattern disturb information that are clearly seen for the normal HH-parameter, so the usage of noise shows the real situation, that we could simulate in our brain with a help of HH-model. Now make some resulting graphs for each cluster with Unidirectional coupling for gE=0 mS/cm^2.

Table 6.1 shows that with increasing sodium conductance(gNa), the time shift between the main AP_{spike} become to decrease and the number of artefact-spikes begin to increase that leads to the spontaneous activity and as the result to the wrong data in modelling. The results which, are obtained here are similar for cluster2, cluster3 and cluster4:

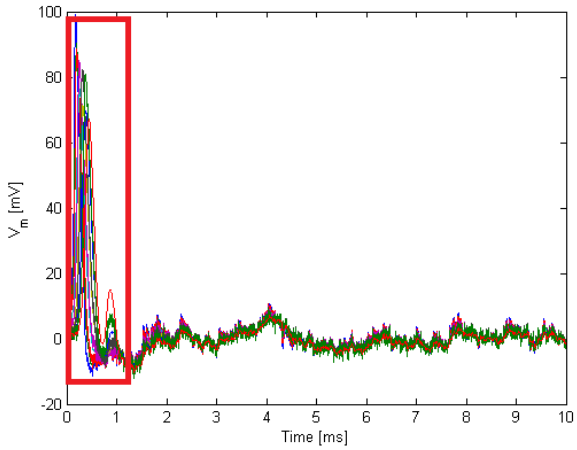

gNa=120 $mScm^{-2}$

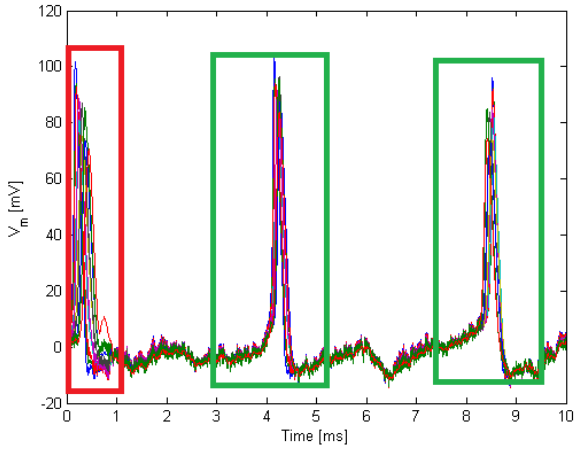

gNa=140 $mScm^{-2}$

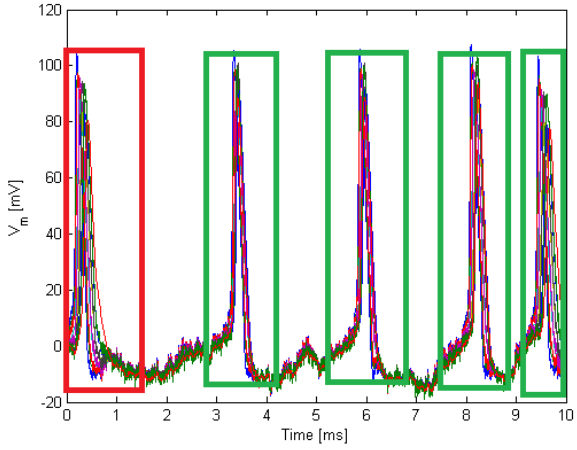

gNa=180 $mScm^{-2}$

Table 6.1: The red - main AP_{spike}, which occur when we make simulations for HH-model with a gNa=120 $mScm^{-2}$. Green - artifacts, which appear when, we increase sodium conductance, and as the result increase spontaneous activity.

Bibliography

Angelborg CA, Engstrm H (1973): The normal organ of CortiBasic Mechanisms of Hearing. New York: *Academic Press*, pp.125-182

Bear MF, Connors BW, Paradiso MA (2007): Neuroscience: Exploring the Brain, third edition, Lippincott Williams-Wilkins

Belluzzi O and Sacchi O (1991): A five conductance model of the action potential in the rat sympathetic neurone, *Progr. Biophys. Molec. Biol.*, 55, 130.

Bloom W, Fawcett DW (1975): A textbook of Histology (Saunders, Philadelphia)

Brown MC (1994): Antidromic responses of single units from the spiral ganglion, *J. Neurophysiol.* 71, 1835-1847.

Brugge JF, Anderson DJ, Hind JE, and Rose JE (1969): Time structure of discharges in single auditory nerve fibers of the squerrel monkey in response to complex periodic sounds. *Journal of Neurophysiology*, 32(3):386-401.1

Cells of the Nervous system: `http://www.columbia.edu/cu/psychology/courses/1010/mangels/neuro/neurocells/neurocells.html` accessed on 02.06.14

Chiu SY, Ritchie JM, Rogart RB and Stagg D (1979): A quantitative description

of membrane currents in rabbit myelinated nerve, *J. Physiol.*, 313, 149166.

Cohen LT, Saunders E, and Richardson LM (2004): Spatial spread of neural excitation: comparison of compound action potential and forward-making data in cochlear implant recipients. *International Journal of Audiology*, 43:346-355.

Dallos P, Fakler B (2002): Prestin, a new type of motor protein, *Nature Rev. Molec.Bio.* 3, 104-111

DeSchutter E and Smolen P (1999): Calcium dynamics in large neuronal models, in Methods in Neuronal Modeling: From Ions to Networks, 2nd ed., Koch, C. and Segev, I., Eds., *MIT Press*, Cambridge, MA, pp. 211250.

Destexhe A, Mainen ZF, Sejnowski TJ (1994): Synthesis of models for excitable membranes, synaptic transmission, and neuromodulation using a common kinetic framework, *J. Comput Neurosci.*,Aug; 1(3):195-230

Diller N, Lai WK, Almqvist B, Frohne C, Mller-Deile J, Stecker M, and von Wallenberg E (2002): Mesurement of the electrically evoked compound action potential via a neural response telemetry system. *The Annals of Otology, Rhinology and Laryngology*, 111:407-414. 1

Eatock R.A., Hurley K.M. (2003): Functional development of hair cells, *Curr. Topics Dev. Bio.* 57, 389-448

Engström H (1958): Structure and innervation of the inner ear sensory epithelia. *Int Rev Cytol* 7:535-585

Fettiplace R, Hackney CM (2006): The sensory and motor roles of auditory hair

cells, *Nature Rev. FettiplaceNeurosci.* 7, 19-29

Fohlmeister JF and Miller RF (1997): Impulse encoding mechanisms of ganglion cells in the tiger salamander retina, *J. Neurophysiol.*, 78, 19351947.

Fohlmeister JF and Miller RF (1997): Mechanisms by which cell geometry controls repetitive impulse firing in retinal ganglion cells, *J. Neurophysiol.*, 78, 19481964.

Forge A (1987): Specializations of the lateral membrane of inner hair cells. *Her Res* 31: 99-110.

Frankenhaeuser B (1964): Sodium permeability in toad nerve and in squid nerve, *J. Physiol.*, 152, 159166.

Furness DN, Hackney CM (1990): Comparative ultrastructure of subsurface cisternae in inner and outer hair cells of the guinea pig cochlea. *Eur Arch Otorhinolaryngol* 247: 12-15.

Glueckert R, Pfaler K, A. Kinnefors H. Rask-Anderson, and A Schrott-Fischer (2005b) The human spiral ganglion: New insights into ultrastructure, survival rate and implications for cochlear implants. *Audiology - Neurothology*, 10:258-273.

Guinan JJ Jr (1996): Physiology of olivocochlear efferents. In: Dallos P, Poppler AN, Fay RR(eds) The Cochlear. New York: *Springer Verlag*, pp.435-502

Hodgkin AL, Huxley AF (1952a): The components of membrane conductance in the giant axon of Loligo. *J. Physiol. (Lond.)* 116: 473-96.

Hodgkin AL, Huxley AF (1952b): Currents carried by sodium and potassium ions through the membrane of the giant axon of Loligo. *J. Physiol. (Lond.)* 116: 449-72.

Hodgkin AL, Huxley AF (1952c): The dual effect of membrane potential on sodium conductance in the giant axon of Loligo. *J. Physiol. (Lond.)* 116: 497-506.

Hodgkin AL, Huxley AF (1952d): A quantitative description of membrane current and its application to conduction and excitation in nerve. *J. Physiol. (Lond.)* 117: 500-44.

Horackova M, Nonner W, and Stämpfli R (1968): Action potentials and voltage clamp currents of single rat Ranvier nodes, *Proc. Int. Union Physiol. Sci.*, 7, 198

Jagger DJ, Housley GD (2003): Membrane properties of type II spiral ganglion neurones identified in a neonatal rat cochlear slice, *J Physiol.* 552, 525-533.

Javel E: Shapes of cat auditory nerve fiber tuning curves. *Hearing Research*, 81:167-88, 1994. 1

Junge D (1992): Nerve and Muscle Excitation, 3rd ed., 263 pp. *Sinauer Assoc.*, Sunderland, Mass.

Kiang NYS (1966): Discharge pattern of single fibers in the cats auditory nerve. *MIT press*, Cambridge,MA

Kimura RS (1966): Hairs of the cochlear sensory cells and their attachment to the tectorial membrane. *Acta Otolaryngol* 61:55-72

Kimura RS, Bongiorno CL, and Iverson NA (1987) : Synapses and ephapses in the spiral ganglion. *Acta oto-laryngologica.* Supplementum, 438:1-18

LeMasurier M, Gillespie PG (2005).: Hair-cell mechanotransduction and cochlear amplification, *Neuron.* 48, 403-415.

Liberman M.C. and Oliver M.E.(1984): Morphometry of intracellularly labeled neurons in the auditory nerve: correlations with functional properties. *The Journal of comparative neurology*, 223:163-176, 1,3.2.3

Lim DJ (1986): Functional Structure of the organ of Corti: a review. *Hear Res* 22:117-146

Liu W, Bstrom M, Kinnefors A, Linthicum F, Rask-Andersen H (2012): Expression of myelin basic protein in the human auditory nerve - an immunohistochemical and comparative study.*Auris Nasus Larynx*, 39(1):18-24.

Liu W, Glueckert R, Linthicum FH, Rieger G, Blumer M, Bitsche M, Pechriggl E, Rask-Andersen H, Schrott-Fischer A (2014): Possible role of gap junction intercellular channels and connexin 43 in satellite glial cells (SGCs) for preservation of human spiral ganglion neurons. *Cell Tissue Res.* 355: 267-278.

Lodish H, Berk A, Kaiser CA, Krieger M, Scott MP, Bretscher A, Ploegh H, Matsudaira P (2008): Molecular Cell Biology, sixth edition, chapter 10: Biomembrane Structure. W.H. Freeman and Company, New York

Machery O., Carlyon R.P., van Wieringen A., Deeks J.M., and Wouters J. (2008): Higher sensitivity of human auditory nerve fibers to positive electrical currents. *Journal of the Association for Research in Otolaryngology*:JARO, 9(2):241-251

Malmivuo J, Plonsey R (1995): Bioelectromagnetism

Martini F, Nath J (2012) :Fundamentals of Anatomy and Physiology ninths edi-

tion pp.374-415

McCormick DA and Huguenard JR (1992): A model of the electrophysiological properties of thalamocortical relay neurons, *J. Neurophysiol.*, 68, 13841400.

Nadol JB Jr (1988): Comparative anatomy of the cochlea and auditory nerve in mammals. *Hear Res.* Aug;34(3):253-66.

Ota CY and Kimura RS (1980): Ultrastructural study of the human spiral ganglion. *Acta oto-laryngologica*, 89:53-62,(document),1,3.2.2

Owen A (2003): The organ of Corti and auditory hair cells `http://www.nano.susx.ac.uk/research/hair-cell.org/Alan-Owen/EDUCATIONPAGE/Education-files/Cochlea-files/Cochlear-cells/CochlearCells-frame.htm` accessed on 31.07.14

Popper AN, Fay RR: The Cochlea (1996). New York: *Springer Verlag*, pp.186-257

Potrusil T, Wenger C, Glueckert R, Schrott-Fischer A, Rattay F (2012): Morphometric classification and spatial organization of spiral ganglion neurons in the human cochlea: Consequences for single fiber response to electrical stimulation. *Journal of Neuroscience* 214(5): 120-135.

Potrusil T (2013): Human Cochlear Nerve Model:Data Collection and Simulation, Dissertation

Pikovsky A, Rosenblum M and Kurth J (2001): Syncronization, A universal concept in in Nonlinear Sviences. *Cambridge University Press*,UK

Purves D (2007): Neuroscience: Third edition Sunderland, Massachusetts, USA

Raphael Y, Lenoir M, Wroblewski R, Pujol R (1991): The sensory epithelium and its innervation in the mole rat cochlea. *J Comp Neurol* 314: 367-382

Rattay F, Greenberg RG, Resatz S: Neuron Modeling in Finn WE, LoPresti PG (2003): Handbook of neuroprosthetic Methods pp. 46-78

Rattay F (1990): Electrical Nerve Stimulation: Theory, Experiments and Applications, *Springer-Verlag*, New York

Rattay F(1993): Stimulation of artificial neural reactions produced with electric fields, Simulation Practice Theory, 1, 137-152

Rattay F, Lutter P, Felix H (2001): A model of the electrically excited human cochlear neuron . I. Contribution of neural substructures to the generation and propagation of spikes. *Hearing Research* 153:43-63.

Rattay F, Leao RN, Felix H (2001): A model of the electrically excited human cochlear neuron. II. Influence of the three-dimensional cochlear structure on neural excitability. *Hearing Research* 153:64-79.

Rattay F, Potrusil T, Wenger C, Wise AK, Glueckert R, Schrott-Fischer A (2013): Impact of Morphometry, Myelinization and Synaptic Current Strength on Spike Conduction in Human and Cat Spiral Ganglion Neurons PLoS One. 8(11).

Rattay F and Lutter P (1997) : Speech Sound representation in the auditory nerve: computer simulation studies on inner ear mechanisms. *Zeitschrift für angewandte Mathematik und Mechanik*, 77:935-943

Rattay F,Mladenka A, and Pontes Pinto J (1998) : Classifying auditory nerve patterns with neural nets: a modelling study with low level signals. Stimulation Practise and Theory, 6:493-503

Rattay F (1999): The basic mechanism for the electrical stimulation of the nervous system. *Neuroscience*, 89(2):335-346

Reid MA, Flores-Otero J, Davis RL (2004): Firing Patterns of Type II Spiral Ganglion Neurons In Vitro, *J. Neurosci.* 24, 733-742.

Robertson D (1984): Horseradish peroxidase injection of physiologically characterized afferent and efferent neurons in the guinea pig spiral ganglion, *Hearing Res.* 15, 113-121

Robertson D, Sellick PM, Patuzzi R (1999): The continuing search for outer hair cell afferents in the guinea pig spiral ganglion, *Hearing Res.* 136, 151-158.

Ryugo DK (1992): The auditory nerve: Peripheral innervation, cell body morphology and central projections, in The Mammalian Auditory Pathway: Neuroanatomy, D.B. Webster, A.N. Popper, Fay R.R.,(Eds) (*Springer-Verlag*, New-York)

Schwarz JR and Eikhof G (1987): Na currents and action potentials in rat myelinated nerve fibres at 20 and 37C, *Pflügers Arch.*, 409, 569577

Shamma SA (1985) : Speech processing in the auditory system. i: The representation of speech sounds in the responses of the auditory nerve. *The Journal of the Acoustical Society of America*, 78(5):1612-21

Silbernagl S (2009): Color atlas of physiology, 6th edition, pp. 42

Smith CA, Cjostrand FS (1961a): Structure of the nerve endings on the external hair cells of the guinea pig cochlea as studied by serial sections. *J Ultrastruct Res* 5:523-556

Spoendlin H (1973): Innervation of the cochlear receptor. Basic Mechanisms in Hearing. New York: *Academic Press*, pp.185-230.

Spoendlin H (1967): The Innervation of the organ of Corti. *J Laryngol Otol* 81:717-738

Spoendlin H and Schrott A (1989) : Analysis of the human auditory nerve. *Hearing Research*, 43: 25-38, 1,3.1.3, 3.2.1, 3.2.3

Spoendlin H (1971) : Degenration behaviour of the cochlear nerve. *Archiv fr klinische und experimentelle Ohren- Nasen- und Kehlkopfheilkunde*, 200:275-291,(document),1

Svrcek-Seiler WA, Gebeshuber IC, Rattay F, Biro TS, and Markum H (1998): Micromechanical models for brownian motion of hair cell stereocilia. *Journal of Theoretical Biology*, 193:623-630

Sweeney JD, Mortimer JT, and Durand D (1987): Modeling of mammalian myelinated nerve for functional neuromuscular electrostimulation, in *IEEE 9th Annu. Conf. Eng. Med. Biol. Soc.*, Boston, MA, pp. 15771578.

Taylor EG, Hummel JE (2007): Perspectives on similarity from the LISA model. In Proceedings of AnICA07 (an analogy workshop held in conjunction with the 29th Annual Meeting of the Cognitive Science Society).

Traub RD, Jefferys, JG, Miles R, Whittington MA, and Toth KA (1994): branching dendritic model of a rodent CA3 pyramidal neurone, *J. Physiol.*, 481, 7995.

Tylstedt S and Rask-Anderson H (2001): A 3-d model of membrane specializations between human auditory spiral ganglion cells. *Journal of Neurocytology*, 30:465-473.

Tylstedt S, Kinnefors A and Rask-Anderson H (1997): Neural interaction in the human spiral ganglion: A tem study. *Acta oto-laryngologica*, 117:505-512

Tylstedt S, Kinnefors A, and Rask-Anderson H (1997): Neural inreraction in the human spiral ganglion: A tem study. *Acta oto-laryngologica*, 117:505-512. (document), 1, 3.2.2, 4.4

Wangemann P, Schacht J (1996): Homeostatic mechanisms in the cochlea. In Dallos P, Popper AN, Fay R (edc) The Cochlea. New York: *Springer*, pp. 130-185

Warr WB (1992): Organizaton of olivocochlear efferent systems in mammals, in The Mammalian Auditory Pathway: Neuroanatomy, Webster DB, Popper AN, Fay RR,(Eds) (*Springer-Verlag*, New-York)

Wenger C (2012): Human Cochlear Nerve Model, Dissertation

Winslow RL and Knapp AG (1991): Dynamic models of the retinal horizontalcell network, *Prog. Biophys. Mol. Biol.*, 56, 107133.

Young ED (2007): Physiological Acoustics in: Rossing TD (2007) - Springer Handbook of Acoustics. *Springer*. New York.